

# Domain Decomposition Methods for Vector Field Problems

Andrea Toselli.

Courant Institute of Mathematical Sciences  
New York University

May 1999

A dissertation in the Department of Mathematics submitted to the Faculty of the Graduate School of Arts and Science in partial fulfillment of the requirements for the degree of Doctor of Philosophy at New York University.

Approved: \_\_\_\_\_

Olof B. Widlund, Advisor

©Andrea Toselli  
All rights reserved 1999

*A Paola e Martina*

## ACKNOWLEDGMENTS

My deepest gratitude goes to my advisor and friend, Olof Widlund, who, during the past four years, has always guided, directed and, when needed, pushed me. I cannot remember a single occasion when he was not available for me.

Secondly, I would like to thank the following scientists, for some fruitful discussions and useful references: Faker Ben Belgacem, Maximilian Dryja, Mario Casarin, Frank Elliott, Ralf Hiptmair, Axel Klawonn, Luca Pavarino, Alberto Valli, and Barbara Wohlmuth.

A special thanks also goes to Alfio Quarteroni, without whom I would have never come to New York.

Finally, I would like to extend my thanks to my parents and my sister, who have always supported me during all these years.

## ABSTRACT

Finite element approximation of vector equations gives rise to very large, sparse linear systems. In this dissertation, we study some domain decomposition methods for finite element approximations of vector-valued problems, involving the curl and the divergence operators. *Edge* and *Raviart–Thomas* finite element spaces are employed. Problems involving the curl operator arise, for instance, when approximating Maxwell’s equations and the stream function–vorticity formulation of Stokes’ problem, while mixed approximations of second order elliptic equations and stabilized mixed formulations of advection–diffusion equations give rise to problems involving the divergence operator.

We first consider Maxwell’s equations in three dimensional conductive media using implicit time–stepping. We prove that the condition number of a two-level overlapping algorithm is bounded independently of the number of unknowns, the number of subregions, and the time step.

For the same equation in two dimensions, we show that the condition number of certain new iterative substructuring methods increases slowly with the number of unknowns in each substructure, but is independent of the time step and even large jumps of the coefficients. We also analyze similar preconditioners for a three-dimensional vector problem involving the divergence operator, and prove that the preconditioners are quasi-optimal and scalable in this case as well.

For each method, we provide a series of numerical experiments, that confirm our theoretical analysis.

This work generalizes well-known results for scalar second order elliptic equations and has required the development of several new technical tools.

# Contents

Acknowledgments . . . . .	iv
Abstract . . . . .	v
List of Figures . . . . .	ix
List of Tables . . . . .	x
<b>1 Introduction</b>	<b>1</b>
1.1 Continuous problems . . . . .	3
1.2 Two-level overlapping methods . . . . .	5
1.3 Iterative substructuring methods . . . . .	6
<b>2 Function and Finite Element spaces</b>	<b>9</b>
2.1 Sobolev spaces . . . . .	9
2.1.1 The space $H(\text{div}; \mathcal{D})$ . . . . .	11
2.1.2 The space $H(\mathbf{curl}; \mathcal{D})$ in two dimensions . . . . .	13
2.1.3 The space $H(\mathbf{curl}; \mathcal{D})$ in three dimensions . . . . .	14
2.1.4 The kernel and range of the curl and divergence operators . . . . .	16
2.1.5 Regularity results . . . . .	19
2.2 Finite element spaces . . . . .	22
2.2.1 Raviart–Thomas elements . . . . .	23
2.2.2 Nédélec elements in two dimensions . . . . .	25
2.2.3 Nédélec elements in three dimensions . . . . .	27
2.2.4 The kernel and range of the curl and divergence operators . . . . .	29
2.3 Schwarz methods . . . . .	33

<b>3</b>	<b>Overlapping Methods for Nédélec elements</b>	<b>37</b>
3.1	Finite element spaces and discrete problem . . . . .	38
3.2	Description of the algorithm . . . . .	39
3.3	Technical tools . . . . .	40
3.3.1	Some operators . . . . .	40
3.3.2	A partition of unity . . . . .	43
3.4	Main result . . . . .	45
3.5	Extensions . . . . .	51
3.6	Numerical results . . . . .	52
<b>4</b>	<b>Iterative substructuring methods based on individual edges or faces</b>	<b>60</b>
4.1	Introduction . . . . .	60
4.2	An edge space method in two dimensions . . . . .	62
4.2.1	Discrete problem and finite element spaces . . . . .	62
4.2.2	Description of the algorithm . . . . .	63
4.2.3	A stability estimate for the interpolation operator . . . . .	64
4.2.4	Main result . . . . .	66
4.2.5	Numerical results . . . . .	73
4.3	A face space method in three dimensions . . . . .	78
4.3.1	Discrete problem and finite element spaces . . . . .	78
4.3.2	Description of the algorithm . . . . .	79
4.3.3	Technical tools . . . . .	80
A stability estimate for the interpolation operator . . . . .	80	
Trace spaces . . . . .	83	
An extension operator . . . . .	90	
4.3.4	Main result . . . . .	91
4.3.5	Numerical results . . . . .	94
<b>5</b>	<b>Iterative substructuring methods: Neumann–Neumann methods</b>	<b>98</b>
5.1	Introduction . . . . .	98
5.2	Finite element spaces and operators . . . . .	99

5.3	Discrete problem and Schur complement system . . . . .	103
5.4	Description of the algorithms . . . . .	106
5.5	Technical tools . . . . .	109
5.6	Main result . . . . .	114
5.7	Numerical results . . . . .	123
<b>Bibliography</b>		<b>129</b>



# List of Figures

3.1	Two-level method. Inverse of the estimated minimum eigenvalue (asterisk), least-square zero (solid line), first (solid line), and second order (dashed line) fitting polynomials, versus $H/\delta$ . The relative fitting error is 1.0, 1.4 and 3.5 per cent, respectively. Case for $\eta_1 = 1$ , $\eta_2 = 1$ , $n$ equal to 16, 18, and 20. . . . .	58
4.1	Estimated condition number from Table 4.1 (asterisk) and least-square second order logarithmic polynomial (solid line), versus $H/h$ ; relative fitting error about 1.8 per cent. . . . .	76
4.2	Checkerboard distribution of the coefficients in the unit square. . .	77
4.3	Decomposition of the face $F$ . . . . .	81
4.4	Neighborhood of the wire-basket. . . . .	88
4.5	Estimated condition number from Table 4.4 (asterisk) and least-square second order logarithmic polynomial (solid line), versus $H/h$ ; the relative fitting error is about 4.5 per cent. . . . .	97
5.1	Estimated condition number from Table 5.1 (asterisk) and least-square second order logarithmic polynomial (solid line), versus $H/h$ ; relative fitting error about 2.8 per cent. . . . .	127

# List of Tables

3.1	One-level additive Schwarz algorithm. Estimated condition number and number of CG iterations for a residual norm reduction of $10^{-6}$ (in parentheses), versus $n$ , number of subdomains and $H/\delta$ . Case of $\eta_1 = 1, \eta_2 = 1$ . . . . .	53
3.2	Two-level additive Schwarz algorithm. Estimated condition number and number of CG iterations for a residual norm reduction of $10^{-6}$ (in parentheses), versus $n$ , number of subdomains and $H/\delta$ . Case of $\eta_1 = 1, \eta_2 = 1$ . . . . .	54
3.3	One-level additive Schwarz algorithm. Estimated condition number and number of CG iterations for a residual norm reduction of $10^{-6}$ (in parentheses), versus $b$ and $H/\delta$ . Case of $\eta_2 = 1, n = 16$ . . . . .	56
3.4	Two-level additive Schwarz algorithm. Estimated condition number and number of CG iterations for a residual norm reduction of $10^{-6}$ (in parentheses), versus $b$ and $H/\delta$ . Case of $\eta_2 = 1, n = 16$ . . . . .	57
4.1	Estimated condition number and number of CG iterations for a residual norm reduction of $10^{-6}$ (in parentheses), versus $H/h$ and $n$ . Case of $a = 1, b = 1$ . . . . .	74
4.2	Estimated condition number and number of CG iterations for a residual norm reduction of $10^{-6}$ (in parentheses), versus $H/h$ and $b$ . Case of $n = 128$ and $a = 1$ . . . . .	75
4.3	Checkerboard distribution for $b$ : $(b_1, b_2)$ . Estimated condition number and number of CG iterations for a residual norm reduction of $10^{-6}$ (in parentheses), versus $H/h$ and $b_2$ . Case of $n = 128, a = 1$ , and $b_1 = 100$ . . . . .	76

4.4	Estimated condition number and number of conjugate gradient iterations for a residual norm reduction of $10^{-6}$ (in parentheses), versus $H/h$ and $n$ . Case of $a = 1, b = 1$ . . . . .	95
4.5	Estimated condition number and number of conjugate gradient iterations for a residual norm reduction of $10^{-6}$ (in parentheses), versus $H/h$ and $b$ . Case of $n = 24$ and $a = 1$ . . . . .	96
5.1	Estimated condition number and number of CG iterations necessary for a reduction of $10^{-6}$ of the norm of the preconditioned residual (in parentheses), versus $H/h$ and $n$ . Case of $a = 1, b = 1$ . . . . .	125
5.2	Estimated condition number and number of CG iterations necessary for a reduction of $10^{-6}$ of the norm of the preconditioned residual (in parentheses), versus $H/h$ and $b$ . Case of $n = 128$ and $a = 1$ . . .	126
5.3	Checkerboard distribution for $b: (b_1, b_2)$ . Estimated condition number and number of CG iterations for a reduction of $10^{-6}$ of the norm of the preconditioned residual (in parentheses), versus $H/h$ and $b_2$ . Case of $n = 128, a = 1$ , and $b_1 = 100$ . . . . .	128
5.4	Checkerboard distribution for $a: (a_1, a_2)$ . Estimated condition number and number of CG iterations for a reduction of $10^{-6}$ of the norm of the preconditioned residual (in parentheses), versus $H/h$ and $a_2$ . Case of $n = 128, b = 1$ , and $a_1 = 0.01$ . . . . .	128

# Chapter 1

## Introduction

Computational electromagnetics study the numerical approximation of Maxwell's equations. These equations describe electromagnetic phenomena and form a vector system of time-dependent partial differential equations. In the last ten years, computational electromagnetics has become an extremely important research area in numerical analysis. Among the areas of interest are the simulation of antenna propagation in free space, scattering by complicated objects, analysis of optical devices in integrated optics, and calculation of eddy currents in electric conductors.

This thesis focuses on the construction of preconditioners for finite element (FE) approximations of Maxwell's equations and some vector valued problems involving the divergence operator. Many of these results have already appeared as technical reports and some have been submitted for publication; [56, 57, 62]. We note that the results of Chapter 4 have been obtained jointly with Barbara Wohlmuth and Olof Widlund.

For the analysis of Maxwell's equations, suitable Sobolev spaces have to be introduced:  $H(\mathbf{curl}; \Omega)$  and  $H(\text{div}; \Omega)$  are the spaces of square-integrable vectors on the domain  $\Omega$ , with square-integrable curl and divergence, respectively; see [26]. Suitable FE spaces, conforming in  $H(\mathbf{curl}; \Omega)$  and in  $H(\text{div}; \Omega)$ , were introduced in the late 1970's, in particular, the *Nédélec* or *edge element* spaces, conforming in  $H(\mathbf{curl}; \Omega)$ , and the *Raviart-Thomas* spaces, conforming in  $H(\text{div}; \Omega)$ ; see [44, 45]. These approximation spaces ensure the correct type of continuity across the elements of the triangulation. Nédélec FE vectors have a continuous

tangential component across the boundaries, as is physically required for the electric and magnetic fields, while Raviart–Thomas vectors have a continuous normal component, as is required for the electric and magnetic induction; see [18].

The study of efficient ways for solving the resulting algebraic system has recently become the subject of extensive research. In a Domain Decomposition (DD) approach, an approximate solver for the solution of a differential equation in a domain  $\Omega$  is obtained by solving problems over smaller subregions and then patching together the local solutions, by imposing continuity of suitable traces on the interfaces between the subregions. Iterative schemes can naturally be devised, where, starting from an initial guess, one solves the local problems, in parallel or in sequence, in each step. These basic iterative methods give rise to preconditioners that can be employed with Krylov–type methods to accelerate the convergence. Finally, a coarse problem can be added to make the convergence independent of the number of subregions. By their very nature, DD methods can, quite naturally, be implemented on parallel computers and they can give rise to scalable preconditioners.

Many of DD methods can be viewed as *Schwarz* preconditioners; see [54]. A Schwarz preconditioner is defined by a family of subspaces, the sum of which equals the original FE space, and solvers that are employed in these spaces (exact or inexact solvers can be used). The algorithms considered here are *two-level methods*, where the subspaces are related to a partition of the original domain into smaller subdomains, and to a coarse space, built on a coarse triangulation.

We have studied variational problems involving the following bilinear forms

$$a(\mathbf{u}, \mathbf{v}) = \int_{\Omega} a \mathbf{u} \cdot \mathbf{v} \, dx + \int_{\Omega} b \mathbf{curl} \mathbf{u} \cdot \mathbf{curl} \mathbf{v} \, dx, \quad (1.1)$$

and

$$a(\mathbf{u}, \mathbf{v}) = \int_{\Omega} a \mathbf{u} \cdot \mathbf{v} \, dx + \int_{\Omega} b \operatorname{div} \mathbf{u} \operatorname{div} \mathbf{v} \, dx, \quad (1.2)$$

defined in  $H(\mathbf{curl}; \Omega)$  and  $H(\operatorname{div}; \Omega)$ , respectively. The domain  $\Omega$  is a bounded connected polygon in  $\mathbb{R}^2$  or a polyhedron in  $\mathbb{R}^3$ . Dirichlet, Neumann, and Robin conditions can be considered.

The study and analysis of preconditioners for Nédélec and Raviart–Thomas approximations is quite new. Extensive work has started only in the past three years, in order to extend classical Schwarz preconditioners to these vector problems. Two–level overlapping Schwarz preconditioners for  $H(\operatorname{div}; \Omega)$  and  $H(\mathbf{curl}; \Omega)$  were developed for two dimensions, in [6]. Multigrid and multilevel methods were considered in [6, 5, 31, 30, 7], and an iterative substructuring method in [3]. We also mention [27, 25, 13, 39, 40, 16, 52, 53], which report on a study of a class of two- and multi-level methods for mixed approximations of Poisson’s equation. In [56], we have studied a two–level overlapping method for  $H(\mathbf{curl}; \Omega)$  in three dimensions, and in [33], we have extended our results to problems in  $H(\operatorname{div}; \Omega)$  and with variable coefficients. In [57] and [62], we have studied some iterative substructuring methods for problems in two and three dimensions, respectively.

## 1.1 Continuous problems

In this section, we will briefly review some problems involving the curl and divergence operators.

When time-dependent Maxwell’s equations are considered, the electric field  $\mathbf{u}$  satisfies the following equation

$$\mathbf{curl} \left( \mu^{-1} \mathbf{curl} \mathbf{u} \right) + \varepsilon \frac{\partial^2 \mathbf{u}}{\partial t^2} + \sigma \frac{\partial \mathbf{u}}{\partial t} = - \frac{\partial \mathbf{J}}{\partial t}, \quad \text{in } \Omega \times (0, T). \quad (1.3)$$

Here  $\mathbf{J}(\mathbf{x}, t)$  is the current density and  $\varepsilon$ ,  $\mu$ ,  $\sigma$  are positive semi-definite tensors that, in general, describe the electromagnetic properties of the medium. For their meaning and for a general discussion of Maxwell’s equations, see [43, 18, 35]. A similar equation holds for the magnetic field. For a conducting medium and low–frequency fields, the conductivity  $\sigma$  is large and the term in (1.3) involving the second derivative in time can be neglected, giving rise to a parabolic equation.

For a perfect conducting boundary, the electric field satisfies the essential boundary condition

$$\mathbf{u} \times \mathbf{n}_{|\partial\Omega} = 0.$$

A natural boundary condition

$$\mathbf{curl} \mathbf{u} \times \mathbf{n}_{|\partial\Omega} = 0,$$

can also be considered; see [18].

When Equation (1.3) is discretized with an implicit finite difference time scheme, the following equation has to be solved

$$a \mathbf{u} + \mathbf{curl} (b \mathbf{curl} \mathbf{u}) = \mathbf{F}, \quad (1.4)$$

in each time step. Here,  $a$  tends to infinity as the time step goes to zero and, in the general case, depends on  $\varepsilon$  and  $\sigma$ ,  $b$  is equal to  $1/\mu$ , and  $\mathbf{F}$  depends on the current density  $\mathbf{J}$ , as well as on the solution at the previous steps. The variational formulation of (1.4) involves the bilinear form defined in (1.1).

For the spatial approximation of (1.3), Nédélec spaces can be employed; see [44], [45], and Chapter 2. See [8], [41], [42], [15], [9], for the finite element and spectral element approximation of time-dependent Maxwell's equations and [49], for a discussion of approximations of hyperbolic and parabolic equations.

Given a porous medium and a fluid in it, Darcy's law states that the pressure  $p$  and the velocity  $\mathbf{v}$  of the fluid are related by the equation

$$A \mathbf{grad} p = \mathbf{v}, \quad (1.5)$$

where  $A$  is a symmetric positive-definite tensor. In addition the velocity satisfies the equation

$$-\mathbf{div} \mathbf{u} = f, \quad (1.6)$$

where  $f$  is a forcing term. Equations (1.5) and (1.6) give rise to the following mixed system

$$\begin{aligned} A^{-1} \mathbf{v} - \mathbf{grad} p &= 0, \\ -\mathbf{div} \mathbf{v} &= f. \end{aligned} \quad (1.7)$$

Dirichlet

$$p = g_1,$$

or Neumann

$$(A \mathbf{grad} p) \cdot \mathbf{n} = \mathbf{v} \cdot \mathbf{n} = g_2,$$

conditions can be considered on the boundary of the medium. For the approximation of the velocity, Raviart-Thomas spaces can be employed; see [48], [44] [45], [14], and Chapter 2.

Stabilized mixed formulations of the Stokes problem can also give rise to problems involving the divergence operator; see [14, Ch. VI] and the references therein. Still other applications of the space  $H(\text{div}; \Omega)$  are given in [6].

## 1.2 Two-level overlapping methods

Two-level overlapping methods give rise to optimal and scalable preconditioners and their application to scalar second-order problems has been studied extensively; see [54]. We consider some problems involving bilinear forms of (1.1) and (1.2), with strictly positive coefficients  $a$  and  $b$ .

In [6], a two-level overlapping preconditioner for two-dimensional problems involving the bilinear form (1.2) is studied. This result is also valid for  $H(\mathbf{curl}; \Omega)$ . In this thesis, we have extended this result to the three-dimensional case. Our original analysis can be found in [56]. We also note that our results have been then extended to the case of  $H(\text{div}; \Omega)$  and our bounds have been improved, in [33].

To begin a more detailed discussion, consider first a shape-regular triangulation of the domain  $\Omega$ , obtained by refining a coarse triangulation with a mesh size  $H$ .

Consider then a covering of the domain  $\Omega$  into overlapping subdomains and the local FE spaces defined on them. Let  $\delta$  be the width of the parts common to more than one subregion. The local components of the preconditioner are defined in terms of the original bilinear form  $a$  and the local spaces supported on the subdomains. The coarse component employs the FE space defined on the coarse triangulation. Modified bilinear forms are defined for inexact solvers. The local problems employ Dirichlet conditions, except on the part of the boundary that is common to  $\partial\Omega$ , where the original conditions are maintained; the coarse problem inherits the boundary conditions of the original one.

In the following, we will denote by  $A$  the representation of the bilinear form  $a$  on the FE space considered, and by  $B$  a symmetric Schwarz preconditioner, of additive, multiplicative or hybrid form; see [54]. In Chapter 3, we prove that the



condition number of the preconditioned system satisfies

$$\kappa(B^{-1}A) \leq C \left(1 + \frac{H}{\delta}\right)^2. \quad (1.8)$$

Here  $C$  is independent of the dimension of the original problem and the number of subregions. Numerical results also show that it is independent of the ratio between the coefficients  $a$  and  $b$ .

The proof of our results requires that the domain  $\Omega$  be convex and that the triangulation quasi-uniform, since some regularity results for vector fields are employed, together with some global estimates. These two assumptions are not required in the scalar case, where local averages can be employed; see [54]. A similar argument cannot be applied to the spaces  $H(\mathbf{curl}; \Omega)$  and  $H(\text{div}; \Omega)$ , due to their lack of regularity, and a more complicated analysis is required in this case.

### 1.3 Iterative substructuring methods

The method described in the previous section is optimal, but the condition number may possibly increase if the coefficients  $a$  and  $b$  have large jumps. Fast iterative substructuring methods have a condition number that is generally slowly increasing with the number of unknowns, but is independent of even large jumps of the coefficients. They have been successfully applied to scalar and vector problems in  $H^1$ , in both two and three dimensions; see [22, 54]. Their use for three-dimensional problems requires particular care in the choice of the coarse space.

The study of such methods, applied to vector problems in  $H(\mathbf{curl}; \Omega)$  and  $H(\text{div}; \Omega)$  is new. We know of no previous work for  $H(\text{div}; \Omega)$ , and only a few papers on the  $H(\mathbf{curl}; \Omega)$  case; see [3].

In Chapters 4 and 5, we design and analyze some iterative substructuring methods for FE approximations in  $H(\mathbf{curl}; \Omega)$  and  $H(\text{div}; \Omega)$ . Chapter 4 is joint work with Wohlmuth and Widlund, and the original papers [57, 62] have been submitted for publication.

We first consider two-dimensional positive-definite problems, for which the analysis is the same for the  $H(\mathbf{curl}; \Omega)$  and  $H(\text{div}; \Omega)$  cases. The coarse space is a standard coarse space, built on a coarse triangulation, with mesh size  $H$ . The

coarse triangles are called *substructures* and the coefficients  $a$  and  $b$  are supposed to be slowly varying on each substructure, but they may have arbitrary jumps across their boundaries.

In Chapter 4, we study an iterative substructuring method based on individual edges. We consider a partition of the domain  $\Omega$  into subregions that are the union of two substructures that share one edge. The local spaces are the FE spaces defined on each such subregion. We establish the following bound for the condition number

$$\kappa(B^{-1}A) \leq C \left(1 + \log \frac{H}{h}\right)^2, \quad (1.9)$$

where  $h$  is the diameter of the fine triangulation, and the constant  $C$  is independent of the dimension of the problem, the number of substructures, and the jumps of both the coefficients. We also prove that in the two limit cases  $a = 0$  and  $b = 0$ , the condition number remains bounded, and our numerical results also show that these bounds are independent of the ratio  $a/b$ .

We have generalized this previous result to three-dimensional problems in  $H(\operatorname{div}; \Omega)$ . Because of a property of the degrees of freedom for the Raviart–Thomas spaces, the same algorithm can be defined for two-dimensional problems and the estimate (1.9) can again be proven. In this case, the local spaces are related to the unions of two substructures that share a common face.

We remark that the ratio  $H/h$  is related in a simple way to the number of degrees of freedom in each substructure, and, since the analysis is carried out locally, the condition number only depends on the value of this ratio in individual substructures. In our estimates, the fine triangulation needs only be quasi-uniform in each substructure separately.

In Chapter 5, we study a Neumann–Neumann method, where the local spaces are defined on single substructures and establish the same estimate (1.9) for the condition number of the corresponding method. We remark that an important element in the definition of a Neumann–Neumann method is a set of scaling functions defined on the boundaries of the substructures, which involve the values of the coefficients of the partial differential equation. The use of these functions can ensure that the condition number of the corresponding preconditioned system be independent of the jumps of the coefficients across the substructures. We propose

a set of scaling functions, which involve only the values of one coefficient of (1.1) and (1.2). An important feature of our method is that it is independent of jumps of both coefficients. We know of no previous work on a Neumann–Neumann method for Maxwell’s equations or no previous theoretical study of a Neumann–Neumann method for the case where more than one coefficient has jumps.

# Chapter 2

## Function and Finite Element spaces

### 2.1 Sobolev spaces

In this section, we recall some definitions and properties of certain Sobolev spaces. In particular, we will introduce the spaces  $H(\operatorname{div}; \mathcal{D})$  and  $H(\operatorname{curl}; \mathcal{D})$ , suitable for analyzing certain vector problems. For a general theory of the classical Sobolev spaces  $H^s(\mathcal{D})$ , we refer to [1, 46, 28], and for  $H(\operatorname{div}; \mathcal{D})$  and  $H(\operatorname{curl}; \mathcal{D})$ , we refer to [26, 18].

Let  $\mathcal{D} \subset \mathbb{R}^n$ ,  $n = 2, 3$ , be an open bounded connected set, with Lipschitz continuous boundary  $\partial\mathcal{D}$  and exterior normal  $\mathbf{n}$ . Given a generic vector  $\mathbf{u} \in \mathbb{R}^n$ , its Cartesian components are  $\{u_i, i = 1, \dots, n\}$ . Let  $\mathbf{x}$  denote the position vector.

The space  $L^2(\mathcal{D})$  is the space of measurable functions  $q$  such that

$$\int_{\mathcal{D}} |q|^2 dx < +\infty.$$

The scalar product and norm in  $L^2(\mathcal{D})$  are defined, respectively, by

$$(q, p) = (q, p)_{0;\mathcal{D}} := \int_{\mathcal{D}} qp dx, \quad \|q\|^2 = \|q\|_{0;\mathcal{D}}^2 := (q, q)_{0;\mathcal{D}}.$$

The space  $L^2(\partial\mathcal{D})$  is defined in a similar fashion. We also define the space  $L^2(\mathcal{D})^n$ , of vectors  $\mathbf{u}$  with components in  $L^2(\mathcal{D})$ , with scalar product and corresponding norm, still denoted by  $(\cdot, \cdot)_{0;\mathcal{D}}$  and  $\|\cdot\|_{0;\mathcal{D}}^2$ , defined in the obvious way. Finally,  $L_0^2(\mathcal{D})$  is the subspace of  $L^2(\mathcal{D})$  of functions with mean value zero in  $\mathcal{D}$ .

The space  $H^m(\mathcal{D})$ , for  $m$  a positive integer, is the space of square-summable functions, the  $i$ -th derivatives of which are also square-summable, for  $i = 1, \dots, m$ . We will use the space  $H^1(\mathcal{D})$  extensively. The  $H^1$ -seminorm is defined as

$$|q|_{1;\mathcal{D}}^2 := \int_{\mathcal{D}} |\mathbf{grad} q|^2 dx.$$

The subspace of functions in  $H^1(\mathcal{D})$  vanishing on the boundary  $\partial\mathcal{D}$  is denoted by  $H_0^1(\mathcal{D})$ .

We will also need some Sobolev spaces of fractional order; see [1, 46]. For an integer  $m$  greater or equal to zero and  $0 < r < 1$ , the space  $H^{m+r}(\mathcal{D})$  is the space of functions  $q$  in  $H^m(\mathcal{D})$ , such that

$$|q|_{m+r;\mathcal{D}}^2 := \int_{\mathcal{D}} \int_{\mathcal{D}} \frac{|\partial^\alpha q(\mathbf{x}) - \partial^\alpha q(\mathbf{y})|^2}{|\mathbf{x} - \mathbf{y}|^{n+2r}} dx dy < \infty, \quad \|\alpha\| = m.$$

For  $0 < s \leq 1$ , the scaled norm of a function  $q \in H^s(\mathcal{D})$  is defined by

$$\|q\|_{s;\mathcal{D}}^2 := |q|_{s;\mathcal{D}}^2 + \frac{1}{H_{\mathcal{D}}^{2s}} \|q\|_{0;\mathcal{D}}^2, \quad (2.1)$$

where  $H_{\mathcal{D}}$  is the diameter of  $\mathcal{D}$  and the scaling factor is obtained by dilation from a region of unit diameter.

Analogously, for  $0 < s < 1$ , the space  $H^s(\partial\mathcal{D})$  is the space of square-summable functions  $q$  on  $\partial\mathcal{D}$  such that

$$|q|_{s;\partial\mathcal{D}}^2 := \int_{\partial\mathcal{D}} \int_{\partial\mathcal{D}} \frac{|q(\mathbf{x}) - q(\mathbf{y})|^2}{|\mathbf{x} - \mathbf{y}|^{n-1+2s}} dS_x dS_y < \infty,$$

with a scaled norm given by

$$\|q\|_{s;\partial\mathcal{D}}^2 := |q|_{s;\partial\mathcal{D}}^2 + \frac{1}{H_{\mathcal{D}}^{2s}} \|q\|_{0;\partial\mathcal{D}}^2. \quad (2.2)$$

We will also need some dual spaces defined on  $\partial\mathcal{D}$ . For  $s > 0$ , the space  $H^{-s}(\partial\mathcal{D})$  is the dual space of  $H^s(\partial\mathcal{D})$ , equipped with the norm

$$\|q\|_{-s;\partial\mathcal{D}} := \sup_{p \in H^s(\partial\mathcal{D})} \frac{\langle q, p \rangle}{\|p\|_{s;\partial\mathcal{D}}},$$

where  $\langle \cdot, \cdot \rangle$  denotes the duality pairing between  $H^{-s}(\partial\mathcal{D})$  and  $H^s(\partial\mathcal{D})$ . We stress the fact that the scaled  $\|\cdot\|_{s;\partial\mathcal{D}}$ -norm, defined in (2.2), is used in the previous definition.

With obvious modifications, we can define the Sobolev spaces  $H^s(\mathcal{D})^n$  and  $H^s(\partial\mathcal{D})^n$  of vector-valued functions.

From now on, we will denote by  $C$  a positive generic constant, uniformly bounded from above, and by  $c$  a positive generic constant uniformly bounded away from zero.

### 2.1.1 The space $H(\operatorname{div}; \mathcal{D})$

Given a vector function  $\mathbf{u} \in \mathbb{R}^n$ , the divergence operator is defined as

$$\operatorname{div} \mathbf{u} := \sum_{i=1}^n \frac{\partial u_i}{\partial x_i}. \quad (2.3)$$

The space  $H(\operatorname{div}; \mathcal{D})$  consists of square-integrable vectors, with square-integrable divergence. This is a Hilbert space with scalar product and graph norm defined by

$$(\mathbf{u}, \mathbf{v})_{\operatorname{div}; \mathcal{D}} := \int_{\mathcal{D}} \mathbf{u} \cdot \mathbf{v} \, dx + \int_{\mathcal{D}} \operatorname{div} \mathbf{u} \operatorname{div} \mathbf{v} \, dx, \quad \|\mathbf{u}\|_{\operatorname{div}; \mathcal{D}}^2 := (\mathbf{u}, \mathbf{u})_{\operatorname{div}; \mathcal{D}}.$$

Given a vector  $\mathbf{u} \in H(\operatorname{div}; \mathcal{D})$ , it is possible to define its normal component  $\mathbf{u} \cdot \mathbf{n}$  on the boundary  $\partial\mathcal{D}$ , as an element of  $H^{-\frac{1}{2}}(\partial\mathcal{D})$  and the following inequality holds

$$\|\mathbf{u} \cdot \mathbf{n}\|_{-\frac{1}{2}; \partial\mathcal{D}}^2 \leq C \left( \|\mathbf{u}\|_{0; \mathcal{D}}^2 + H_{\mathcal{D}}^2 \|\operatorname{div} \mathbf{u}\|_{0; \mathcal{D}}^2 \right), \quad (2.4)$$

with a constant  $C$  that is independent of  $H_{\mathcal{D}}$ . As usual, the scaling factor is obtained by dilation from a region of unit diameter. The operator that maps a vector in  $H(\operatorname{div}; \mathcal{D})$  into its normal component is thus continuous, and it can be shown to be surjective; see [26, Ch. I, Th. 2.5 and Cor. 2.8].

The following Green's formula holds

$$\int_{\mathcal{D}} \mathbf{u} \cdot \mathbf{grad} \, q \, dx + \int_{\mathcal{D}} \operatorname{div} \mathbf{u} \, q \, dx = \int_{\partial\mathcal{D}} \mathbf{u} \cdot \mathbf{n} \, q \, dS, \quad \mathbf{u} \in H(\operatorname{div}; \mathcal{D}), \, q \in H^1(\mathcal{D}),$$

where the integral on the right hand side is understood as the duality pairing between  $H^{-\frac{1}{2}}(\partial\mathcal{D})$  and  $H^{\frac{1}{2}}(\partial\mathcal{D})$ . The subspace of vectors in  $H(\operatorname{div}; \mathcal{D})$  with vanishing normal component on  $\partial\mathcal{D}$  is denoted by  $H_0(\operatorname{div}; \mathcal{D})$ , the subspace of vectors in  $H(\operatorname{div}; \mathcal{D})$  with vanishing divergence by  $H(\operatorname{div}_0; \mathcal{D})$

$$H(\operatorname{div}_0; \mathcal{D}) := \{\mathbf{u} \in H(\operatorname{div}; \mathcal{D}), \operatorname{div} \mathbf{u} = 0\},$$

and the subspace of vectors in  $H_0(\operatorname{div}; \mathcal{D})$  with vanishing divergence by  $H_0(\operatorname{div}_0; \mathcal{D})$

$$H_0(\operatorname{div}_0; \mathcal{D}) := \{\mathbf{u} \in H_0(\operatorname{div}; \mathcal{D}), \operatorname{div} \mathbf{u} = 0\}.$$

The space  $L^2(\mathcal{D})^n$  has the following orthogonal decompositions, see [18, vol. 3, p. 215, Proposition 1],

$$L^2(\mathcal{D})^n = H(\operatorname{div}_0; \mathcal{D}) \oplus \mathbf{grad} H_0^1(\mathcal{D}), \quad (2.5)$$

$$L^2(\mathcal{D})^n = H_0(\operatorname{div}_0; \mathcal{D}) \oplus \mathbf{grad} H^1(\mathcal{D}), \quad (2.6)$$

$$L^2(\mathcal{D})^n = H_0(\operatorname{div}_0; \mathcal{D}) \oplus \mathbf{grad} \mathcal{H}^1(\mathcal{D}) \oplus \mathbf{grad} H_0^1(\mathcal{D}),$$

where  $\mathcal{H}^1(\mathcal{D})$  is the space of harmonic functions in  $H^1(\mathcal{D})$  and

$$\mathbf{grad} \mathcal{H}^1(\mathcal{D}) = \mathbf{grad} H^1(\mathcal{D}) \cap H(\operatorname{div}_0; \mathcal{D}).$$

These decompositions are the generalization of the Helmholtz decomposition for a smooth vector into a divergence-free and a curl-free part.

Since  $H(\operatorname{div}; \mathcal{D}) \subset L^2(\mathcal{D})^n$ , the decompositions (2.5) and (2.6) give rise to corresponding orthogonal decompositions of  $H(\operatorname{div}; \mathcal{D})$  and  $H_0(\operatorname{div}; \mathcal{D})$ , into the kernel of the divergence operator and its orthogonal complement:

$$H(\operatorname{div}; \mathcal{D}) = H(\operatorname{div}_0; \mathcal{D}) \oplus H^\perp(\operatorname{div}; \mathcal{D}), \quad (2.7)$$

$$H_0(\operatorname{div}; \mathcal{D}) = H_0(\operatorname{div}_0; \mathcal{D}) \oplus H_0^\perp(\operatorname{div}; \mathcal{D}), \quad (2.8)$$

where

$$H^\perp(\operatorname{div}; \mathcal{D}) := H(\operatorname{div}; \mathcal{D}) \cap \mathbf{grad} H_0^1(\mathcal{D}),$$

$$H_0^\perp(\operatorname{div}; \mathcal{D}) := H_0(\operatorname{div}; \mathcal{D}) \cap \mathbf{grad} H^1(\mathcal{D}).$$

We stress the fact that (2.7) and (2.8) are orthogonal both with respect to the  $(\cdot, \cdot)_{0; \mathcal{D}}$  and  $(\cdot, \cdot)_{\operatorname{div}; \mathcal{D}}$  inner products. The decompositions (2.7) and (2.8) ensure that

$$\|\mathbf{u}\|_{0; \mathcal{D}} \leq C H_{\mathcal{D}} \|\operatorname{div} \mathbf{u}\|_{0; \mathcal{D}}, \quad \mathbf{u} \in H^\perp(\operatorname{div}; \mathcal{D}) \cup H_0^\perp(\operatorname{div}; \mathcal{D}). \quad (2.9)$$

### 2.1.2 The space $H(\mathbf{curl}; \mathcal{D})$ in two dimensions

We now consider the case  $\mathcal{D} \subset \mathbb{R}^2$ . Given a scalar function  $q$  and a vector  $\mathbf{u}$ , the vector and scalar curl operators are defined, respectively, by

$$\mathbf{curl} q := \left( \frac{\partial q}{\partial x_2}, -\frac{\partial q}{\partial x_1} \right),$$

and

$$\mathbf{curl} \mathbf{u} := \frac{\partial u_2}{\partial x_1} - \frac{\partial u_1}{\partial x_2}. \quad (2.10)$$

The space  $H(\mathbf{curl}; \mathcal{D})$  consists of square-integrable vectors, with square-integrable curl. This is a Hilbert space with scalar product and graph norm defined by

$$(\mathbf{u}, \mathbf{v})_{\mathbf{curl}; \mathcal{D}} := \int_{\mathcal{D}} \mathbf{u} \cdot \mathbf{v} \, dx + \int_{\mathcal{D}} \mathbf{curl} \mathbf{u} \, \mathbf{curl} \mathbf{v}, \, dx, \quad \|\mathbf{u}\|_{\mathbf{curl}; \mathcal{D}}^2 := (\mathbf{u}, \mathbf{u})_{\mathbf{curl}; \mathcal{D}}.$$

We define the unit tangent vector  $\mathbf{t}$  on the boundary  $\partial\mathcal{D}$  by

$$\mathbf{t} := (-n_2, n_1).$$

For a generic vector  $\mathbf{u}$ , its tangential component on the boundary is

$$\mathbf{u} \cdot \mathbf{t} = \mathbf{n} \times \mathbf{u}.$$

Due to the definitions (2.3) and (2.10), a vector  $\mathbf{u} = (u_1, u_2)$  belongs to  $H(\mathbf{curl}; \mathcal{D})$  if and only if the vector  $\mathbf{v} = (-u_2, u_1)$  belongs to  $H(\mathbf{div}; \mathcal{D})$ . In addition,

$$\mathbf{v} \cdot \mathbf{n} = -\mathbf{u} \cdot \mathbf{t}.$$

It is then clear that, using the results for  $H(\mathbf{div}; \mathcal{D})$ , for a generic vector  $\mathbf{u} \in H(\mathbf{curl}; \mathcal{D})$ , it is possible to define its tangential component on the boundary as an element of  $H^{-\frac{1}{2}}(\partial\mathcal{D})$  and that the following inequality holds

$$\|\mathbf{u} \cdot \mathbf{t}\|_{-\frac{1}{2}; \partial\mathcal{D}}^2 \leq C \left( \|\mathbf{u}\|_{0; \mathcal{D}}^2 + H_{\mathcal{D}}^2 \|\mathbf{curl} \mathbf{u}\|_{0; \mathcal{D}}^2 \right),$$

with a constant  $C$  that is independent of  $H_{\mathcal{D}}$ . The operator that maps a vector in  $H(\mathbf{curl}; \mathcal{D})$  into its tangential component is thus continuous and surjective; see [26, Ch. I, Th. 2.11]. The previous inequality is proven first for a domain of unit



diameter and then for an arbitrary domain, by a scaling argument. We recall that the scaled  $H^{\frac{1}{2}}$ -norm is used in the definition of the dual norm  $\|\cdot\|_{-\frac{1}{2};\partial\mathcal{D}}$ .

The following Green's formula also holds

$$\int_{\mathcal{D}} \operatorname{curl} \mathbf{u} q \, dx - \int_{\mathcal{D}} \mathbf{u} \cdot \operatorname{curl} q \, dx = \int_{\partial\mathcal{D}} \mathbf{u} \cdot \mathbf{t} q \, dS, \quad \mathbf{u} \in H(\mathbf{curl}; \mathcal{D}), \, q \in H^1(\mathcal{D}),$$

where, as usual, the integral on the right hand side is understood as the duality pairing between  $H^{-\frac{1}{2}}(\partial\mathcal{D})$  and  $H^{\frac{1}{2}}(\partial\mathcal{D})$ .

The subspace of vectors in  $H(\mathbf{curl}; \mathcal{D})$  with vanishing tangential component on  $\partial\mathcal{D}$  is denoted by  $H_0(\mathbf{curl}; \mathcal{D})$ , the subspace of vectors in  $H(\mathbf{curl}; \mathcal{D})$  with vanishing curl by  $H(\mathbf{curl}_0; \mathcal{D})$ , and the subspace of vectors in  $H_0(\mathbf{curl}; \mathcal{D})$  with vanishing curl by  $H_0(\mathbf{curl}_0; \mathcal{D})$ .

Since  $H(\mathbf{curl}; \mathcal{D}) \subset L^2(\mathcal{D})^n$  and  $\mathbf{grad} H^1(\mathcal{D}) \subset H(\mathbf{curl}; \mathcal{D})$ , the decompositions (2.5) and (2.6) give rise to the following orthogonal decompositions of  $H_0(\mathbf{curl}; \mathcal{D})$  and  $H(\mathbf{curl}; \mathcal{D})$ ,

$$H_0(\mathbf{curl}; \mathcal{D}) = \mathbf{grad} H^1(\mathcal{D}) \oplus H_0^\perp(\mathbf{curl}; \mathcal{D}), \quad (2.11)$$

$$H(\mathbf{curl}; \mathcal{D}) = \mathbf{grad} H^1(\mathcal{D}) \oplus H^\perp(\mathbf{curl}; \mathcal{D}), \quad (2.12)$$

where

$$H_0^\perp(\mathbf{curl}; \mathcal{D}) := H(\operatorname{div}_0; \mathcal{D}) \cap H_0(\mathbf{curl}; \mathcal{D}), \quad (2.13)$$

$$H^\perp(\mathbf{curl}; \mathcal{D}) := H_0(\operatorname{div}_0; \mathcal{D}) \cap H(\mathbf{curl}; \mathcal{D}).$$

We note that (2.11) and (2.12) are orthogonal both with respect to the  $(\cdot, \cdot)_{0;\mathcal{D}}$  and  $(\cdot, \cdot)_{\mathbf{curl};\mathcal{D}}$  inner products, and that they are valid also for  $n = 3$ ; see Section 2.1.3.

### 2.1.3 The space $H(\mathbf{curl}; \mathcal{D})$ in three dimensions

We will now consider the case  $\mathcal{D} \subset \mathbb{R}^3$ . Given a vector  $\mathbf{u}$ , the vector curl operator is defined by

$$\mathbf{curl} \mathbf{u} := \begin{bmatrix} \frac{\partial u_3}{\partial x_2} - \frac{\partial u_2}{\partial x_3} \\ \frac{\partial u_1}{\partial x_3} - \frac{\partial u_3}{\partial x_1} \\ \frac{\partial u_2}{\partial x_1} - \frac{\partial u_1}{\partial x_2} \end{bmatrix}.$$

The space  $H(\mathbf{curl}; \mathcal{D})$  consists of square-integrable vectors, with square-integrable curl. This is a Hilbert space with scalar product and graph norm defined by

$$(\mathbf{u}, \mathbf{v})_{\mathbf{curl}; \mathcal{D}} := \int_{\mathcal{D}} \mathbf{u} \cdot \mathbf{v} \, dx + \int_{\mathcal{D}} \mathbf{curl} \, \mathbf{u} \cdot \mathbf{curl} \, \mathbf{v}, \, dx, \quad \|\mathbf{u}\|_{\mathbf{curl}; \mathcal{D}}^2 := (\mathbf{u}, \mathbf{u})_{\mathbf{curl}; \mathcal{D}}.$$

We remark that we will use the same notation  $H(\mathbf{curl}; \mathcal{D})$  for the space in two and three dimensions.

The tangential component of a vector  $\mathbf{u}$  on the boundary  $\partial\mathcal{D}$  is defined by

$$\mathbf{u}_t := \mathbf{u} - (\mathbf{u} \cdot \mathbf{n})\mathbf{n} = (\mathbf{n} \times \mathbf{u}) \times \mathbf{n}.$$

Since  $|\mathbf{u}_t| = |\mathbf{n} \times \mathbf{u}|$ , the vector  $\mathbf{u}$  has vanishing tangential component if and only if  $\mathbf{n} \times \mathbf{u} = 0$ . With an abuse of terminology, we will, in the following, refer to  $\mathbf{n} \times \mathbf{u}$  as the tangential component.

Given a vector  $\mathbf{u} \in H(\mathbf{curl}; \mathcal{D})$ , it is possible to define its tangential component  $\mathbf{n} \times \mathbf{u}$  on the boundary  $\partial\mathcal{D}$ , as a vector of  $H^{-\frac{1}{2}}(\partial\mathcal{D})^3$  and the following trace inequality holds

$$\|\mathbf{n} \times \mathbf{u}\|_{-\frac{1}{2}; \partial\mathcal{D}}^2 \leq C \left( \|\mathbf{u}\|_{0; \mathcal{D}}^2 + H_{\mathcal{D}}^2 \|\mathbf{curl} \, \mathbf{u}\|_{0; \mathcal{D}}^2 \right),$$

with a constant  $C$  that is independent of  $H_{\mathcal{D}}$ . The previous inequality is proven first for a domain of unit diameter and then for an arbitrary domain, by a scaling argument. We recall that the scaled  $H^{\frac{1}{2}}$ -norm is used in the definition of the dual norm  $\|\cdot\|_{-\frac{1}{2}; \partial\mathcal{D}}$ .

The operator that maps a vector in  $H(\mathbf{curl}; \mathcal{D})$  into its tangential component is thus continuous, but it is not surjective; see [26, Ch. I, Th. 2.11]. The space of tangential traces of  $H(\mathbf{curl}; \mathcal{D})$  is a proper subspace of  $H^{-\frac{1}{2}}(\partial\mathcal{D})^3$  and it can be fully characterized; see [2] and the references therein for a more detailed analysis.

The following Green's formula holds

$$\int_{\mathcal{D}} \mathbf{curl} \, \mathbf{u} \cdot \mathbf{v} \, dx - \int_{\mathcal{D}} \mathbf{u} \cdot \mathbf{curl} \, \mathbf{v} \, dx = \int_{\partial\mathcal{D}} (\mathbf{n} \times \mathbf{u}) \cdot \mathbf{v} \, dS, \quad \mathbf{u} \in H(\mathbf{curl}; \mathcal{D}), \, \mathbf{v} \in H^1(\mathcal{D})^3.$$

As in the two-dimensional case, the subspace of vectors in  $H(\mathbf{curl}; \mathcal{D})$  with vanishing tangential component on  $\partial\mathcal{D}$  is denoted by  $H_0(\mathbf{curl}; \mathcal{D})$ , the subspace of vectors in  $H(\mathbf{curl}; \mathcal{D})$  with vanishing curl by  $H(\mathbf{curl}_0; \mathcal{D})$ , and the subspace of vectors in  $H_0(\mathbf{curl}; \mathcal{D})$  with vanishing curl by  $H_0(\mathbf{curl}_0; \mathcal{D})$ .

In the three-dimensional case, Equations (2.5) and (2.6) give rise to the same orthogonal decompositions, given in (2.11) and (2.12).

### 2.1.4 The kernel and range of the curl and divergence operators

In this section, we will characterize the kernel and the range of the curl and divergence operators. This characterization depends on the domain  $\mathcal{D}$  where the Sobolev spaces, previously introduced, are defined. We will review some results valid for a particular set of Lipschitz domains and refer to [18, vol. 3, Sect. IX.1.3] for the case of more general smooth domains, and to [4] for a generalization to a larger class of Lipschitz domains.

We recall that  $\mathcal{D} \subset \mathbb{R}^n$ ,  $n = 2, 3$ , is an open bounded connected set, with Lipschitz continuous boundary  $\partial\mathcal{D}$ . We only consider the case where  $\mathcal{D}$  is simply connected and its boundary consists of one connected component. We notice that these two conditions are equivalent for  $n = 2$ . The results presented in this section can be found in [18, vol. 3, Sect. IX.1.3], to which we refer for the proofs.

We clearly have that the kernel of the gradient operator consists of the constants, when defined in  $H^1(\mathcal{D})$ , and of the zero function, when defined in  $H_0^1(\mathcal{D})$ .

The following proposition characterizes the kernel of the curl operator as the range of the gradient operator, for simply-connected domains; see [18, vol. 3, pp. 217-221].

**Proposition 2.1.1** *If  $\mathcal{D}$  is simply connected, then, for  $n = 2, 3$ ,*

$$H(\mathbf{curl}_0; \mathcal{D}) = \mathbf{grad} H^1(\mathcal{D}). \quad (2.14)$$

**Remark 2.1.1** *In the case where  $\mathcal{D}$  is not simply connected,  $\mathbf{grad} H^1(\mathcal{D})$  is a proper subspace of  $H(\mathbf{curl}_0; \mathcal{D})$ , and its orthogonal complement in  $H(\mathbf{curl}_0; \mathcal{D})$  can be fully characterized and is of finite dimension equal to the number of cuts necessary to make  $\mathcal{D}$  simply connected; see [18, vol. 3, p. 219, Prop. 2]. We also note that (2.12) is a decomposition of the space  $H(\mathbf{curl}; \mathcal{D})$  into the kernel of the curl operator and its orthogonal complement, only with the hypothesis of Proposition 2.1.1. In this case, we have, for  $n = 2$ ,*

$$\|\mathbf{u}\|_{0;\mathcal{D}} \leq C H_{\mathcal{D}} \|\mathbf{curl} \mathbf{u}\|_{0;\mathcal{D}}, \quad \mathbf{u} \in H^\perp(\mathbf{curl}; \mathcal{D}), \quad (2.15)$$

and, for  $n = 3$ ,

$$\|\mathbf{u}\|_{0;\mathcal{D}} \leq C H_{\mathcal{D}} \|\mathbf{curl} \mathbf{u}\|_{0;\mathcal{D}}, \quad \mathbf{u} \in H^{\perp}(\mathbf{curl}; \mathcal{D}). \quad (2.16)$$

The next proposition characterizes the kernel of the curl operator in  $H_0(\mathbf{curl}; \mathcal{D})$  and, for the case  $n = 2$ , that of the divergence in  $H_0(\text{div}; \mathcal{D})$ ; see Section 2.1.2, for a discussion of the relation between  $H(\mathbf{curl}; \mathcal{D})$  and  $H(\text{div}; \mathcal{D})$  in two dimensions. This result can be found in [18, vol 3, p. 222, Prop. 3] and [18, vol 3, p. 224, Cor. 5].

**Proposition 2.1.2** *If the boundary  $\partial\mathcal{D}$  is connected, then*

$$H_0(\mathbf{curl}_0; \mathcal{D}) = \mathbf{grad} H_0^1(\mathcal{D}), \quad n = 2, 3, \quad (2.17)$$

$$H_0(\text{div}_0; \mathcal{D}) = \mathbf{curl} H_0^1(\mathcal{D}), \quad n = 2. \quad (2.18)$$

**Remark 2.1.2** *In the case where  $\partial\mathcal{D}$  consists of more than one connected component, the subspace of  $H^1(\mathcal{D})$  of functions that are constant on each connected component of  $\partial\mathcal{D}$  replaces  $H_0^1(\mathcal{D})$  in (2.17) and (2.18). When there is only one connected component, the gradients (and curls, for  $n = 2$ ) of these two spaces coincide and (2.11) is a decomposition of the space  $H_0(\mathbf{curl}; \mathcal{D})$  into the kernel of the curl operator and its orthogonal complement. In this case, we have, for  $n = 2$ ,*

$$\|\mathbf{u}\|_{0;\mathcal{D}} \leq C H_{\mathcal{D}} \|\mathbf{curl} \mathbf{u}\|_{0;\mathcal{D}}, \quad \mathbf{u} \in H_0^{\perp}(\mathbf{curl}; \mathcal{D}), \quad (2.19)$$

and, for  $n = 3$ ,

$$\|\mathbf{u}\|_{0;\mathcal{D}} \leq C H_{\mathcal{D}} \|\mathbf{curl} \mathbf{u}\|_{0;\mathcal{D}}, \quad \mathbf{u} \in H_0^{\perp}(\mathbf{curl}; \mathcal{D}). \quad (2.20)$$

The following two propositions complete the characterization of the kernel of the divergence operator. For  $n = 3$ , we will need the space of vectors in  $H^1(\mathcal{D})^3$ , with vanishing tangential component

$$H_{t_0}^1(\mathcal{D})^3 := \{\mathbf{u} \in H^1(\mathcal{D})^3, \mathbf{n} \times \mathbf{u}|_{\partial\mathcal{D}} = 0\}.$$

**Proposition 2.1.3** *If  $\mathcal{D}$  is simply connected and  $n = 3$ , we have*

$$H_0(\text{div}_0; \mathcal{D}) = \mathbf{curl} H_{0t}^1(\mathcal{D})^3 = \mathbf{curl} H_0^1(\mathcal{D})^3. \quad (2.21)$$

A proof can be found in [18, vol. 3, p. 224, Prop. 4 and Rem. 5]. We note that in the case where  $\mathcal{D}$  is not simply connected,  $\mathbf{curl} H_{0t}^1(\mathcal{D})^3$  is a proper subspace of  $H_0(\operatorname{div}_0; \mathcal{D})$  and its orthogonal complement is the same finite dimensional space mentioned in Remark 2.1.1.

**Proposition 2.1.4** *If the boundary  $\partial\mathcal{D}$  is connected, we have*

$$\begin{aligned} H(\operatorname{div}_0; \mathcal{D}) &= \mathbf{curl} H^1(\mathcal{D}), & n = 2, \\ H(\operatorname{div}_0; \mathcal{D}) &= \mathbf{curl} H^1(\mathcal{D})^3, & n = 3. \end{aligned}$$

A proof can be found in [18, vol. 3, p. 222, Prop. 3]. We note that in the case where  $\partial\mathcal{D}$  consists of  $m > 1$  connected components,  $\mathbf{curl} H^1(\mathcal{D})$  and  $\mathbf{curl} H^1(\mathcal{D})^3$  are proper subspaces of  $H(\operatorname{div}_0; \mathcal{D})$  and their orthogonal complements have dimension  $m - 1$ .

The following corollary is a direct consequence of Proposition 2.1.4 and gives a necessary and sufficient condition for the existence of a vector potential for a divergence-free vector.

**Corollary 2.1.1** *Let  $\partial\mathcal{D}$  be connected. A necessary and sufficient condition for a vector  $\mathbf{u} \in L^2(\mathcal{D})^n$  to be of the form  $\mathbf{u} = \mathbf{curl} q$ , with  $q \in H^1(\mathcal{D})$  if  $n = 2$ , or  $\mathbf{u} = \mathbf{curl} \mathbf{v}$ , with  $\mathbf{v} \in H^1(\mathcal{D})^3$  if  $n = 3$ , is*

$$\operatorname{div} \mathbf{u} = 0.$$

Incidentally, we observe that, due to Propositions 2.1.4 and 2.1.3, for  $n = 3$ , the range of the curl operator on  $H(\mathbf{curl}; \mathcal{D})$  and  $H_0(\mathbf{curl}; \mathcal{D})$  coincides with  $\mathbf{curl} H^1(\mathcal{D})^3$  and  $\mathbf{curl} H_{0t}^1(\mathcal{D})^3$ , respectively. The following proposition generalizes Corollary 2.1.1 to the case of more regular vectors, and ensures that a divergence-free vector potential can be found in three dimensions; see [26, Ch. I, Th. 3.4, Cor. 3.3 and Rem. 3.12].

**Proposition 2.1.5** *Let  $n = 3$  and let  $\partial\mathcal{D}$  be connected. For  $s \in [0, 1]$ , a necessary and sufficient condition for a vector  $\mathbf{u} \in H^s(\mathcal{D})^3$  to be of the form  $\mathbf{u} = \mathbf{curl} \mathbf{v}$ , with  $\mathbf{v} \in H^{1+s}(\mathcal{D})^3$  and  $\operatorname{div} \mathbf{v} = 0$ , is*

$$\operatorname{div} \mathbf{u} = 0.$$

We end this section with a characterization of the range of the divergence operator.

**Proposition 2.1.6** *The divergence operator is continuous and surjective from  $H(\operatorname{div}; \mathcal{D})$  into  $L^2(\mathcal{D})$ , and from  $H_0(\operatorname{div}; \mathcal{D})$  into  $L_0^2(\mathcal{D})$ .*

*Proof.* The proof is quite simple and only the surjectivity needs to be checked. Let  $q \in L^2(\mathcal{D})$ . If  $p \in H^1(\mathcal{D})$  is the solution of the following Dirichlet problem

$$\begin{aligned}\Delta p &= q, & \text{in } \mathcal{D}, \\ p &= 0, & \text{on } \partial\mathcal{D},\end{aligned}$$

then  $\mathbf{u} := \mathbf{grad} p \in H(\operatorname{div}; \mathcal{D})$  and  $\operatorname{div} \mathbf{u} = q$ . If, on the other hand,  $q \in L_0^2(\mathcal{D})$  and  $p \in H^1(\mathcal{D})$  is the solution of the following Neumann problem

$$\begin{aligned}\Delta p &= q, & \text{in } \mathcal{D}, \\ \frac{\partial p}{\partial n} &= 0, & \text{on } \partial\mathcal{D},\end{aligned}$$

then  $\mathbf{u} := \mathbf{grad} p \in H_0(\operatorname{div}; \mathcal{D})$  and  $\operatorname{div} \mathbf{u} = q$   $\square$

## 2.1.5 Regularity results

In this section, we will give some regularity results for vector-valued functions.

Given the spaces

$$\begin{aligned}H_T(\mathcal{D}) &:= H_0(\operatorname{div}; \mathcal{D}) \cap H(\mathbf{curl}; \mathcal{D}), \\ H_N(\mathcal{D}) &:= H(\operatorname{div}; \mathcal{D}) \cap H_0(\mathbf{curl}; \mathcal{D}),\end{aligned}$$

the following proposition is a classical result and a proof can be found in [4, Th. 2.17].

**Proposition 2.1.7** *If the domain  $\mathcal{D}$  is convex, then the spaces  $H_T(\mathcal{D})$  and  $H_N(\mathcal{D})$  are continuously embedded in  $H^1(\mathcal{D})^n$ .*

In order to prove a more general result, we need a regularity result for the Laplace operator that can be found in [17, Corollary 18.18]. In the following, we assume that  $\mathcal{D}$  is a Lipschitz polyhedron in three dimensions and that the largest angle between the faces of  $\mathcal{D}$  is  $\omega$ .

**Lemma 2.1.1** *Let  $\mathcal{D} \subset \mathbb{R}^3$  be a bounded, open, convex, polyhedron and  $s \neq -\frac{1}{2}$  a real number, such that*

$$s < \min \left\{ \frac{3}{2}, \frac{\pi}{\omega} - 1 \right\}.$$

*Then the Laplace operator  $\Delta$  defines an isomorphism:*

$$\Delta : H^{2+s}(\mathcal{D}) \cap H_0^1(\mathcal{D}) \longleftrightarrow H^s(\mathcal{D}). \quad (2.22)$$

**Remark 2.1.3** *Since, for every fixed bounded, convex, polyhedron the maximum angle  $\omega$  is strictly smaller than  $\pi$ , Lemma 2.1.1 implies that there exists a real number  $s_{\mathcal{D}} > 0$ , such that the mapping (2.22) is an isomorphism, for any  $s \in [0, s_{\mathcal{D}})$ . We will always assume that  $s_{\mathcal{D}}$  is less than  $1/2$ .*

We are now ready to prove an embedding theorem.

**Theorem 2.1.1** *Given a bounded, open, convex, polyhedron  $\mathcal{D} \subset \mathbb{R}^3$ , then there exists a real number  $s_{\mathcal{D}} \in (0, 1/2)$ , such that, for every  $t \in [0, s_{\mathcal{D}})$ , the space of functions  $\mathbf{w} \in H_N(\mathcal{D})$ , satisfying the conditions*

$$\operatorname{div} \mathbf{w} \in H^t(\mathcal{D}), \quad (2.23)$$

$$\operatorname{curl} \mathbf{w} \in H^t(\mathcal{D})^3, \quad (2.24)$$

*is continuously embedded in  $H^{1+t}(\mathcal{D})^3$ .*

*Proof.* The argument is the same as in the proofs of similar embedding theorems, given in [4, Proposition 3.7]. These proofs employ the existence and regularity of the vector potential of Proposition 2.1.5 and the regularity result for the Laplace operator given in Lemma 2.1.1.

Let  $s_{\mathcal{D}} \in (0, 1/2)$  be the exponent of Remark 2.1.3 and let  $t \in [0, s_{\mathcal{D}})$ . Given  $\mathbf{w} \in H_N(\mathcal{D})$ , satisfying (2.23) and (2.24), define

$$\mathbf{u} = \operatorname{curl} \mathbf{w} \in H^t(\mathcal{D})^3.$$

Let  $\mathcal{O}$  be an open ball that contains  $\overline{\mathcal{D}}$  and let  $\tilde{\mathbf{u}}$  be the extension by zero of  $\mathbf{u}$  to  $\mathcal{O} \setminus \mathcal{D}$ ;  $\tilde{\mathbf{u}}$  belongs to  $H^t(\mathcal{O})^3$ , as  $t < 1/2$ . Since, by Stokes' theorem, the normal component of  $\mathbf{u}$  on  $\Gamma$  is zero,  $\tilde{\mathbf{u}}$  belongs to  $H(\operatorname{div}, \mathcal{O})$ , and  $\operatorname{div} \tilde{\mathbf{u}} = 0$  in  $\mathcal{O}$ .

The vector  $\tilde{\mathbf{u}}$  satisfies the hypothesis of Proposition 2.1.5. There then exists a vector  $\mathbf{v} \in H^{1+t}(\mathcal{O})^3$ , satisfying

$$\begin{aligned}\tilde{\mathbf{u}} &= \mathbf{curl} \mathbf{v}, \\ \operatorname{div} \mathbf{v} &= 0.\end{aligned}$$

Consider now the vector  $\mathbf{v}$  in  $\mathcal{O} \setminus \mathcal{D}$ : Since  $\mathcal{D} \subset \mathbb{R}^3$  is simply connected,  $\mathcal{O} \setminus \mathcal{D}$  is also simply connected. From

$$\mathbf{curl} \mathbf{v} = \tilde{\mathbf{u}} = 0, \quad \text{in } \mathcal{O} \setminus \mathcal{D},$$

we deduce that there exists a function  $q \in H^{2+t}(\mathcal{O} \setminus \mathcal{D})$ , such that  $\mathbf{v} = \mathbf{grad} q$  in  $\mathcal{O} \setminus \mathcal{D}$ .

Define now  $\chi$  by

$$-\Delta \chi = \operatorname{div} \mathbf{w}, \quad \text{in } \mathcal{D}, \tag{2.25}$$

$$\chi = q, \quad \text{on } \mathcal{D}. \tag{2.26}$$

Then the vector  $\mathbf{grad} \chi$  has zero curl and divergence equal to  $(-\operatorname{div} \mathbf{w})$  in  $\mathcal{D}$ , and satisfies the boundary conditions

$$\mathbf{grad} \chi \times \mathbf{n} = \mathbf{grad} q \times \mathbf{n} = \mathbf{v} \times \mathbf{n}, \quad \text{on } \partial \mathcal{D};$$

It is easy to see that the vector  $(\mathbf{w} - \mathbf{v} + \mathbf{grad} \chi)$  has zero divergence and curl in  $\mathcal{D}$  and has zero tangential trace on  $\partial \mathcal{D}$ . By [26, Remark 3.9], it then follows that it vanishes and consequently

$$\mathbf{w} = \mathbf{v} - \mathbf{grad} \chi.$$

Consider now the Poisson problem given by (2.25) and (2.26). The function  $q|_{\partial \mathcal{D}}$  belongs to  $H^{3/2+t}(\partial \mathcal{D})$ . Using Lemma 2.1.1, by the surjectivity of the trace map from  $H^{2+t}(\mathcal{D})$  onto  $H^{3/2+t}(\partial \mathcal{D})$  and by (2.23), the solution of (2.25) and (2.26) belongs to  $H^{2+t}(\mathcal{D})$  and, finally,  $\mathbf{w}$  belongs to  $H^{1+t}(\mathcal{D})^3$ .  $\square$

**Remark 2.1.4** *In Theorem 2.1.1, the constraint  $t < s_{\mathcal{D}} < 1/2$  is necessary for the extension by zero of  $\mathbf{curl} \mathbf{w}$  to be in  $H^t(\mathcal{D})^3$ . Theorem 2.1.1 is stated in [4, Remark 3.8] without proof. Observe that the  $H^{2+t}$  regularity of problem (2.25) and (2.26), for  $t \geq 0$ , is employed. The conclusion of Theorem 2.1.1 is false for a general non-convex polyhedron.*



## 2.2 Finite element spaces

Let  $\Omega$  be a bounded, open polygon or polyhedron and let  $\mathcal{T}_h$  be a family of triangulations of  $\Omega$ . We suppose that  $\mathcal{T}_h$  consists of triangles or rectangles in two dimensions, and of tetrahedra or parallelepipeds in three dimensions.  $h$  is the maximum diameter of the triangulation. We suppose that  $\mathcal{T}_h$  is *shape-regular*, that is, for each element in  $\mathcal{T}_h$ , the ratio between its diameter and the radius of the circle, or sphere in three dimensions, inscribed in it, is bounded from above, by a constant that is independent of  $h$ ; see [49, Def. 3.4.1]. In case the ratio between the largest and the smallest diameter of  $\mathcal{T}_h$  is bounded independently of  $h$ , the triangulation is called *quasi-uniform*.

Given an open set  $\mathcal{D}$  in  $\mathbb{R}^n$ ,  $n = 1, 2, 3$ , we now define some polynomial spaces. Let  $\mathbb{P}_k(\mathcal{D})$ ,  $k \geq 0$ , be the set of polynomials of total degree at most  $k$  defined on  $\mathcal{D}$ , and let  $\mathbb{P}_k(\mathcal{D})^n$ , for  $n = 2, 3$ , be the set of vectors of  $\mathbb{R}^n$ , the components of which belong to  $\mathbb{P}_k(\mathcal{D})$ . Their subspaces consisting of homogeneous polynomials of degree  $k$  are denoted by  $\tilde{\mathbb{P}}_k(\mathcal{D})$  and  $\tilde{\mathbb{P}}_k(\mathcal{D})^n$ , respectively. In addition, let  $\mathbb{Q}_k(\mathcal{D})$  be the set of polynomials of degree at most  $k$  in each variable. For  $n = 2$ , let  $\mathbb{Q}_{k_1, k_2}(\mathcal{D})$  be the set of polynomials of degree  $k_1$  in the first variable and  $k_2$  in the second variable. We clearly have  $\mathbb{Q}_{k, k}(\mathcal{D}) = \mathbb{Q}_k(\mathcal{D})$ . For  $n = 3$ , the space  $\mathbb{Q}_{k_1, k_2, k_3}(\mathcal{D})$  has an analogous definition.

We first introduce the usual spaces of continuous, piecewise polynomial functions, contained in  $H^1(\Omega)$ , for  $k \geq 1$ , see [49, Sect. 3.2],

$$\begin{aligned} \mathcal{S}_h^k(\Omega) &:= \left\{ q \in H^1(\Omega); q|_K \in \mathbb{P}_k(K), \forall K \in \mathcal{T}_h \right\}, \\ \mathcal{S}_{0;h}^k(\Omega) &:= \left\{ q \in H_0^1(\Omega); q|_K \in \mathbb{P}_k(K), \forall K \in \mathcal{T}_h \right\}, \end{aligned}$$

if  $\mathcal{T}_h$  is made of triangles or tetrahedra, and

$$\begin{aligned} \mathcal{S}_h^k(\Omega) &:= \left\{ q \in H^1(\Omega); q|_K \in \mathbb{Q}_k(K), \forall K \in \mathcal{T}_h \right\}, \\ \mathcal{S}_{0;h}^k(\Omega) &:= \left\{ q \in H_0^1(\Omega); q|_K \in \mathbb{Q}_k(K), \forall K \in \mathcal{T}_h \right\}, \end{aligned}$$

if  $\mathcal{T}_h$  is made of rectangles or parallelepipeds.

The corresponding nodal interpolation operator is denoted by  $\Pi_h^{\mathcal{S}^k}$ . When there is no ambiguity, we will simply use the notations  $\mathcal{S}_h(\Omega)$ ,  $\mathcal{S}_{0;h}(\Omega)$ , and  $\Pi_h^{\mathcal{S}}$ .

We will also need some finite element spaces which are conforming only in  $L^2(\Omega)$ . For  $k \geq 1$ , see [49, Sect. 3.2],

$$\begin{aligned}\mathcal{W}_h^k(\Omega) &:= \{q \in L^2(\Omega); q|_K \in \mathbb{P}_{k-1}(K), \forall K \in \mathcal{T}_h\}, \\ \mathcal{W}_{0;h}^k(\Omega) &:= \{q \in L_0^2(\Omega); q|_K \in \mathbb{P}_{k-1}(K), \forall K \in \mathcal{T}_h\},\end{aligned}$$

if  $\mathcal{T}_h$  is made of triangles or tetrahedra, and

$$\begin{aligned}\mathcal{W}_h^k(\Omega) &:= \{q \in L^2(\Omega); q|_K \in \mathbb{Q}_{k-1}(K), \forall K \in \mathcal{T}_h\}, \\ \mathcal{W}_{0;h}^k(\Omega) &:= \{q \in L_0^2(\Omega); q|_K \in \mathbb{Q}_{k-1}(K), \forall K \in \mathcal{T}_h\},\end{aligned}$$

if  $\mathcal{T}_h$  is made of rectangles or parallelepipeds.

We will denote the  $L^2$ -projection onto the spaces  $\mathcal{W}_h^k(\Omega)$  and  $\mathcal{W}_{0;h}^k(\Omega)$  by  $\Pi_h^{\mathcal{W}^k}$  and  $\Pi_h^{\mathcal{W}_0^k}$ , respectively. As before, we will drop the superscript  $k$ , when there is no ambiguity.

### 2.2.1 Raviart–Thomas elements

The Raviart–Thomas spaces are conforming in  $H(\operatorname{div}; \Omega)$  and were originally introduced in [48] in two dimensions and then extended in [44] to the three dimensional case; see also [14, 49].

We will first consider the case of triangulations made of triangles, for  $n = 2$ , and of tetrahedra, for  $n = 3$ . Given a triangle or a tetrahedron  $K$ , we consider the polynomial space

$$\mathbb{D}_k(K) := \mathbb{P}_{k-1}(K)^n \oplus \mathbf{x} \tilde{\mathbb{P}}_{k-1}(K), \quad k \geq 1.$$

A function  $\mathbf{u}$  in  $\mathbb{D}_k(K)$  is uniquely defined by the following degrees of freedom

$$\int_f \mathbf{u} \cdot \mathbf{n} p, \quad p \in \mathbb{P}_{k-1}(f), \quad (2.27)$$

for each edge ( $n = 2$ ) or face ( $n = 3$ )  $f$  of  $K$ . For  $k > 1$ , we add

$$\int_K \mathbf{u} \cdot \mathbf{p}, \quad \mathbf{p} \in \mathbb{P}_{k-2}(K)^n.$$

It can be proven that this finite element is conforming in  $H(\operatorname{div}; \Omega)$ ; see [44, 14]. Thus, the following finite element spaces are well-defined

$$\begin{aligned}\mathcal{RT}_h^k(\Omega) &:= \{\mathbf{u} \in H(\operatorname{div}; \Omega); \mathbf{u}|_K \in \mathbb{D}_k(K), \forall K \in \mathcal{T}_h\}, \\ \mathcal{RT}_{0;h}^k(\Omega) &:= \{\mathbf{u} \in H_0(\operatorname{div}; \Omega); \mathbf{u}|_K \in \mathbb{D}_k(K), \forall K \in \mathcal{T}_h\}.\end{aligned}$$

The corresponding interpolation operator is denoted by  $\Pi_h^{\mathcal{RT}^k}$ . When there is no ambiguity, we will simply use the notations  $\mathcal{RT}_h(\Omega)$ ,  $\mathcal{RT}_{0;h}(\Omega)$ , and  $\Pi_h^{\mathcal{RT}}$ .

For the case  $k = 1$ , the elements of the local space have the simple form

$$\mathbb{D}_1(K) = \{\mathbf{u} = \mathbf{a} + b \mathbf{x}, \mathbf{a} \in \mathbb{P}_0(K)^n, b \in \mathbb{P}_0(K)\}.$$

It is immediate to check that the normal components of a vector in  $\mathbb{D}_1(K)$  are constant on each edge ( $n = 2$ ) or face ( $n = 3$ )  $f$ . These values  $\{\lambda_f(\mathbf{u}), f \subset \partial K\}$  can be taken as the degrees of freedom. As in the case of nodal elements, the  $L^2$ -norm of a vector  $\mathbf{u} \in \mathbb{D}_1(K)$  can be bounded from above and below by means of its degrees of freedom

$$c \sum_{f \subset \partial K} \left( H_f^{n/2} \lambda_f(\mathbf{u}) \right)^2 \leq \|\mathbf{u}\|_{0;K}^2 \leq C \sum_{f \subset \partial K} \left( H_f^{n/2} \lambda_f(\mathbf{u}) \right)^2, \quad (2.28)$$

where  $H_f$  is the diameter of  $f$  and the constants  $c$  and  $C$  only depend on the aspect ratio of the element  $K$ . The proof given for nodal elements in [49, Prop. 6.3.1] can easily be adapted to the present case, and similar estimates can also be obtained for the case  $k > 1$ .

We will now consider the case of triangulations made of rectangles ( $n = 2$ ) and parallelepipeds ( $n = 3$ ). The local spaces are defined as follows:

$$\begin{aligned}\mathbb{S}_k(K) &:= \mathbb{Q}_{k,k-1}(K) \times \mathbb{Q}_{k-1,k}(K), \quad n = 2, \\ \mathbb{S}_k(K) &:= \mathbb{Q}_{k,k-1,k-1}(K) \times \mathbb{Q}_{k-1,k,k-1}(K) \times \mathbb{Q}_{k-1,k-1,k}(K), \quad n = 3.\end{aligned}$$

A function  $\mathbf{u}$  in  $\mathbb{S}_k(K)$  is uniquely defined by the following degrees of freedom

$$\int_f \mathbf{u} \cdot \mathbf{n} p, \quad p \in \mathbb{Q}_{k-1}(f), \quad (2.29)$$

for each edge ( $n = 2$ ) or face ( $n = 3$ )  $f$  of  $K$ . For  $k > 1$ , we add

$$\begin{aligned}\int_K \mathbf{u} \cdot \mathbf{p}, \quad \mathbf{p} \in \mathbb{Q}_{k-2,k-1}(K) \times \mathbb{Q}_{k-1,k-2}(K), \quad n = 2, \\ \int_K \mathbf{u} \cdot \mathbf{p}, \quad \mathbf{p} \in \mathbb{Q}_{k-2,k-1,k-1}(K) \times \mathbb{Q}_{k-1,k-2,k-1}(K) \times \mathbb{Q}_{k-1,k-1,k-2}(K), \quad n = 3.\end{aligned}$$

The global spaces are defined as

$$\begin{aligned}\mathcal{RT}_h^k(\Omega) &:= \{\mathbf{u} \in H(\operatorname{div}; \Omega); \mathbf{u}|_K \in \mathbb{S}_k(K), \forall K \in \mathcal{T}_h\}, \\ \mathcal{RT}_{0;h}^k(\Omega) &:= \{\mathbf{u} \in H_0(\operatorname{div}; \Omega); \mathbf{u}|_K \in \mathbb{S}_k(K), \forall K \in \mathcal{T}_h\}.\end{aligned}$$

For the case  $k = 1$ , the local space is

$$\mathbb{S}_1(K) = \{\mathbf{u}, u_i = a_i + b_i x_i, \mathbf{a}, \mathbf{b} \in \mathbb{P}_0(K)^n\}.$$

It is easy to check the normal components of a vector in  $\mathbb{S}_1(K)$  are constant on each edge ( $n = 2$ ) or face ( $n = 3$ )  $f$ . These values  $\{\lambda_f(\mathbf{u}), f \subset \partial K\}$  can be taken as the degrees of freedom. The bounds in (2.28) are also valid for a vector  $\mathbf{u}$  in  $\mathbb{S}_1(K)$ .

For all the spaces defined in this section, the corresponding nodal interpolation operator  $\Pi_h^{\mathcal{RT}^k}$  is not defined in the whole space  $H(\operatorname{div}; \Omega)$ ; some additional regularity is required. In particular, the normal component on  $\partial K$  of a vector  $\mathbf{u} \in H(\operatorname{div}; \Omega)$  generally only belongs to  $H^{-1/2}(\partial K)$ , and the degrees of freedom (2.27) and (2.29) are not defined in general. These degrees of freedom are certainly well-defined if the trace of a vector  $\mathbf{u}$  on the boundary of a generic element is sufficiently regular, that is, if  $\mathbf{u}$  belongs to  $H^r(\Omega)^n$  for  $r > 1/2$ . The following error estimate can be proven using standard arguments as in [49, Sect. 3.4.2]

$$\|\mathbf{u} - \Pi_h^{\mathcal{RT}^k} \mathbf{u}\|_{0;\Omega} \leq Ch^r |\mathbf{u}|_{r;\Omega}, \quad \frac{1}{2} < r \leq k. \quad (2.30)$$

The constant  $C$  depends only on the aspect ratios of the elements of  $\mathcal{T}_h$  and the exponent  $r$ . See also [44] for other error estimates and [14, Sect. III.3.3] for additional comments.

### 2.2.2 Nédélec elements in two dimensions

Nédélec elements (also called *edge* elements) are finite elements which are conforming in  $H(\mathbf{curl}; \Omega)$ . Just as, in two dimensions, vectors in  $H(\mathbf{curl}; \Omega)$  are obtained from those in  $H(\operatorname{div}; \Omega)$  by a rotation of 90 degrees, Nédélec finite element vectors are obtained from those in the Raviart–Thomas spaces in the same way. However, we will see that the two families of elements are completely different in three dimensions.

In two dimensions ( $n = 2$ ), it is enough to rotate the vectors in the Raviart–Thomas spaces introduced in the previous section. In the case of triangles the local spaces are thus

$$\mathcal{R}_k(K) := \left\{ \mathbf{u} + \mathbf{v}, \mathbf{u} \in \mathbb{P}_{k-1}(K)^2, \mathbf{v} \in \tilde{\mathbb{P}}_k(K)^2, \mathbf{v} \cdot \mathbf{x} = 0 \right\}, \quad k \geq 1,$$

and a function  $\mathbf{u}$  in  $\mathcal{R}_k(K)$  is uniquely defined by the following degrees of freedom:

$$\int_e \mathbf{u} \cdot \mathbf{t}_e p, \quad p \in \mathbb{P}_{k-1}(e),$$

for each edge  $e$ , and, in addition, for  $k > 1$ ,

$$\int_K \mathbf{u} \cdot \mathbf{p}, \quad \mathbf{p} \in \mathbb{P}_{k-2}(K)^n.$$

Here  $\mathbf{t}_e$  is the unit vector that is tangent to  $e$ .

In the case  $k = 1$ , the local space  $\mathcal{R}_1(K)$  has the form

$$\mathcal{R}_1(K) = \left\{ \mathbf{u} = \begin{bmatrix} a_1 + bx_2 \\ a_2 - bx_1 \end{bmatrix}, \mathbf{a} \in \mathbb{P}_0(K)^2, b \in \mathbb{P}_0(K) \right\}.$$

It is easy to check that a vector in  $\mathcal{R}_1(K)$  has a constant tangential component on each edge of  $K$ , and the corresponding degrees of freedom  $\{\lambda_e(\mathbf{u}), e \subset \partial K\}$  can be taken as the values of the tangential component on the three edges  $e$  of  $K$ . They can be written as

$$\lambda_e(\mathbf{u}) = \frac{1}{H_e} \int_e \mathbf{n} \times \mathbf{u} ds, \quad e \subset \partial K,$$

and the degrees of freedom in the global space will be associated to the edges of the triangulation. By direct computation, the curl of a vector in  $\mathcal{R}_1(K)$  is constant.

In the case of rectangles the local spaces are defined as

$$\mathcal{Q}_k(K) := \mathbb{Q}_{k-1,k}(K) \times \mathbb{Q}_{k,k-1}(K),$$

and the corresponding degrees of freedom are

$$\int_e \mathbf{u} \cdot \mathbf{t}_e p, \quad p \in \mathbb{Q}_{k-1}(e),$$

for each edge  $e$  of  $K$ , and, in addition, for  $k > 1$ ,

$$\int_K \mathbf{u} \cdot \mathbf{p}, \quad \mathbf{p} \in \mathbb{Q}_{k-1,k-2}(K) \times \mathbb{Q}_{k-2,k-1}(K). \quad n = 2.$$

In the case  $k = 1$ , the local space  $\mathcal{Q}_k(K)$  has the form

$$\mathcal{Q}_1(K) = \left\{ \mathbf{u} = \begin{bmatrix} a_1 + b_1 x_2 \\ a_2 + b_2 x_1 \end{bmatrix}, \mathbf{a} \in \mathbb{P}_0(K)^2, \mathbf{b} \in \mathbb{P}_0(K)^2 \right\},$$

and a vector in  $\mathcal{Q}_1(K)$  has a constant tangential component on each edge of  $K$ , and the corresponding degrees of freedom  $\{\lambda_e(\mathbf{u}), e \subset \partial K\}$  can be taken as the values of the tangential component on the four edges  $e$  of  $K$ . The degrees of freedom in the global space will be associated to the edges of the triangulation and, by direct computation, the curl of a vector in  $\mathcal{Q}_1(K)$  is constant.

Given these local spaces, the global ones, conforming in  $H(\mathbf{curl}; \Omega)$  and  $H_0(\mathbf{curl}; \Omega)$ , are defined in the obvious way and are denoted by  $\mathcal{ND}_h^k(\Omega)$  and  $\mathcal{ND}_{0,h}^k(\Omega)$ , respectively, or by  $\mathcal{ND}_h(\Omega)$  and  $\mathcal{ND}_{0,h}(\Omega)$ , when there is no ambiguity. Clearly, inequalities (2.28) and (2.30) still hold for the Nédélec spaces in two dimensions.

### 2.2.3 Nédélec elements in three dimensions

We will now consider the three dimensional case,  $n = 3$ . We refer to [44, 26] as general references for this section.

For triangulations made of tetrahedra, the local spaces on a generic tetrahedron  $K$  are defined as

$$\mathcal{R}_k(K) := \left\{ \mathbf{u} + \mathbf{v}; \mathbf{u} \in \mathbb{P}_{k-1}(K)^3, \mathbf{v} \in \tilde{\mathbb{P}}_k(K)^3, \mathbf{v} \cdot \mathbf{x} = 0 \right\}, \quad k \geq 1;$$

see [26, Sect. III.5.3]. A vector in  $\mathbf{u} \in \mathcal{R}_k(K)$  is uniquely defined by the following degrees of freedom, see [44],

$$\int_e \mathbf{u} \cdot \mathbf{t}_e p, \quad p \in \mathbb{P}_{k-1}(e), \tag{2.31}$$

for the six edges  $e$  of  $K$ , and, for  $k > 1$ ,

$$\int_f (\mathbf{u} \times \mathbf{n}) \cdot \mathbf{p}, \quad \mathbf{p} \in \mathbb{P}_{k-2}(f)^2,$$

for the four faces  $f$  of  $K$ , and, additionally, for  $k > 2$ ,

$$\int_K \mathbf{u} \cdot \mathbf{p}, \quad \mathbf{p} \in \mathbb{P}_{k-3}(K)^3.$$

Here  $\mathbf{t}_e$  denotes the unit vector in the direction of the edge  $e$ . It can be proven that this finite element is conforming in  $H(\mathbf{curl}; \Omega)$ , see [44], and the following finite element spaces are therefore well-defined

$$\begin{aligned} \mathcal{ND}_h^k(\Omega) &:= \{\mathbf{u} \in H(\mathbf{curl}; \Omega); \mathbf{u}|_K \in \mathcal{R}_k(K), \forall K \in \mathcal{T}_h\}, \\ \mathcal{ND}_{0;h}^k(\Omega) &:= \{\mathbf{u} \in H_0(\mathbf{curl}; \Omega); \mathbf{u}|_K \in \mathcal{R}_k(K), \forall K \in \mathcal{T}_h\}. \end{aligned}$$

The corresponding interpolation operator is denoted by  $\Pi_h^{\mathcal{ND}^k}$ , and, as usual, we will drop the superscript  $k$ , when there is no ambiguity.

In the case  $k = 1$ , the elements of the local space  $\mathcal{R}_k(K)$  have the simple form

$$\mathcal{R}_1(K) = \{\mathbf{u} = \mathbf{a} + \mathbf{b} \times \mathbf{x}, \mathbf{a}, \mathbf{b} \in \mathbb{P}_0(K)^3\}.$$

It is immediate to see that the tangential components of a vector in  $\mathcal{R}_1(K)$  are constant on the six edges  $e$  of  $K$ . These values  $\{\lambda_e(\mathbf{u}), e \subset \partial K\}$  can be taken as the degrees of freedom. Also in this case, for  $\mathbf{u} \in \mathcal{R}_1(K)$ , by the same argument as in the proof of [49, Prop. 6.3.1], we have

$$c \sum_{e \subset \partial K} \left( H_e^{3/2} \lambda_e(\mathbf{u}) \right)^2 \leq \|\mathbf{u}\|_{0;K}^2 \leq C \sum_{e \subset \partial K} \left( H_e^{3/2} \lambda_e(\mathbf{u}) \right)^2, \quad (2.32)$$

where  $H_e$  is the length of  $e$  and the constants  $c$  and  $C$  only depend on the aspect ratio of the element  $K$ . A similar estimate can also be obtained for the case  $k > 1$ .

We will now consider triangulations made of parallelepipeds. In this case, the local spaces defined on a parallelepiped  $K$  are, see [44],

$$\mathcal{Q}_k(K) := \mathcal{Q}_{k-1,k,k}(K) \times \mathcal{Q}_{k,k-1,k}(K) \times \mathcal{Q}_{k,k,k-1}(K),$$

and the corresponding degrees of freedom are

$$\int_e \mathbf{u} \cdot \mathbf{t}_e p, \quad p \in \mathbb{P}_{k-1}(e), \quad (2.33)$$

for the twelve edges  $e$  of  $K$ , and, for  $k > 1$ ,

$$\int_f (\mathbf{u} \times \mathbf{n}) \cdot \mathbf{p}, \quad \mathbf{p} \in \mathcal{Q}_{k-2,k-1}(f) \times \mathcal{Q}_{k-1,k-2}(f),$$

for the six faces  $f$  of  $K$ , and

$$\int_K \mathbf{u} \cdot \mathbf{p}, \quad \mathbf{p} \in \mathbb{Q}_{k-1,k-2,k-2}(K) \times \mathbb{Q}_{k-2,k-1,k-2}(K) \times \mathbb{Q}_{k-2,k-2,k-1}(K).$$

The global spaces  $\mathcal{ND}_h^k(\Omega)$  and  $\mathcal{ND}_{0,h}^k(\Omega)$ , which are conforming in  $H(\mathbf{curl}; \Omega)$  and  $H_0(\mathbf{curl}; \Omega)$ , respectively, are defined in the obvious way.

The interpolation operator on the space  $\mathcal{ND}_h^k(\Omega)$  is not defined in the whole space  $H(\mathbf{curl}; \Omega)$ ; additional regularity is required. Different choices, and consequently different error estimates, are possible; see [44, 26, 42, 3, 4, 7]. Here, we only remark that the interpolant  $\Pi_h^{\mathcal{ND}^k} \mathbf{u}$  is not defined for a generic vector  $\mathbf{u}$  in  $H^r(\Omega)^3$  for  $1/2 < r \leq 1$ , as it was the case for the Raviart–Thomas spaces, since the degrees of freedom (2.31) and (2.33) involve the tangential component of  $\mathbf{u}$  on the edges, which is not necessarily defined. If we require that  $\mathbf{u} \in H^r(\Omega)^3$  for  $r > 1$ , then the trace of  $\mathbf{u}$  is defined on the edges. The following error estimate can then be proven using standard arguments as in [49, Sect. 3.4.2]

$$\left\| \mathbf{u} - \Pi_h^{\mathcal{ND}^k} \mathbf{u} \right\|_{0;\Omega} \leq Ch^r |\mathbf{u}|_{r;\Omega}, \quad 1 < r \leq k, \quad k > 1, \quad (2.34)$$

where the constant  $C$  depends only on the aspect ratios of the elements of  $\mathcal{T}_h$  and the exponent  $r$ . We note that (2.34) is only valid for  $k > 1$ , since the local spaces  $\mathcal{R}_1(K)$  and  $\mathcal{Q}_1(K)$  do not contain the whole space  $\mathbb{P}_1(K)^3$  and that  $\mathbf{u}$  must be in  $H^r(\Omega)^3$  for  $r > 1$ ; see [49, Sect. 3.4].

## 2.2.4 The kernel and range of the curl and divergence operators

We now suppose that the domain  $\Omega$  is a simply connected polygon or polyhedron, with a connected boundary. In Section 2.1.4, we have seen that the range of the divergence operator in  $H(\text{div}; \Omega)$  is  $L^2(\Omega)$  and the kernel of the curl operator in  $H(\mathbf{curl}; \Omega)$  is the space  $\mathbf{grad} H^1(\Omega)$ . In two dimensions, the kernel of the divergence operator is  $\mathbf{curl} H^1(\Omega)$ , and in three dimensions it coincides with  $\mathbf{curl} H(\mathbf{curl}; \Omega)$ . Similar properties hold for the spaces of functions satisfying homogeneous boundary conditions.

In this section, we will state analogous properties for the finite element spaces previously introduced. These results are well-known and can, for instance, be



found in [26, 20, 10, 14, 29, 4]. In particular, we refer to [29] for the proofs of the results in this section. The case when  $\Omega$  is not simply connected or its boundary is not connected, is treated in [4] and does not present any particular difficulties.

The following lemma is well-known and is often referred to as commuting-diagram property; a rigorous proof can be found in [29, Th. 2.30].

**Proposition 2.2.1** *Let  $\mathcal{T}_h$  be shape-regular and the functions  $q$ ,  $\mathbf{u}$ ,  $\mathbf{v}$  sufficiently regular. Then, the following identities hold*

$$\mathbf{grad} \left( \Pi_h^{\mathcal{S}^k} q \right) = \Pi_h^{\mathcal{N}\mathcal{D}^k} \left( \mathbf{grad} q \right), \quad (2.35)$$

$$\mathbf{curl} \left( \Pi_h^{\mathcal{N}\mathcal{D}^k} \mathbf{u} \right) = \Pi_h^{\mathcal{W}^k} \left( \mathbf{curl} \mathbf{u} \right), \quad n = 2, \quad (2.36)$$

$$\mathbf{curl} \left( \Pi_h^{\mathcal{S}^k} q \right) = \Pi_h^{\mathcal{R}\mathcal{T}^k} \left( \mathbf{curl} q \right), \quad n = 2, \quad (2.37)$$

$$\mathbf{curl} \left( \Pi_h^{\mathcal{N}\mathcal{D}^k} \mathbf{u} \right) = \Pi_h^{\mathcal{R}\mathcal{T}^k} \left( \mathbf{curl} \mathbf{u} \right), \quad n = 3, \quad (2.38)$$

$$\mathbf{div} \left( \Pi_h^{\mathcal{R}\mathcal{T}^k} \mathbf{v} \right) = \Pi_h^{\mathcal{W}^k} \left( \mathbf{div} \mathbf{v} \right). \quad (2.39)$$

We remark that Proposition 2.2.1 is proved by local arguments on each element of  $\mathcal{T}_h$ , and the result is thus valid for an arbitrary Lipschitz domain. Proposition 2.2.1 implies that the interpolants of the finite element spaces, that we have introduced, preserve the kernel of the relevant operators. An analogous result is valid for the spaces that satisfy homogeneous boundary conditions.

The following Proposition characterizes the kernel of the curl operator; see [29, Th. 2.36] for a proof.

**Proposition 2.2.2** *If  $\Omega$  is simply connected, with a connected boundary, the kernels of the curl operator defined in  $\mathcal{N}\mathcal{D}_h^k(\Omega)$  and  $\mathcal{N}\mathcal{D}_{0;h}^k(\Omega)$  are  $\mathbf{grad} \mathcal{S}_h^k(\Omega)$  and  $\mathbf{grad} \mathcal{S}_{0;h}^k(\Omega)$ , respectively.*

We can now define the following decompositions of the Nédélec spaces into the kernel of the curl operator and its orthogonal complement:

$$\mathcal{N}\mathcal{D}_h^k(\Omega) = \mathbf{grad} \mathcal{S}_h^k(\Omega) \oplus \mathcal{N}\mathcal{D}_h^{k;\perp}(\Omega), \quad (2.40)$$

$$\mathcal{N}\mathcal{D}_{0;h}^k(\Omega) = \mathbf{grad} \mathcal{S}_{0;h}^k(\Omega) \oplus \mathcal{N}\mathcal{D}_{0;h}^{k;\perp}(\Omega). \quad (2.41)$$

These decompositions are the discrete analogs of (2.12) and (2.11). We note that, in general, the spaces  $\mathcal{ND}_h^{k;\perp}(\Omega)$  and  $\mathcal{ND}_{0;h}^{k;\perp}(\Omega)$  are not included in  $H^\perp(\mathbf{curl}; \Omega)$  and  $H_0^\perp(\mathbf{curl}; \Omega)$ .

The following Proposition states the analog of (2.15), (2.16), (2.19), and (2.20). Its proof can be found in [26, Ch. III, Prop. 5.1].

**Proposition 2.2.3** *Let  $\Omega$  be convex and  $\mathcal{T}_h$  quasi-uniform. Then, for  $n = 2$ ,*

$$\|\mathbf{u}\|_{0;\Omega} \leq C H_\Omega \|\mathbf{curl} \mathbf{u}\|_{0;\Omega}, \quad \mathbf{u} \in \mathcal{ND}_h^{k;\perp}(\Omega) \cup \mathcal{ND}_{0;h}^{k;\perp}(\Omega), \quad (2.42)$$

and, for  $n = 3$ ,

$$\|\mathbf{u}\|_{0;\Omega} \leq C H_\Omega \|\mathbf{curl} \mathbf{u}\|_{0;\Omega}, \quad \mathbf{u} \in \mathcal{ND}_h^{k;\perp}(\Omega) \cup \mathcal{ND}_{0;h}^{k;\perp}(\Omega). \quad (2.43)$$

We remark that, if  $\Omega$  is only simply connected or  $\mathcal{T}_h$  is not quasi-uniform, (2.42) and (2.43) remain valid, but the constants may depend on  $h$ .

We now consider the characterization of the kernel of the divergence operator. For the two-dimensional case, we can use the results for  $H(\mathbf{curl}; \Omega)$  and prove results analogous to Propositions 2.2.2. In particular, the kernels of the divergence operator defined in  $\mathcal{RT}_h^k(\Omega)$  and  $\mathcal{RT}_{0;h}^k(\Omega)$  are  $\mathbf{curl} \mathcal{S}_h^k(\Omega)$  and  $\mathbf{curl} \mathcal{S}_{0;h}^k(\Omega)$  and the following decompositions hold

$$\mathcal{RT}_h^k(\Omega) = \mathbf{curl} \mathcal{S}_h^k(\Omega) \oplus \mathcal{RT}_h^{k;\perp}(\Omega), \quad (2.44)$$

$$\mathcal{RT}_{0;h}^k(\Omega) = \mathbf{curl} \mathcal{S}_{0;h}^k(\Omega) \oplus \mathcal{RT}_{0;h}^{k;\perp}(\Omega). \quad (2.45)$$

For the three-dimensional case, the following result can be found in [29, Th. 2.36].

**Proposition 2.2.4** *If  $\Omega \subset \mathbb{R}^3$  is simply connected, with a connected boundary, the kernels of the divergence operator defined in  $\mathcal{RT}_h^k(\Omega)$  and  $\mathcal{RT}_{0;h}^k(\Omega)$  are  $\mathbf{curl} \mathcal{ND}_h^k(\Omega)$  and  $\mathbf{curl} \mathcal{ND}_{0;h}^k(\Omega)$ .*

We can now define the following decompositions of the Raviart–Thomas spaces into the kernel of the divergence operator and its orthogonal complement, for  $n = 3$ ,

$$\mathcal{RT}_h^k(\Omega) = \mathbf{curl} \mathcal{ND}_h^k(\Omega) \oplus \mathcal{RT}_h^{k;\perp}(\Omega), \quad (2.46)$$

$$\mathcal{RT}_{0;h}^k(\Omega) = \mathbf{curl} \mathcal{ND}_{0;h}^k(\Omega) \oplus \mathcal{RT}_{0;h}^{k;\perp}(\Omega). \quad (2.47)$$

These decompositions are the discrete analogs of (2.7) and (2.8).

We end this section with a characterization of the range of the divergence operator; see [29, Th. 2.36].

**Proposition 2.2.5** *The divergence operator is surjective from  $\mathcal{RT}_h^k(\Omega)$  into  $\mathcal{W}_h^k(\Omega)$ , and from  $\mathcal{RT}_{0;h}^k(\Omega)$  into  $\mathcal{W}_{0;h}^k(\Omega)$ .*

## 2.3 Schwarz methods

In this section, we will recall some standard results on Schwarz methods. We refer to [23, 54, 61, 50] and to the references therein for an introduction to Schwarz methods.

Let  $V$  be a finite dimensional space and let  $a(\cdot, \cdot)$  be a symmetric coercive bilinear form on  $V$ . We consider the the following problem: Find  $u \in V$ , such that

$$a(u, v) = F(v) \quad \forall v \in V, \quad (2.48)$$

where  $F(\cdot)$  is a linear functional defined on  $V$ .

A Schwarz preconditioner for the solution of (2.48) is built from the inverses of suitable operators defined on a set of subspaces.

Suppose that the space  $V$  admits the decomposition

$$V = \sum_{i=0}^J V_i,$$

and that  $J + 1$  symmetric positive-definite bilinear forms

$$\tilde{a}_i(u, v), \quad u, v \in V_i,$$

are defined on the subspaces. Let us now define the following operators for  $i = 0, \dots, J$ :

$$Q_i : V \longrightarrow V_i \subset V, \quad (2.49)$$

$$\tilde{a}_i(Q_i u, v) = a(u, v), \quad \forall v \in V_i, \quad (2.50)$$

and the additive Schwarz operator

$$Q_{ad} := \sum_{j=0}^J Q_j : V \longrightarrow V. \quad (2.51)$$

An additive Schwarz method provides the new equation

$$Q_{ad} u = g,$$

which can be much better conditioned than the original problem given by (2.48); it can be solved effectively with the conjugate gradient method, without any further

preconditioner, employing  $a(\cdot, \cdot)$  as the inner product. The right hand side  $g$  can be chosen so that the new problem has the same solution as the original one. Iterative multiplicative schemes can also be designed. The error  $e_{n+1}$  at the  $(n+1)$ -th step satisfies the equation

$$e_{n+1} = E_{mu} e_n := (I - Q_J) \cdots (I - Q_0) e_n, \quad n \geq 0, \quad (2.52)$$

and the multiplicative Schwarz operator is defined by

$$Q_{mu} := I - E_{mu}.$$

The three following fundamental lemmas state the convergence properties of the additive and multiplicative algorithms. We refer to [23, 54] for proofs and additional comments.

**Lemma 2.3.1** *Let  $Q_i$  and  $Q_{ad}$  be defined by (2.49), (2.50), and (2.51). We have*

$$a(Q_{ad}^{-1}u, u) = \inf_{u = \sum u_i} \sum_{i=0}^J \tilde{a}_i(u_i, u_i). \quad (2.53)$$

*Equivalently, if a representation,  $u = \sum u_i$ , can be found, such that*

$$\sum_{i=0}^J \tilde{a}_i(u_i, u_i) \leq C_0^2 a(u, u) \quad \forall u \in V, \quad (2.54)$$

*then*

$$a(Q_{ad}u, u) \geq C_0^{-2} a(u, u) \quad \forall u \in V. \quad (2.55)$$

**Lemma 2.3.2** *Let  $\|\cdot\|_a$  be the norm induced by  $a(\cdot, \cdot)$  and let  $\omega$  be a constant such that*

$$a(u_i, u_i) \leq \omega \tilde{a}_i(u_i, u_i), \quad u_i \in V_i, \quad i = 0, \dots, J. \quad (2.56)$$

*Then*

$$\|Q_i\|_a := \sup_{u \in V} \frac{\|Q_i u\|_a}{\|u\|_a} \leq \omega. \quad (2.57)$$

*If, in addition,  $\omega \in [0, 2)$  and  $\mathcal{E} = \{\varepsilon_{ij}\}$  are the smallest constants for which*

$$|a(u_i, u_j)| \leq \varepsilon_{ij} \|u_i\|_a \|u_j\|_a \quad \forall u_i \in V_i \quad \forall u_j \in V_j, \quad i, j \geq 1, \quad (2.58)$$

*holds, then*

$$a(Q_{ad}u, u) \leq C_1 a(u, u), \quad u \in V, \quad (2.59)$$

*where  $C_1 = \omega(\varrho(\mathcal{E}) + 1)$ , with  $\varrho(\mathcal{E})$  the spectral radius of  $\mathcal{E}$ .*

**Lemma 2.3.3** *Assume that Lemma 2.3.1 and 2.3.2 hold. Then,*

a) *the condition number  $\kappa(Q_{ad})$  of the operator  $Q_{ad}$  of the additive Schwarz method satisfies*

$$\kappa(Q_{ad}) \leq \omega(\varrho(\mathcal{E}) + 1)C_0^2; \quad (2.60)$$

b) *the norm of the error operator of the multiplicative Schwarz method,  $E_{mu}$ , satisfies*

$$\|E_{mu}\|_a \leq \sqrt{1 - \frac{2 - \hat{\omega}}{(2\hat{\omega}^2\varrho(\mathcal{E})^2 + 1)C_0^2}}, \quad (2.61)$$

where  $\hat{\omega} := \max\{1, \omega\}$ .

We will also consider a particular hybrid algorithm in Chapter 5. This algorithm will be multiplicative with respect to the levels and additive with respect to the local solvers. We will be able to analyze it using only Lemmas 2.3.1 and 2.3.2.

We will now give the expressions of the matrix representations of the local operators  $\{Q_i\}$ . It will then be clear that the additive Schwarz operator is the product the original matrix and a suitable preconditioner. A similar expression can be found for the multiplicative method.

Introduce a specific set of basis functions for  $V$  and its subspaces  $\{V_i\}$ . Let  $A$  and  $A_i$  be the stiffness matrices of the bilinear forms  $a(\cdot, \cdot)$  and  $\tilde{a}_i(\cdot, \cdot)$  on  $V$  and  $V_i$ , respectively, with respect to these bases. By identifying  $V$  and  $V_i$  with the sets of degrees of freedom relative to the bases introduced, we can write, with an abuse of notation,

$$A : V \rightarrow V; \quad A_i : V_i \rightarrow V_i, \quad i = 0, \dots, J,$$

and (2.48) gives rise to the following linear system in  $V$

$$Au = f.$$

We define the extension operators

$$R_i^T : V_i \longrightarrow V, \quad i = 0, \dots, J,$$

as the natural extensions from the local to the global spaces, mapping the degrees in  $V_i$  into the corresponding degrees of freedom in  $V$ . Here, the transpose operator

is taken with respect to the Euclidean inner product. If  $V$  is a finite element space defined on a triangulation of a domain  $\Omega$ , the local spaces  $\{V_i, i = 1, \dots, J\}$  are often taken as finite element spaces defined on smaller subdomains  $\{\Omega_i \subset \Omega\}$ . The extensions  $\{R_i^T\}$  then map the local degrees of freedom into the corresponding global ones. If a two-level method is considered a coarse space  $V_0$  has to be introduced. A possible choice for  $V_0$  is a finite element space defined on a coarse triangulation, such that the fine mesh is a refinement of the coarse one. The extension  $R_0^T$  is then the natural operator that maps the degrees of freedom of the coarse space into the ones of the fine space.

Due to (2.49) and (2.50), it is immediate that the operators  $Q_i$  has the following representation, still denoted by  $Q_i$ ,

$$\begin{aligned} Q_i &: V \longrightarrow V, \\ Q_i &= (R_i^T A_i^{-1} R_i) A, \end{aligned}$$

and that the additive operator  $Q_{ad}$  can be written as

$$\begin{aligned} Q_{ad} &: V \longrightarrow V, \\ Q_{ad} &= \sum_{i=0}^J Q_i = \sum_{i=0}^J (R_i^T A_i^{-1} R_i) A. \end{aligned}$$

It is then clear that the additive preconditioner is

$$B_{ad} := \sum_{i=0}^J R_i^T A_i^{-1} R_i.$$

## Chapter 3

# Overlapping Methods for Nédélec elements

In this chapter, we will describe and analyze a two-level overlapping method for the Nédélec approximation of problems involving the bilinear form

$$a(\mathbf{u}, \mathbf{v}) := \eta_1 \int_{\Omega} \mathbf{u} \cdot \mathbf{v} + \eta_2 \int_{\Omega} \mathbf{curl} \mathbf{u} \cdot \mathbf{curl} \mathbf{v}, \quad \mathbf{u}, \mathbf{v} \in H(\mathbf{curl}; \Omega),$$

where  $\Omega$  is a bounded Lipschitz polyhedron in three dimensions and  $\eta_1$  and  $\eta_2$  are positive quantities. We will prove that the condition number of the corresponding preconditioned system is bounded independently of the number of unknowns and the number of subdomains. This bound grows quadratically with the relative overlap and linearly with the ratio  $\eta_1/\eta_2$ . We will also prove that, in the limit case  $\eta_2 = 0$ , the condition number remains bounded independently of the relative overlap, and we will present some numerical results, which suggest that the condition number grows only linearly with the relative overlap and is independent of possibly large ratios of the coefficients. When Dirichlet conditions are considered, we require that the domain  $\Omega$  be convex. Our result can easily be generalized to treat the case of variable coefficients.

In the following, we will always assume that  $\Omega$  is convex, but in Section 3.5, we will show that this restriction is not needed when Neumann conditions are employed.

Our analysis of overlapping methods is inspired by [6], where a Schwarz method for a conforming finite element problem in  $H(\mathbf{div}; \Omega)$  in two dimensions is studied.



Their result is also valid for  $H(\mathbf{curl}; \Omega)$  in two dimensions; see [55]. In addition, we will also use technical tools and results originally developed in [29], where a multigrid method is studied for a Raviart–Thomas finite element approximation in three dimensions. We note that we prove a regularity property that will enable us to extend the tools in [29] and [32] to a general convex polyhedron; see Theorem 2.1.1. We also note that the results in this chapter were first presented in [56]. The author and Hiptmair have then extended them to the case of  $H(\operatorname{div}; \Omega)$  and have improved some bounds in [33].

We will carry out our analysis for tetrahedral meshes but our results are equally valid for meshes built on parallelepipeds. In addition, we will only consider a Schwarz additive preconditioner in full detail. Multiplicative and hybrid operators can also be considered and Krylov subspace methods different than conjugate gradient, such as GMRES, can also be employed as accelerators. The extension of our analysis to other Schwarz methods is completely routine; see [54] for a more detailed discussion. We also remark that we will only consider the case when the problems defined on the subspaces are solved exactly. The extension to the case when inexact solvers are employed can be carried out by using Lemma 2.3.2; see [54, Assumption 3].

### 3.1 Finite element spaces and discrete problem

Let

$$\mathcal{T}_H = \{\Omega_i, i = 1, \dots, J\},$$

be a triangulation of  $\Omega$ , of maximum diameter  $H$ , consisting of tetrahedra and let  $\mathcal{T}_h$  be a refinement of  $\mathcal{T}_H$ , with characteristic diameter  $h$ . We suppose that  $\mathcal{T}_H$  and  $\mathcal{T}_h$  are shape-regular and quasi-uniform. For  $k \geq 1$ , we define the fine and coarse spaces

$$\begin{aligned} V^k &= V := \mathcal{N}\mathcal{D}_{0,h}^k(\Omega), \\ V_0^k &= V_0 := \mathcal{N}\mathcal{D}_{0,H}^k(\Omega), \end{aligned}$$

conforming in  $H_0(\mathbf{curl}; \Omega)$ ; see Section 2.2.3. We remark that, in this chapter, we will use the subscript 0 for quantities related to the coarse triangulation.

We will also need the finite element spaces  $\mathcal{S}_{0;h}^k(\Omega)$  and  $\mathcal{S}_{0;H}^k(\Omega)$ , contained in  $H_0^1(\Omega)$ , defined in Section 2.2, and define

$$\begin{aligned} Z^k &= Z := \mathbf{grad} \mathcal{S}_{0;h}^k(\Omega), \\ Z_0^k &= Z_0 := \mathbf{grad} \mathcal{S}_{0;H}^k(\Omega). \end{aligned}$$

The kernel of the curl operator has already been studied in Section 2.2.4. Here, we remark that, since  $\Omega$  is convex, Proposition 2.2.2 holds and  $Z$  and  $Z_0$  are the kernels of the curl operator defined on  $V$  and  $V_0$ , respectively. If we set

$$\begin{aligned} Z^{\perp,k} &= Z^\perp := \mathcal{N}\mathcal{D}_{0;h}^{k;\perp}(\Omega), \\ Z_0^{\perp,k} &= Z_0^\perp := \mathcal{N}\mathcal{D}_{0;H}^{k;\perp}(\Omega), \end{aligned}$$

we have the following orthogonal decompositions

$$V^k = Z^k \oplus Z^{\perp,k}, \tag{3.1}$$

$$V_0^k = Z_0^k \oplus Z_0^{\perp,k}; \tag{3.2}$$

see (2.41).

## 3.2 Description of the algorithm

We will consider the following problem:

Find  $\mathbf{u} \in V^k$  such that

$$a(\mathbf{u}, \mathbf{v}) = (\mathbf{f}, \mathbf{v}) \quad \forall \mathbf{v} \in V^k, \tag{3.3}$$

where  $\mathbf{f} \in L^2(\Omega)^3$ . The case of  $\mathcal{N}\mathcal{D}_h^k(\Omega)$  (Neumann boundary conditions) is treated in Section 3.5.

Let us consider a covering  $\{\Omega'_i, i = 1, \dots, J\}$  of  $\Omega$ , such that each subregion  $\Omega'_i$  is the union of fine tetrahedra of  $\mathcal{T}_h$ , and contains  $\Omega_i$ . Define the overlapping parameter  $\delta$  as

$$\delta := \min_{i=1, \dots, J} \{\text{dist}(\partial\Omega'_i, \Omega_i)\}.$$

We will assume that the following property holds (finite covering): see [54, Sect 1.3.1].

**Assumption 3.2.1** *The overlapping subregions  $\{\Omega'_i\}$  can be colored using  $N_c$  colors, in such a way that regions with the same color do not intersect.*

We note that more general partitions are possible and that the non overlapping subregions  $\{\Omega_i\}$  do not need to be related to the coarse elements in  $\mathcal{T}_H$ . Our results remain equally valid for this more general case and we can then interpret the ratio that appears in our bounds as

$$\frac{H}{\delta} = \frac{\max_{K \in \mathcal{T}_H} \{H_K\}}{\min_{i=1, \dots, J} \{\text{dist}(\partial\Omega'_i, \Omega_i)\}}.$$

Consequently, our preconditioner will be effective if the diameter of the subregions  $\{\Omega_i\}$  is comparable to the diameter of  $\mathcal{T}_H$ .

In order to define a Schwarz algorithm, we have to define a family of subspaces and some bilinear forms defined on them. For  $i = 1, \dots, J$ , we define the subspaces  $V_i \subset V$ , by setting the degrees of freedom outside  $\Omega'_i$  to zero,

$$V_i^k = V_i := V^k \cap H_0(\mathbf{curl}; \Omega'_i), \quad i = 1, \dots, J.$$

The space  $V$  then admits the following decomposition

$$V = V_0 + \sum_{i=1}^J V_i. \tag{3.4}$$

We will employ the original bilinear form  $a(\cdot, \cdot)$  on both the coarse space and the local spaces. The effect of approximate solvers can be dealt with in a standard way, using Lemma 2.3.2. The coarse and local operators  $Q_i$  are now defined by (2.49) and (2.50), using  $\tilde{a}_i(\cdot, \cdot) = a(\cdot, \cdot)$ , and the additive Schwarz operator  $Q_{ad}$  is defined by (2.51).

## 3.3 Technical tools

### 3.3.1 Some operators

In this section, we will introduce some projections; see [29, Ch. 5].

As already noted in Section 2.2.4, the decompositions given in (3.1) and (3.2) are discrete analogs of (2.12). But, while the following inclusions hold

$$\begin{aligned} V_0 &\subset V \subset H_0(\mathbf{curl}; \Omega), \\ Z_0 &\subset Z \subset \mathbf{grad} H_0^1(\Omega), \end{aligned}$$

the space  $Z_0^\perp$  is not contained in  $Z^\perp$ , and neither of them is contained in  $H_0^\perp(\mathbf{curl}; \Omega)$ . This fact makes the analysis of multilevel methods for  $H(\mathbf{curl}; \Omega)$ -conforming elements particularly cumbersome. In order to obtain suitable projections onto  $Z_0^\perp$  and  $Z^\perp$ , Hiptmair [29] has introduced auxiliary subspaces, defined by an orthogonal projection onto  $H_0^\perp(\mathbf{curl}; \Omega)$ :

$$\Theta : H_0(\mathbf{curl}; \Omega) \longrightarrow H_0^\perp(\mathbf{curl}; \Omega).$$

In particular,  $\Theta \mathbf{u}$  is defined by

$$\Theta \mathbf{u} := \mathbf{u} - \mathbf{grad} q,$$

where  $q \in H_0^1(\Omega)$  satisfies

$$(\mathbf{grad} q, \mathbf{grad} p) = (\mathbf{u}, \mathbf{grad} p), \quad \forall p \in H_0^1(\Omega).$$

It is readily seen that  $\Theta$  preserves the curl and is an orthogonal projection in  $L^2(\Omega)^3$  as well. We now define  $\vartheta_0$  and  $\vartheta$  as the restrictions of  $\Theta$  to  $Z_0^\perp$  and  $Z^\perp$ , respectively, and the following spaces:

$$\begin{aligned} Z_0^+ &:= \vartheta_0(Z_0^\perp) = \Theta(Z_0^\perp), \\ Z^+ &:= \vartheta(Z^\perp) = \Theta(Z^\perp). \end{aligned}$$

We note that we use different notations than those in [29]. The spaces  $Z_0^+$  and  $Z^+$  are finite dimensional. They are not finite element spaces, but the curls of these functions are finite element functions. It can be proven that  $Z_0^+$  is contained in  $Z^+$ , and that they are both contained in  $H_0^\perp(\mathbf{curl}; \Omega)$ . Moreover the operators

$$\begin{aligned} \vartheta_0 &: Z_0^\perp \longrightarrow Z_0^+, \\ \vartheta &: Z^\perp \longrightarrow Z^+, \end{aligned}$$

are isomorphisms. Their inverses satisfy the following  $L^2$ -bounds; see [29, Lemma 5.15].

**Lemma 3.3.1** *Let  $k \geq 2$  and suppose that  $\Omega$  is convex and that the triangulations  $\mathcal{T}_H$  and  $\mathcal{T}_h$  are shape regular and quasi-uniform. Then, there exists a constant  $C$ , depending only on  $k$  and  $\Omega$ , such that*

$$\|\mathbf{v}\| \leq C (\|\vartheta_0(\mathbf{v})\| + H \|\mathbf{curl} \mathbf{v}\|), \quad \mathbf{v} \in Z_0^{\perp,k}, \quad (3.5)$$

$$\|\mathbf{v}\| \leq C (\|\vartheta(\mathbf{v})\| + h \|\mathbf{curl} \mathbf{v}\|), \quad \mathbf{v} \in Z^{\perp,k}. \quad (3.6)$$

*Proof.* We will only prove (3.5). The proof of (3.6) can be carried out in exactly the same way.

Consider  $\mathbf{v} \in Z_0^{\perp,k}$ . Since  $\mathbf{curl}(\vartheta_0 \mathbf{v}) = \mathbf{curl} \mathbf{v} \in H^t(\Omega)$ ,  $t < \frac{1}{2}$ , Theorem 2.1.1 and (2.13) ensure that  $\vartheta_0 \mathbf{v} \in H^{1+t}(\Omega)$ , for  $t < s_\Omega$ . Moreover,

$$\|\vartheta_0 \mathbf{v}\|_{1+t;\Omega} \leq C \|\mathbf{curl}(\vartheta_0 \mathbf{v})\|_{t;\Omega}.$$

The vector  $\Pi_H^{\mathcal{N}\mathcal{D}^k}(\vartheta_0 \mathbf{v})$  is thus well-defined; it has already been defined in Section 2.2.3. Using (2.34), the triangle inequality, and an inverse estimate, we can prove

$$\begin{aligned} \left\| \Pi_H^{\mathcal{N}\mathcal{D}^k}(\vartheta_0 \mathbf{v}) \right\| &\leq C \left( \|\vartheta_0 \mathbf{v}\| + H^{1+t} \|\mathbf{curl}(\vartheta_0 \mathbf{v})\|_{t;\Omega} \right) \\ &\leq C (\|\vartheta_0 \mathbf{v}\| + H \|\mathbf{curl}(\vartheta_0 \mathbf{v})\|). \end{aligned} \quad (3.7)$$

In order to find a bound for  $\mathbf{v}$ , we remark that, since  $\partial\Omega$  is connected and since

$$\mathbf{curl}(\mathbf{v} - \vartheta_0 \mathbf{v}) = 0,$$

Proposition 2.1.2 ensures that there exists a function  $q \in H_0^1(\Omega)$ , such that  $\mathbf{v} - \vartheta_0 \mathbf{v} = \mathbf{grad} q$ . Employing (2.35), we obtain

$$\mathbf{v} - \Pi_H^{\mathcal{N}\mathcal{D}^k}(\vartheta_0 \mathbf{v}) = \Pi_H^{\mathcal{N}\mathcal{D}^k}(\mathbf{grad} q) = \mathbf{grad} \left( \Pi_H^{\mathcal{N}\mathcal{D}^k} q \right) := \mathbf{grad} p,$$

where  $p \in \mathcal{S}_{0;h}^k(\Omega)$ . We then obtain

$$\begin{aligned} \|\mathbf{v}\|^2 &= \left( \mathbf{v}, \Pi_H^{\mathcal{N}\mathcal{D}^k}(\vartheta_0 \mathbf{v}) + \mathbf{grad} p \right) \\ &= \left( \mathbf{v}, \Pi_H^{\mathcal{N}\mathcal{D}^k}(\vartheta_0 \mathbf{v}) \right) \leq \|\mathbf{v}\| \left\| \Pi_H^{\mathcal{N}\mathcal{D}^k}(\vartheta_0 \mathbf{v}) \right\|. \end{aligned} \quad (3.8)$$

Inequality (3.5) follows by combining (3.7) and (3.8).  $\square$

**Remark 3.3.1** *Lemma 3.3.1 is the main result of this section. The proof given here is the same as in [29, Lemma 5.15] for a cube, but Theorem 2.1.1 allows us to extend that to the case of a general convex polyhedron. We remark that a quasi-uniform mesh is required, since an inverse estimate is used.*

We end this section, by introducing a projection onto the coarse space  $Z_0^+$ . We recall that, because of (2.20), the  $L^2$ -norm of the curl is an equivalent norm in  $Z_0^+ \subset H_0^\perp(\mathbf{curl}; \Omega)$ . Define  $P_0$  by

$$P_0 : H_0^\perp(\mathbf{curl}; \Omega) \longrightarrow Z_0^+, \quad (3.9)$$

$$(\mathbf{curl}(P_0 \mathbf{v}), \mathbf{curl} \mathbf{w}) = (\mathbf{curl} \mathbf{v}, \mathbf{curl} \mathbf{w}), \quad \mathbf{w} \in Z_0^+. \quad (3.10)$$

The operator  $P_0$  is well defined, by the Lax-Milgram lemma, and it does not increase the  $L^2$ -norm of the curl. It satisfies an error estimate given in the following lemma.

**Lemma 3.3.2** *Let  $k \geq 1$  and let  $\Omega$  be a convex polyhedron. Then,*

$$\|(I - P_0)\mathbf{v}\| \leq C H \|\mathbf{curl} \mathbf{v}\|, \quad \mathbf{v} \in H_0^\perp(\mathbf{curl}; \Omega),$$

with  $C$  independent of  $h$ ,  $H$ , and  $\mathbf{v}$ .

*Proof.* The proof is the same as the one of [29, Lemma 5.19]. We remark that it requires a regularity result that is only valid for convex polyhedra.  $\square$

### 3.3.2 A partition of unity

We now consider the covering  $\{\Omega'_i, i = 1, \dots, J\}$ . A partition of unity  $\{\tilde{\chi}_i, i = 1, \dots, J\}$ , relative to the family  $\{\Omega'_i\}$ , is a set of continuous functions, satisfying the following properties,

$$\text{supp}(\tilde{\chi}_i) \subset \Omega'_i, \quad 0 \leq \tilde{\chi}_i \leq 1, \quad \sum_{i=1}^J \tilde{\chi}_i = 1. \quad (3.11)$$

Let now  $\{\chi_i\}$  be the functions obtained from  $\{\tilde{\chi}_i\}$ , by interpolating into the finite element space  $\mathcal{S}_h^1(\Omega)$  of piecewise, linear continuous functions on  $\mathcal{T}_h$ ; by the linearity of the interpolation operator, they also satisfy the same properties (3.11).

Moreover, we have

$$\|\mathbf{grad} \chi_i\|_{L^\infty(\Omega)} \leq C \delta^{-1}, \quad i = 1, \dots, J. \quad (3.12)$$

The following lemma holds; see [23, Lemma 3.2], for a similar result for nodal elements.

**Lemma 3.3.3** *Let  $\mathbf{v} \in V = V^k$  and let  $\{\chi_i, i = 1, \dots, J\}$  be a piecewise linear partition of unity relative to  $\{\Omega'_i\}$ . The following inequalities hold,*

$$\|\Pi_h^{\mathcal{N}^{\mathcal{D}^k}}(\chi_i \mathbf{v})\| \leq C \|\chi_i \mathbf{v}\|, \quad i = 1, \dots, J, \quad (3.13)$$

$$\|\mathbf{curl} \left( \Pi_h^{\mathcal{N}^{\mathcal{D}^k}}(\chi_i \mathbf{v}) \right)\| \leq C \|\mathbf{curl}(\chi_i \mathbf{v})\|, \quad i = 1, \dots, J, \quad (3.14)$$

with constants  $C$  independent of  $\mathbf{v}$ ,  $i$ ,  $h$ , and  $H$ .

*Proof.* We recall that the degrees of freedom in  $V^k$  involve integrals of the tangential components over the edges and the faces, as well as moments of  $\mathbf{v}$  computed over each tetrahedron in  $\mathcal{T}_h$ ; see Section 2.2.3.

Let us first consider (3.13). The vector  $\mathbf{v}$  has continuous tangential component across the edges and faces of the tetrahedra; since the scalar function  $\chi_i$  belongs to  $C(\Omega)$ , the vector  $\chi_i \mathbf{v}$  satisfies the same conditions and, thus, the degrees of freedom are well defined.

The interpolation operator  $\Pi_h^{\mathcal{N}^{\mathcal{D}^k}}$  is local, i.e. the values of  $\Pi_h^{\mathcal{N}^{\mathcal{D}^k}} \mathbf{v}$  in each tetrahedron  $K \in \mathcal{T}_h$  only depend on those of  $\mathbf{v}$  in the same element; therefore, the degrees of freedom are calculated on each  $K$  and the interpolated function is built from the appropriate basis functions. We therefore need only consider one tetrahedron. We also note that the vector  $\chi_i \mathbf{v}$  is a polynomial of degree  $k+1$  over each element. On the reference tetrahedron the interpolation operator is bounded in the  $L^2$ -norm, when applied to the finite dimensional space  $\mathbb{P}_{k+1}$ . Consequently, it is easily seen, by a scaling argument, that, on any tetrahedron  $K$ ,  $\Pi_h^{\mathcal{N}^{\mathcal{D}^k}}$  is bounded by a constant that only depends on the degree  $k$  and the shape-regularity constant of the triangulation, but is independent of the diameter of  $K$ . Inequality (3.13) is obtained by summing over all the elements of  $\mathcal{T}_h$ .

Let us next consider inequality (3.14). The vector  $\mathbf{curl}(\chi_i \mathbf{v})$  is a  $C^\infty$  function in each element and has a continuous normal component. Therefore, the interpolant  $\Pi_h^{\mathcal{RT}^k}(\mathbf{curl}(\chi_i \mathbf{v}))$  is well defined; see Section 2.2.1. Employing (2.38), we obtain

$$\mathbf{curl}(\Pi_h^{\mathcal{ND}^k}(\chi_i \mathbf{v})) = \Pi_h^{\mathcal{RT}^k}(\mathbf{curl}(\chi_i \mathbf{v})).$$

The inequality

$$\|\Pi_h^{\mathcal{RT}^k}(\mathbf{curl}(\chi_i \mathbf{v}))\| \leq C \|\mathbf{curl}(\chi_i \mathbf{v})\|,$$

can be then obtained in the same way as (3.13), and this proves (3.14).  $\square$

### 3.4 Main result

In this section, we will prove an upper bound for the condition number of the additive Schwarz operator  $Q_{ad}$ .

**Lemma 3.4.1** *The largest eigenvalue of the additive operator  $Q_{ad}$  is bounded from above by  $(N_c + 1)$ , where  $N_c$  is defined in Assumption 3.2.1.*

*Proof.* The proof can be carried out in a standard way by a coloring argument; see Lemma 5.6.3 or [54, p. 165].  $\square$

In order to bound the lowest eigenvalue, we use Lemma 2.3.1. We first have to find a stable decomposition according to (3.4).

**Lemma 3.4.2** *For every  $\mathbf{u} \in V^k$ ,  $k \geq 2$ , we have*

$$\sum_{i=0}^J a(\mathbf{u}_i, \mathbf{u}_i) \leq C_0^2 a(\mathbf{u}, \mathbf{u}), \quad (3.15)$$

with

$$C_0^2 = C \left(1 + \frac{\eta_1}{\eta_2}\right) \left(1 + \left(\frac{H}{\delta}\right)^2\right).$$

*The constant  $C$  depends on  $k$ , the domain  $\Omega$ , the number of colors  $N_c$ , and the shape-regularity and quasi-uniformity constants for  $\mathcal{T}_H$  and  $\mathcal{T}_h$ , but is independent of  $h$ ,  $H$ ,  $\delta$ ,  $\eta_1$ ,  $\eta_2$ , and  $\mathbf{u}$ .*



*Proof.* The vector  $\mathbf{u}$  has the following decomposition

$$\mathbf{u} = \mathbf{grad} q + \mathbf{w}, \quad (3.16)$$

according to (3.1), where  $\mathbf{grad} q \in Z$  and  $\mathbf{w} \in Z^\perp$ . We will decompose  $\mathbf{grad} q$  and  $\mathbf{w}$  separately.

Let us first consider the gradient term. Using the domain decomposition theory for scalar elliptic operators (see [23] or [54, Ch. 5]), we can obtain a decomposition  $q = \sum q_i$ , for  $q \in \mathcal{S}_{0,h}(\Omega) \subset H_0^1(\Omega)$ , and the following bound:

$$\begin{aligned} \sum_{i=0}^J a(\mathbf{grad} q_i, \mathbf{grad} q_i) &= \eta_1 \sum_{i=0}^J |q_i|_{1,\Omega}^2 \leq C \left(1 + \frac{H}{\delta}\right) \eta_1 |q|_{1,\Omega}^2 \\ &= C \left(1 + \frac{H}{\delta}\right) a(\mathbf{grad} q, \mathbf{grad} q); \end{aligned}$$

see [54, Theorem 2, Section 5.3].

Consider now  $\mathbf{w} \in Z^\perp$ . We will find a non-conforming approximation of  $\mathbf{w}$ , as described in [29], by first projecting onto  $Z^+$ , then onto the coarse space  $Z_0^+$  and finally onto  $Z_0^\perp$ . We will, then, divide the remainder into a sum of functions supported on the individual subdomains  $\{\Omega'_i\}$ .

The first step is performed in the following way:

Define

$$\mathbf{w}^+ := \Theta(\mathbf{w}) \in Z^+,$$

and consider the splitting

$$\mathbf{w}^+ = \mathbf{v}_0^+ + \mathbf{v}^+,$$

where

$$\begin{aligned} \mathbf{v}_0^+ &:= P_0 \mathbf{w}^+ \in Z_0^+, \\ \mathbf{v}^+ &:= (I - P_0) \mathbf{w}^+ \in Z^+, \end{aligned}$$

and the operator  $P_0$  is defined in Section 3.3.1. Since  $\vartheta$  and  $\vartheta_0$  are invertible on  $Z^\perp$  and  $Z_0^\perp$ , respectively, the following vectors are well defined

$$\begin{aligned} \mathbf{v}_0 &:= \vartheta_0^{-1}(\mathbf{v}_0^+) \in Z_0^\perp, \\ \mathbf{v} &:= \vartheta^{-1}(\mathbf{v}^+) \in Z^\perp. \end{aligned}$$

The sum  $\mathbf{v}_0 + \mathbf{v} = \mathbf{w}'$  is not equal to the original vector  $\mathbf{w}$ , but it can easily be seen that the difference  $(\mathbf{w} - \mathbf{w}')$  is curl-free and, thus, by Proposition 2.1.2 and (2.35), is the gradient of a function  $p \in \mathcal{S}_{0,h}(\Omega)$ . Consequently, we have found the decomposition

$$\mathbf{w} = \mathbf{v}_0 + \mathbf{v} + \mathbf{grad} p. \quad (3.17)$$

Before proceeding, we have to find some bounds for the terms in (3.17) and their curls. Since the operators  $\Theta$ ,  $\vartheta$ , and  $\vartheta_0$  preserve the curl and  $P_0$  does not increase the  $L^2$ -norm of the curl, it can be easily seen that

$$\|\mathbf{curl} \mathbf{v}_0\| \leq \|\mathbf{curl} \mathbf{w}\|, \quad (3.18)$$

$$\|\mathbf{curl} \mathbf{v}\| \leq \|\mathbf{curl} \mathbf{w}\|. \quad (3.19)$$

We employ Lemma 3.3.1 to bound the  $L^2$ -norm of  $\mathbf{v}_0$  and  $\mathbf{v}$ . Consider  $\mathbf{v}_0$  first. By (3.5), we find

$$\|\mathbf{v}_0\| \leq C \left( \|\mathbf{v}_0^+\| + H \|\mathbf{curl} \mathbf{v}_0\| \right) = C \left( \|\mathbf{v}_0^+\| + H \|\mathbf{curl} \mathbf{v}_0^+\| \right),$$

and, by Lemma 3.3.2,

$$\|\mathbf{v}_0\| \leq C \|\mathbf{curl} \mathbf{w}^+\| = C \|\mathbf{curl} \mathbf{w}\|. \quad (3.20)$$

We next consider  $\mathbf{v}$ . Applying Lemma 3.3.1 and 3.3.2, we find, in a similar way,

$$\begin{aligned} \|\mathbf{v}\| &\leq C \left( \|\mathbf{v}^+\| + h \|\mathbf{curl} \mathbf{v}\| \right) = C \left( \|\mathbf{v}^+\| + h \|\mathbf{curl} \mathbf{v}^+\| \right) \\ &\leq C \left( H \|\mathbf{curl} \mathbf{w}^+\| + h \|\mathbf{curl} \mathbf{v}^+\| \right) \leq C H \|\mathbf{curl} \mathbf{w}\|. \end{aligned} \quad (3.21)$$

Since the  $L^2$ -norms of  $\mathbf{v}_0$  and  $\mathbf{v}$  are bounded, we can bound the  $L^2$ -norm of  $\mathbf{grad} p$  in (3.17) in terms of the  $H(\mathbf{curl}; \Omega)$ -norm of  $\mathbf{w}$ . The  $\mathbf{grad} p$  term can therefore be decomposed in the same way as the gradient part of  $\mathbf{u}$  in (3.16).

We now decompose the vector  $\mathbf{v}$  as a sum of terms in  $\{V_i, i = 1, \dots, J\}$ . With  $\{\chi_i\}$ , the piecewise linear partition of unity relative to the covering  $\{\Omega'_i\}$ , we define

$$\mathbf{w}_i = \Pi_h^{\mathcal{N}_{\mathcal{D}^k}}(\chi_i \mathbf{v}) \in V_i, \quad i = 1, \dots, J.$$

The function  $\mathbf{w}' = \mathbf{v}_0 + \mathbf{v}$  is thus decomposed as  $\mathbf{w}' = \sum_{i=0}^J \mathbf{w}_i$ , with

$$\mathbf{w}_0 = \mathbf{v}_0.$$

We have to check that the sum of the squares of the  $\mathbf{a}$ -norm of the  $\mathbf{w}_i$  is bounded by the square of the  $\mathbf{a}$ -norm of  $\mathbf{w}$ . The bounds for  $\mathbf{w}_0$  are given by (3.18) and (3.20).

By inequality (3.13) of Lemma 3.3.3, we can write

$$\|\mathbf{w}_i\| \leq C \|\chi_i \mathbf{v}\| \leq C \|\mathbf{v}\|,$$

and, by (3.21),

$$\|\mathbf{w}_i\| \leq C H \|\mathbf{curl} \mathbf{w}\|. \quad (3.22)$$

Employing (3.14), we can also write

$$\begin{aligned} \|\mathbf{curl} \mathbf{w}_i\|_{0,\Omega} &\leq C \|\mathbf{curl}(\chi_i \mathbf{v})\|_{0,\Omega} \\ &\leq C (\|\mathbf{grad} \chi_i \times \mathbf{v}\|_{0,\Omega} + \|\chi_i \mathbf{curl} \mathbf{v}\|_{0,\Omega}) \\ &\leq C \left( \|\mathbf{grad} \chi_i\|_{L^\infty(\Omega)} \|\mathbf{v}\|_{0,\Omega'_i} + \|\chi_i\|_{L^\infty(\Omega'_i)} \|\mathbf{curl} \mathbf{v}\|_{0,\Omega'_i} \right) \\ &\leq C \left( \delta^{-1} \|\mathbf{v}\|_{0,\Omega} + \|\mathbf{curl} \mathbf{v}\|_{0,\Omega} \right), \end{aligned}$$

where we have used (3.12) for the last inequality. Finally, by (3.19) and (3.21), we obtain

$$\begin{aligned} \|\mathbf{curl} \mathbf{w}_i\| &\leq C \left( \frac{H}{\delta} \|\mathbf{curl} \mathbf{w}\| + \|\mathbf{curl} \mathbf{w}\| \right) \\ &\leq C \left( 1 + \frac{H}{\delta} \right) \|\mathbf{curl} \mathbf{w}\|. \end{aligned} \quad (3.23)$$

By summing over  $i$  and employing Assumption 3.2.1, (3.18), (3.20), (3.22), (3.23), and the equivalence of the graph and the energy norm, we find

$$\sum_{i=0}^J a(\mathbf{w}_i, \mathbf{w}_i) \leq C \left( 1 + \frac{\eta_1}{\eta_2} \right) \left( 1 + \left( \frac{H}{\delta} \right)^2 \right) a(\mathbf{w}, \mathbf{w}). \quad (3.24)$$

Since (3.16) is also an  $\mathbf{a}$ -orthogonal decomposition, inequality (3.15) holds.  $\square$

**Lemma 3.4.3** *The conclusion of Lemma 3.4.2 is also valid for  $k = 1$ .*

*Proof.* The proof is similar to the one in [31, Section 5.2] and employs the decomposition of  $V^2$  and the hierarchical decomposition of the degrees of freedom for the Nédélec spaces.

The vectors in  $Z^1$  are gradients of scalar functions in  $\mathcal{S}_{0,h}^1(\Omega)$  and can be decomposed using the theory for scalar elliptic operators. Thus, we only need to find a decomposition for a generic  $\mathbf{w} \in Z^{\perp,1}$ . Since  $\mathbf{w} \in V^2$ , we can proceed as in the proof of Lemma 3.4.2 (see Equations (3.16) and (3.17)) and we find a decomposition

$$\mathbf{w} = \mathbf{grad} \left( q^{(2)} + p^{(2)} \right) + \mathbf{v}_0^{(2)} + \mathbf{v}^{(2)} := \mathbf{grad} \tilde{q}^{(2)} + \mathbf{v}_0^{(2)} + \mathbf{v}^{(2)},$$

where  $\tilde{q}^{(2)} \in \mathcal{S}_{0,h}^2(\Omega)$ ,  $\mathbf{v}_0^{(2)} \in Z_0^{\perp,2}$ , and  $\mathbf{v}^{(2)} \in Z^{\perp,2}$ . The vectors  $\mathbf{v}_0^{(2)}$  and  $\mathbf{v}^{(2)}$  satisfy the following bounds (see (3.18), (3.20), (3.19), (3.21))

$$\begin{aligned} \|\mathbf{curl} \mathbf{v}_0^{(2)}\| &\leq \|\mathbf{curl} \mathbf{w}\|, \\ \|\mathbf{v}_0^{(2)}\| &\leq C \|\mathbf{curl} \mathbf{w}\|, \\ \|\mathbf{curl} \mathbf{v}^{(2)}\| &\leq \|\mathbf{curl} \mathbf{w}\|, \\ \|\mathbf{v}^{(2)}\| &\leq C H \|\mathbf{curl} \mathbf{w}\|. \end{aligned} \tag{3.25}$$

Interpolating in  $V^1$ , we obtain

$$\begin{aligned} \mathbf{w} &= \Pi_h^{\mathcal{N}\mathcal{D}^1} \left( \mathbf{grad} \tilde{q}^{(2)} + \mathbf{v}_0^{(2)} + \mathbf{v}^{(2)} \right) \\ &= \Pi_h^{\mathcal{N}\mathcal{D}^1} \left( \mathbf{grad} \tilde{q}^{(2)} \right) + \Pi_H^{\mathcal{N}\mathcal{D}^1} \mathbf{v}_0^{(2)} + \left( \Pi_h^{\mathcal{N}\mathcal{D}^1} \mathbf{v}^{(2)} + \left( \Pi_h^{\mathcal{N}\mathcal{D}^1} - \Pi_H^{\mathcal{N}\mathcal{D}^1} \right) \mathbf{v}_0^{(2)} \right). \end{aligned}$$

Equality (2.35) ensures that there exists a unique  $p \in \mathcal{S}_{0,h}^1(\Omega)$ , such that

$$\Pi_h^{\mathcal{N}\mathcal{D}^1} \left( \mathbf{grad} \tilde{q}^{(2)} \right) = \mathbf{grad} p.$$

By setting

$$\begin{aligned} \mathbf{v}_0 &:= \Pi_H^{\mathcal{N}\mathcal{D}^1} \mathbf{v}_0^{(2)} \in V_0^1, \\ \mathbf{v} &:= \Pi_h^{\mathcal{N}\mathcal{D}^1} \mathbf{v}^{(2)} + \left( \Pi_h^{\mathcal{N}\mathcal{D}^1} - \Pi_H^{\mathcal{N}\mathcal{D}^1} \right) \mathbf{v}_0^{(2)} \in V^1, \end{aligned}$$

we have found the decomposition

$$\mathbf{w} = \mathbf{v}_0 + \mathbf{v} + \mathbf{grad} p,$$

which is the analog of (3.17). We now have to find some bounds for  $\mathbf{v}_0$  and  $\mathbf{v}$ . Since  $\mathbf{v}_0$  and  $\mathbf{v}$  are piecewise quadratic functions, the same argument as in the proof of Lemma 3.3.3 gives

$$\begin{aligned}
\|\Pi_H^{\mathcal{N}\mathcal{D}^1} \mathbf{v}_0^{(2)}\| &\leq C \|\mathbf{v}_0^{(2)}\|, \\
\|\Pi_h^{\mathcal{N}\mathcal{D}^1} \mathbf{v}^{(2)}\| &\leq C \|\mathbf{v}^{(2)}\|, \\
\|\mathbf{curl} \Pi_H^{\mathcal{N}\mathcal{D}^1} \mathbf{v}_0^{(2)}\| &\leq C \|\mathbf{curl} \mathbf{v}_0^{(2)}\|, \\
\|\mathbf{curl} \Pi_h^{\mathcal{N}\mathcal{D}^1} \mathbf{v}^{(2)}\| &\leq C \|\mathbf{curl} \mathbf{v}^{(2)}\|, \\
\|\mathbf{curl} (\Pi_h^{\mathcal{N}\mathcal{D}^1} - \Pi_H^{\mathcal{N}\mathcal{D}^1}) \mathbf{v}_0^{(2)}\| &\leq C \|\mathbf{curl} \mathbf{v}_0^{(2)}\|,
\end{aligned} \tag{3.26}$$

while [31, Lemma 5.2] ensures that

$$\|(\Pi_h^{\mathcal{N}\mathcal{D}^1} - \Pi_H^{\mathcal{N}\mathcal{D}^1}) \mathbf{v}_0^{(2)}\| \leq CH \|\mathbf{v}_0^{(2)}\|. \tag{3.27}$$

Combining (3.25), (3.26), and (3.27), we obtain

$$\begin{aligned}
\|\mathbf{curl} \mathbf{v}_0\| &\leq \|\mathbf{curl} \mathbf{w}\|, \\
\|\mathbf{v}_0\| &\leq C \|\mathbf{curl} \mathbf{w}\|, \\
\|\mathbf{curl} \mathbf{v}\| &\leq \|\mathbf{curl} \mathbf{w}\|, \\
\|\mathbf{v}\| &\leq CH \|\mathbf{curl} \mathbf{w}\|,
\end{aligned}$$

and, by setting

$$\mathbf{v}_i := \Pi_h^{\mathcal{N}\mathcal{D}^1} (\chi_i \mathbf{v}), \quad i = 1, \dots, J,$$

we can now proceed as in the proof of Lemma 3.4.2.  $\square$

Combining Lemmas 5.6.1, 3.4.1, Theorem 3.4.2, and Theorem 3.4.3, we obtain the final result.

**Theorem 3.4.1** *Let  $k \geq 1$ . There exists a constant  $C$ , such that the condition number  $\kappa(Q_{ad})$  of the additive Schwarz preconditioner satisfies*

$$\kappa(Q_{ad}) \leq C \left(1 + \frac{\eta_1}{\eta_2}\right) \left(1 + \left(\frac{H}{\delta}\right)^2\right).$$

*Here,  $C$  may depend on the domain  $\Omega$ , on the the number of colors  $N_c$ , and on the shape-regularity and quasi-uniformity constants of  $\mathcal{T}_H$  and  $\mathcal{T}_h$ , but is independent of  $h$ ,  $H$ ,  $\eta_1$ , and  $\eta_2$ .*

### 3.5 Extensions

The bound in Theorem 3.4.1 tends to infinity as the coefficient  $\eta_2$  tends to zero. This is due to the fact that the decompositions considered in Lemmas 3.4.2 and 3.4.3 are not stable in the  $L^2$ -norm. However, the numerical results in the next section show that the condition number of the additive method remains bounded and is independent of the overlap  $H/\delta$ , as  $\eta_2$  becomes small. In fact, the condition numbers appears to be bounded independently of the ratio  $\eta_1/\eta_2$ . Here, we show that in the limit case  $\eta_2 = 0$ , a stable decomposition can be found and, consequently, the overlapping preconditioner considered is still optimal. We remark that Lemmas 3.4.2 and 3.4.3 remain valid in the limit case  $\eta_1 = 0$ .

Given a function  $\mathbf{u} \in V$ , consider the decomposition

$$\begin{aligned}\mathbf{u}_0 &= \mathbf{0} \in V_0, \\ \mathbf{u}_i &= \Pi_h^{\mathcal{N}\mathcal{D}^k}(\chi_i \mathbf{u}) \in V_i.\end{aligned}$$

Lemma 3.3.3 and Assumption 3.2.1 ensure that this is a stable decomposition with respect to the  $L^2$ -norm, and, consequently, Lemma 3.4.1 holds for  $\eta_2 = 0$ , with a constant  $C_0$  that is independent of  $h$ ,  $H$ ,  $\mathbf{u}$ ,  $\delta$ , and  $\eta_1$ . Thus, in this limit case, a coarse space is not needed.

For the Neumann problem, convexity is not necessary.

**Theorem 3.5.1** *When the whole space  $H(\mathbf{curl}; \Omega)$  is considered, the conclusions of Lemmas 3.4.1 and 3.4.2 are still valid, for a general polyhedral domain.*

*Proof.* The proof of Lemma 3.4.1 is the same. For the lower bound of the additive method, the proof can be carried out as in [32, Theorem 5]. The domain  $\Omega$  is embedded in a larger convex domain,  $\tilde{\Omega}$ , and the decomposition for  $H_0(\mathbf{curl}; \tilde{\Omega})$ , together with an extension theorem, is exploited.  $\square$

We conclude this section with some remarks on our assumptions. A *convex* polyhedral domain is considered for the Dirichlet problem: this is necessary for the Embedding Theorem 2.1.1 to hold. As pointed out in Remark 2.1.4, the theorem is not valid for a general non-convex domain, unless the boundary is sufficiently

regular. This assumption is also required for the proof of Lemma 3.3.2. *Quasi-uniform* triangulations are assumed, for the proof of the inequalities in Lemma 3.3.1.

## 3.6 Numerical results

In this section, we present some numerical results to find out how the rate of convergence of two Schwarz algorithms depends on the overlap, the number of subdomains, and the coefficients  $\eta_1$  and  $\eta_2$ . We consider the Dirichlet problem (3.3) in the unit cube  $\Omega$ , with uniform triangulations  $\mathcal{T}_h$  and  $\mathcal{T}_H$ . The fine triangulation  $\mathcal{T}_h$  consists of  $n^3$  cubical elements, with  $h = 1/n$ . The number of subdomains  $n_{sub}$  equals the number of coarse elements in  $\mathcal{T}_H$ .

We have tested the following Schwarz algorithms:

- (i) The conjugate gradient method applied to the *additive one-level* Schwarz operator

$$Q_{as1} = \sum_{i=1}^J Q_i.$$

- (ii) The conjugate gradient method applied to the *additive two-level* operator

$$Q_{as2} = Q_0 + \sum_{i=1}^J Q_i.$$

For the two algorithms, Tables 3.1 and 3.2 show the estimated condition number and the number of conjugate gradient iterations necessary to obtain a reduction of  $10^{-6}$  of the residual norm, as a function of the problem size, the number of subregions, and the relative overlap. The estimate of the condition number is obtained from the parameters calculated during the conjugate gradient iteration, using the method described in [47]. We observe:

- When the number of subdomains and the relative overlap are fixed, the condition number and the number of iterations appear to be bounded independently of the problem size.

Table 3.1: One-level additive Schwarz algorithm. Estimated condition number and number of CG iterations for a residual norm reduction of  $10^{-6}$  (in parentheses), versus  $n$ , number of subdomains and  $H/\delta$ . Case of  $\eta_1 = 1$ ,  $\eta_2 = 1$ .

$n$	$n_{sub}$	$H/\delta$			
		8	4	2	1.33
8	$2^3$	-	14.10 (23)	8.95 (20)	8.94 (15)
16	$2^3$	28.05 (25)	13.32 (21)	-	-
16	$4^3$	-	33.51 (29)	15.13 (23)	27.30 (28)
16	$8^3$	-	-	57.31 (35)	-
24	$3^3$	50.94 (30)	22.62 (24)	-	-
24	$6^3$	-	67.39 (35)	22.99 (26)	21.25 (27)
24	$12^3$	-	-	73.69 (38)	-
32	$4^3$	80.86 (36)	34.82 (25)	-	-
32	$8^3$	-	117.18 (43)	37.33 (29)	28.85 (28)
40	$5^3$	115.93 (41)	50.41 (29)	-	-
40	$10^3$	-	177.46 (46)	55.35 (31)	44.52 (29)
48	$6^3$	143.05 (43)	66.60 (32)	-	-
48	$12^3$	-	243.85 (55)	74.57 (35)	60.03 (33)



Table 3.2: Two-level additive Schwarz algorithm. Estimated condition number and number of CG iterations for a residual norm reduction of  $10^{-6}$  (in parentheses), versus  $n$ , number of subdomains and  $H/\delta$ . Case of  $\eta_1 = 1$ ,  $\eta_2 = 1$ .

$n$	$n_{sub}$	$H/\delta$			
		8	4	2	1.33
8	$2^3$	-	8.94 (19)	8.98 (20)	9.05 (15)
16	$2^3$	14.05 (21)	8.49 (19)	-	-
16	$4^3$	-	8.61 (19)	9.86 (21)	27.54 (28)
16	$8^3$	-	-	10.59 (19)	-
24	$3^3$	13.86 (21)	8.45 (19)	-	-
24	$6^3$	-	8.43 (19)	9.05 (19)	21.93 (27)
24	$12^3$	-	-	9.39 (18)	-
32	$4^3$	13.02 (20)	8.30 (18)	-	-
32	$8^3$	-	8.37 (19)	8.78 (19)	21.39 (25)
40	$5^3$	13.12 (20)	8.29 (18)	-	-
40	$10^3$	-	8.29 (18)	8.68 (19)	22.28 (25)
48	$6^3$	12.91 (20)	8.36 (18)	-	-
48	$12^3$	-	8.32 (18)	8.64 (18)	22.93 (24)

- For both algorithms, the condition number initially decreases with  $H/\delta$ , when the number of subregions is fixed. For larger values of the relative overlap, the number of colors  $N_c$  increases, and, consequently, the condition number increases, in accordance with our analysis.
- For a fixed value of the relative overlap, the condition number grows rapidly with the number of subregions for the one-level algorithm, while it appears to be bounded independently of the number of subregions, for the two-level case. The two-level algorithm behaves better than the one-level method in all the cases considered in Tables 3.1 and 3.2, except for problems of small size and large overlap.
- We have compared the number of iterations obtained with our two-level method, with those given in [54, p. 50], for a two-level overlapping preconditioner employed with GMRES, for the Laplace equation in two dimensions. Taking into account that a different precision is required there and that the number of conjugate gradient iterations varies logarithmically with the required precision, we can conclude that our iteration counts are comparable with those for similar preconditioners for Laplace equation.

In a second study, we further analyze the upper bound of the inverse of the minimum eigenvalue, given in Lemmas 3.4.2 and 3.4.3. We recall that the estimate for the corresponding preconditioner for the scalar Laplace equation gives an upper bound that is linear in  $H/\delta$ ; see [54, Theorem 2, Section 5.3] and [23]. Figure 3.1 shows the inverse of the estimated condition number and some polynomial least-square fits, versus  $H/\delta$ . We observe that the inverse of the smallest eigenvalue appears to grow linearly for  $H/\delta \geq 4$  and is practically constant for  $H/\delta \leq 4$ . This suggests that the leading term of its asymptotic expansion is linear in  $H/\delta$  and the bounds given in Lemmas 3.4.2 and 3.4.3 probably are not sharp. We also show the quadratic polynomial least-square fit in the whole interval  $(1, 10]$ .

We have also considered the effect on our method when the ratio between the coefficients  $\eta_1$  and  $\eta_2$  is changed. We recall that the bounds obtained in Lemmas 3.4.2 and 3.4.3 remain bounded when  $\eta_1/\eta_2$  tends to zero, but blow up when  $\eta_1/\eta_2$

Table 3.3: One-level additive Schwarz algorithm. Estimated condition number and number of CG iterations for a residual norm reduction of  $10^{-6}$  (in parentheses), versus  $b$  and  $H/\delta$ . Case of  $\eta_2 = 1$ ,  $n = 16$ .

$\eta_1$	8 subdomains		64 subdomains		
	$H/\delta$		$H/\delta$		
	8	4	4	2	1.33
1e-06	29.44 (26)	13.58 (22)	34.50 (31)	14.50 (25)	14.36 (24)
1e-05	29.44 (26)	13.58 (22)	34.50 (31)	14.50 (25)	14.36 (24)
0.0001	29.43 (26)	13.58 (22)	34.50 (31)	14.50 (25)	14.36 (24)
0.001	29.43 (26)	13.58 (22)	34.49 (31)	14.51 (25)	14.37 (24)
0.01	29.40 (26)	13.58 (22)	34.49 (31)	14.62 (25)	15.11 (25)
0.1	29.20 (26)	13.52 (22)	34.41 (31)	16.04 (25)	28.18 (28)
1	28.05 (25)	13.32 (21)	33.50 (29)	15.13 (23)	27.30 (28)
10	22.34 (22)	11.80 (18)	25.81 (25)	10.19 (20)	24.98 (29)
100	11.51 (17)	8.04 (15)	11.54 (18)	7.99 (17)	26.71 (26)
1000	8.11 (14)	8.00 (12)	8.14 (14)	7.99 (14)	26.96 (25)
10000	8.53 (13)	8.00 (10)	8.70 (14)	8.01 (12)	26.98 (23)
1e+05	8.95 (14)	8.02 (9)	9.17 (15)	8.05 (10)	26.98 (22)
1e+06	9.13 (14)	8.02 (9)	9.24 (15)	8.06 (10)	26.99 (22)

Table 3.4: Two-level additive Schwarz algorithm. Estimated condition number and number of CG iterations for a residual norm reduction of  $10^{-6}$  (in parentheses), versus  $b$  and  $H/\delta$ . Case of  $\eta_2 = 1$ ,  $n = 16$ .

$\eta_1$	8 subdomains		64 subdomains		
	$H/\delta$		$H/\delta$		
	8	4	4	2	1.33
1e-06	13.30 (21)	8.99 (20)	8.94 (20)	13.44 (24)	14.31 (24)
1e-05	13.30 (21)	8.99 (20)	8.94 (20)	13.44 (24)	14.31 (24)
0.0001	13.30 (21)	8.99 (20)	8.94 (20)	13.44 (24)	14.31 (24)
0.001	13.30 (21)	8.99 (20)	8.94 (20)	13.43 (24)	14.32 (24)
0.01	13.30 (21)	8.98 (20)	8.93 (20)	13.35 (24)	19.51 (26)
0.1	13.29 (21)	8.89 (20)	8.86 (20)	12.64 (23)	27.83 (27)
1	14.05 (21)	8.49 (19)	8.61 (19)	9.86 (21)	27.54 (28)
10	13.48 (19)	8.43 (17)	9.03 (18)	8.67 (19)	24.99 (29)
100	9.94 (16)	8.04 (15)	8.59 (18)	8.74 (18)	26.67 (26)
1000	8.11 (15)	8.07 (13)	8.30 (17)	8.82 (17)	26.97 (26)
10000	8.55 (15)	8.08 (13)	8.91 (17)	8.88 (15)	27.03 (23)
1e+05	8.92 (14)	8.09 (12)	9.40 (18)	8.92 (14)	27.04 (24)
1e+06	9.00 (14)	8.09 (12)	9.47 (18)	8.93 (14)	27.04 (24)

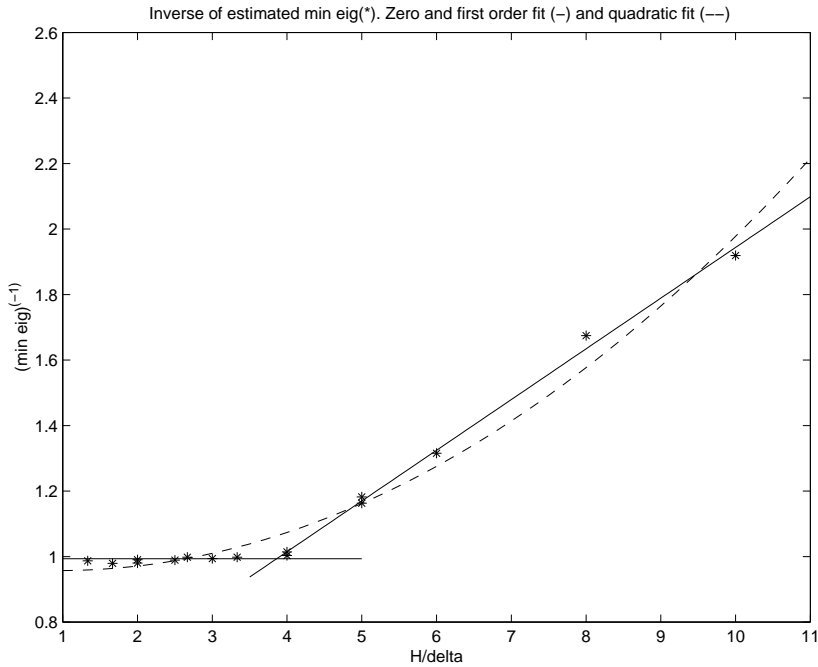


Figure 3.1: Two-level method. Inverse of the estimated minimum eigenvalue (asterisk), least-square zero (solid line), first (solid line), and second order (dashed line) fitting polynomials, versus  $H/\delta$ . The relative fitting error is 1.0, 1.4 and 3.5 per cent, respectively. Case for  $\eta_1 = 1$ ,  $\eta_2 = 1$ ,  $n$  equal to 16, 18, and 20.

tends to infinity. In addition, an optimal bound is given in Section 3.5, for the case  $\eta_2 = 0$ , which is independent of the number of subdomains and the overlap.

Tables 3.3 and 3.4 show the estimated condition number and the number of conjugate gradient iterations in order to obtain a reduction of  $10^{-6}$  of the residual norm, as functions of  $\eta_1$ , the number of subregions, and the relative overlap, for the two algorithms, applied to a problem of fixed size and a fixed  $\eta_2$ . We observe:

- When the coefficient  $\eta_1$  is fixed, the observations made concerning Tables 3.1 and 3.2 are still valid.
- For a fixed number of subregions and a fixed overlap, the condition number and the number of iterations are practically constant as a function of  $\eta_1$ , when  $\eta_1 < 1$ . The same behavior is observed for the two-level algorithm, when  $\eta_1 > 1$ . Moreover, the condition number of the one-level method decreases

when  $\eta_1$  increases. When  $\eta_1$  is large, the condition number is less insensitive to the overlap and the number of subregions; this is consistent with the our analysis for the case  $\eta_2 = 0$ , in which a coarse space is not needed.

# Chapter 4

## Iterative substructuring methods based on individual edges or faces

### 4.1 Introduction

In this chapter, we study some iterative substructuring methods (also called Schur complement methods) for some Raviart–Thomas and Nédélec element approximations, in two and three dimensions.

In a substructuring method, the local spaces are related to a partition of the original domain  $\Omega$  into non-overlapping subdomains, called *substructures*. Depending on the particular method, the substructures can be the elements of a coarse mesh or arbitrary connected subsets of  $\Omega$ , consisting of unions of elements of the fine mesh. The lack of generous overlap results in bounds for the condition number that are not optimal, but which can be made independent of the jumps of the coefficients. This last property is not in general guaranteed for overlapping methods.

If the degrees of freedom of the local spaces are related to the edges (or faces, in three dimensions) of the substructures, we speak of *edge space* (or *face space*) methods. In case they are related to the entire boundaries of the substructures, they give rise to *Neumann–Neumann* methods; see [22, 54] and Chapter 5.

In this chapter, we will study an edge space method for  $H(\mathbf{curl}; \Omega)$  and  $H(\mathbf{div}; \Omega)$ , in two dimensions, and a face space method for  $H(\mathbf{div}; \Omega)$ , in three dimensions. We note that we only know of one study of iterative substructuring

methods in  $H(\mathbf{curl}; \Omega)$ , in three dimensions. In [3] an iterative method for the case of two substructures is studied. To our knowledge, methods for the case of an arbitrary number of substructures still remains to be developed and analyzed.

The analysis presented in this chapter, on edge space and face space methods in two and three dimensions, is contained in [57] and [62], respectively.

Many Schwarz methods have been designed and analyzed for the case of  $H^1(\Omega)$  in two and three dimensions; see, e.g. [23, 22, 54]. The substructuring methods presented in this chapter all employ standard coarse spaces, built on coarse triangulations. The choice of the coarse space for a Schur complement method in  $H^1(\Omega)$  is a delicate matter, in three dimensions; see, e.g. [22, 60]. Thus, if a standard subspace built on a coarse triangulation is employed in a *vertex-based* algorithm, the condition number of the method cannot be both quasi-optimal and independent of the jumps of the coefficients across the inner edges of the substructures; see [22]. In particular, if only edge, face, and interior spaces are used in addition to a conventional coarse space, the condition number can be made independent of the jumps but it will grow algebraically with the number of unknowns in each subdomain. If, on the other hand, local vertex spaces are added then a logarithmic bound can be found for the condition number of the iteration operator, but this bound will not, in general, be independent of the jumps of the coefficients. The reason is that the standard, vertex based interpolation operator onto the coarse space has a norm that grows algebraically in three dimensions. For this reason, other coarse spaces and iterative substructuring methods have been introduced, among them the *wire-basket based* algorithms (see [22]), and the *balancing* methods (see [37, 36, 16]). (We recall that the wire-basket is the union of the boundaries of the faces which separate the substructures.) In this respect, there is an interesting difference between  $H^1(\Omega)$  and  $H(\text{div}; \Omega)$  in three dimensions, since our new method for  $H(\text{div}; \Omega)$  uses a standard coarse space that is just a smaller instance of the original finite element problem. At the same time, we are able to maintain the same kind of quasi-optimality and independence of the jumps as the best, more complicated algorithms for the  $H^1(\Omega)$  case. This is a consequence of a certain stability result, given in Lemma 4.3.1, for the interpolant for the Raviart-Thomas space, the degrees of freedoms of which are defined by averages of the normal



component over the faces of the triangulation.

## 4.2 An edge space method in two dimensions

In this section, we will present some results for the space  $H(\mathbf{curl}; \Omega)$  in two dimensions. The analysis of the corresponding algorithm for  $H(\mathbf{div}; \Omega)$  in two dimensions follows from that for  $H(\mathbf{curl}; \Omega)$  and the observation that the functions in  $H(\mathbf{div}; \Omega)$  and in the Raviart–Thomas spaces are obtained from those in  $H(\mathbf{curl}; \Omega)$  and in the Nédélec spaces, respectively, by a rotation of ninety degrees; see Sections 2.1.2 and 2.2.2.

### 4.2.1 Discrete problem and finite element spaces

Let  $\Omega$  be a bounded polygon in  $\mathbb{R}^2$ . We consider problems involving the bilinear form

$$a(\mathbf{u}, \mathbf{v}) := \int_{\Omega} (a \operatorname{curl} \mathbf{u} \operatorname{curl} \mathbf{v} + B \mathbf{u} \cdot \mathbf{v}) \, dx, \quad \mathbf{u}, \mathbf{v} \in H(\mathbf{curl}; \Omega), \quad (4.1)$$

where the coefficient matrix  $B$  is a symmetric uniformly positive definite matrix-valued function with  $b_{i,j} \in L^\infty(\Omega)$ ,  $1 \leq i, j \leq 2$ , and  $a \in L^\infty(\Omega)$  is a positive function bounded away from zero.

Let  $\mathcal{T}_H$  be a triangulation of  $\Omega$ , of maximum diameter  $H$ , consisting of triangles or rectangles, and let  $\mathcal{T}_h$  be a *shape-regular* and *quasi-uniform* refinement of  $\mathcal{T}_H$ , with characteristic diameter  $h$ . A generic element of  $\mathcal{T}_h$  and  $\mathcal{T}_H$  will be denoted by  $t$  and  $T$ , respectively. The sets of edges of the triangulations  $\mathcal{T}_h$  and  $\mathcal{T}_H$ , are denoted by  $\mathcal{E}_h$  and  $\mathcal{E}_H$ , respectively, and a generic edge by  $e$  and  $E$ . The elements of  $\mathcal{T}_H$  will be called substructures. For each interior edge  $E \in \mathcal{E}_H$  there are two elements  $T_i, T_j \in \mathcal{T}_H$  such that  $\bar{E} := \partial T_i \cap \partial T_j$ , and we set

$$\bar{T}_E := \bar{T}_i \cup \bar{T}_j.$$

We also suppose that the coefficients  $a$  and  $B$  are constant on each substructure  $T$  and equal to  $a_T$  and  $B_T$ , respectively. They may have arbitrary jumps across the edges of the substructures. In addition, the matrices  $\{B_T\}$  satisfy

$$\beta_T \eta^T \eta \leq \eta^T B_T \eta \leq \gamma_T \eta^T \eta, \quad \forall \eta \in \mathbb{R}^2,$$

where  $\beta_T$  and  $\gamma_T$  are positive constants, which can depend on the substructure  $T$ .

In this section, we will only consider, in full detail, triangulations based on triangles, but note that our results are equally valid for finite element spaces built on rectangles. We also remark that our analysis is carried out locally for one substructure at a time. We can therefore interpret the factor  $H/h$ , which appears in our estimates, as

$$\max_{T \in \mathcal{T}_H} \max_{\substack{t \in \mathcal{T}_h \\ t \subset T}} \frac{H_T}{H_t}.$$

We consider the lowest order Nédélec elements, defined on the fine and coarse mesh, respectively,

$$\begin{aligned} X_{0;h} &:= \mathcal{N}\mathcal{D}_{0;h}^1(\Omega) = \mathcal{N}\mathcal{D}_{0;h}(\Omega), \\ X_{0;H} &:= \mathcal{N}\mathcal{D}_{0;H}^1(\Omega) = \mathcal{N}\mathcal{D}_{0;H}(\Omega), \end{aligned}$$

conforming in  $H_0(\mathbf{curl}; \Omega)$ ; see Section 2.2.2. In the case  $\mathcal{D}$  is a substructure or the union of two substructures that have a common edge, we will also need the finite element space  $X_{0;h}(\mathcal{D}) \subset H_0(\mathbf{curl}; \mathcal{D})$ , and the space  $\mathcal{S}_{0;h}^1(\mathcal{D}) = \mathcal{S}_{0;h}^1(\mathcal{D})$ , of continuous, piecewise linear functions that vanish on  $\partial\mathcal{D}$ .

## 4.2.2 Description of the algorithm

We consider the approximate problem:

Find  $\mathbf{u} \in X_{0;h}$  such that

$$a(\mathbf{u}, \mathbf{v}) = (\mathbf{f}, \mathbf{v}) \quad \forall \mathbf{v} \in X_{0;h}, \tag{4.2}$$

where  $\mathbf{f} \in L^2(\Omega)^2$ . The generalization to the case of the  $\mathcal{N}\mathcal{D}_h(\Omega)$  (Neumann boundary conditions) does not present any particular difficulty.

In order to define a Schwarz , algorithm, we have to define a decomposition of  $X_{0;h}$  into subspaces and some bilinear forms defined on them. We decompose  $X_{0;h}$  into the coarse space  $X_{0;H}$ , the interior spaces  $\{X_T, T \in \mathcal{T}_H\}$

$$X_T := X_{0;h}(T), \quad T \in \mathcal{T}_H,$$

and the edge spaces  $\{X_E, E \in \mathcal{E}_H\}$

$$X_E := \{\mathbf{v} \in X_{0;h} \mid a(\mathbf{v}, \mathbf{w}) = 0, \mathbf{w} \in X_{T_i} \cup X_{T_j}, \text{supp } \mathbf{v} \subset \overline{T_E}\}.$$

We note that any element  $\mathbf{v} \in X_E$  is the harmonic extension of a function defined on the edge  $E$  to  $T_E$ , and that it is defined uniquely by its value of  $\mathbf{n} \times \mathbf{v}$  on  $E$ . In addition, the coarse space  $X_{0;H}$  is contained in the union of the edge and interior spaces, and, consequently, the decomposition

$$X_{0;h} = X_{0;H} + \sum_{T \in \mathcal{T}_H} X_T + \sum_{E \in \mathcal{E}_H} X_E, \quad (4.3)$$

is not a direct sum.

We will use the original bilinear form  $a(\cdot, \cdot)$  on all the subspaces  $X_{0;h}$ ,  $X_E$ , and  $X_T$ .

### 4.2.3 A stability estimate for the interpolation operator

In this section, we will prove a stability estimate for the interpolation operator

$$\rho_H : X_{0;h} \longrightarrow X_{0;H}.$$

In particular, this interpolant will be logarithmically stable in the  $\|\cdot\|_{\text{curl}}$  norm. We note that the best bound for the  $L^2$ -norm alone involves a factor of  $H/h$ ; this can easily be seen by considering an element  $\mathbf{u}$ , for which all the interior degrees of freedom vanish.

The interpolation operator has already been defined in Section 2.2.2. In particular, we recall that  $\rho_H$  is defined in terms of the degrees of freedom of the coarse space  $X_{0;H}$ , i.e.

$$\lambda_E(\rho_H \mathbf{u}) := \frac{1}{H_E} \int_E \mathbf{n} \times \mathbf{u} \, ds, \quad E \in \mathcal{E}_H. \quad (4.4)$$

As usual, we denote the diameter of a bounded open set  $\mathcal{D}$  by  $H_{\mathcal{D}}$ .

**Lemma 4.2.1** *Let  $T$  be a substructure. Then, there exists a constant  $C > 0$ , which depends only on the aspect ratios of  $T$  and the elements in  $\mathcal{T}_h$ , such that for all  $\mathbf{u} \in X_{0;h}$ ,*

$$\|\text{curl}(\rho_H \mathbf{u})\|_{0;T}^2 \leq \|\text{curl} \mathbf{u}\|_{0;T}^2, \quad (4.5)$$

$$\|\rho_H \mathbf{u}\|_{0;T}^2 \leq C \left( \left(1 + \log \left(\frac{H}{h}\right)\right) \|\mathbf{u}\|_{0;T}^2 + H_T^2 \|\text{curl} \mathbf{u}\|_{0;T}^2 \right). \quad (4.6)$$

*Proof.* By (2.36) in Proposition 2.2.1, we have that

$$(\operatorname{curl}(\rho_H \mathbf{u}))|_T = (Q_H \operatorname{curl}(\mathbf{u}))|_T, \quad (4.7)$$

where  $Q_H$  is the  $L^2$ -projection operator onto the space of constants on  $T \in \mathcal{T}_H$ . Inequality (4.5) follows immediately.

Let  $E$  be an edge of  $\partial T$ , of length  $H_E$ , and let  $v_1$  and  $v_2$  be its endpoints. The restriction of the fine triangulation  $\mathcal{T}_h$  to  $E$  splits  $E$  into a union of nonoverlapping edges of the fine triangulation. Let  $e_1$  and  $e_2$  be the edges, which end at  $v_1$  and  $v_2$ , respectively, and let  $t_1$  and  $t_2$  be the elements in  $\mathcal{T}_h$  to which  $e_1$  and  $e_2$  belong. We now define a continuous, piecewise linear function,  $\vartheta_E$  on  $\partial T$  which satisfies:  $\vartheta_E$  is equal to one on  $E$ , except on  $e_1$  and  $e_2$ , where it decreases linearly to zero; it is extended by zero on  $\partial T \setminus E$ . As shown in [54, Section 5.3.2],  $\vartheta_E$  can be extended to  $T$ , as a continuous piecewise linear function, still denoted by  $\vartheta_E$ , with an absolute value less than or equal to 1, and with a gradient which is bounded by  $C/h$  on  $t_1$  and  $t_2$  and by  $C/r$  elsewhere. Here  $r$  is the distance to the closest of  $v_1$  or  $v_2$ .

Because of (2.28), it is enough to bound  $H_E(\mathbf{n} \times \rho_H \mathbf{u})|_E$ , for each edge  $E \subset \partial T$ . Since the function  $\mathbf{n} \times (\rho_H \mathbf{u})|_E$  is constant, we can use Stokes' theorem, (2.28), and (4.4), and find that

$$\begin{aligned} H_E(\mathbf{n} \times \rho_H \mathbf{u})|_E &= \int_E (\mathbf{n} \times \mathbf{u}) ds \\ &= \int_{\partial T} \vartheta_E (\mathbf{n} \times \mathbf{u}) + \frac{h_{e_1}}{2} (\mathbf{n} \times \mathbf{u}|_{e_1}) + \frac{h_{e_2}}{2} (\mathbf{n} \times \mathbf{u}|_{e_2}) \\ &= \int_T (\vartheta_E \operatorname{curl} \mathbf{u} + \mathbf{grad} \vartheta_E \times \mathbf{u}) + \frac{h_{e_1}}{2} (\mathbf{n} \times \mathbf{u}|_{e_1}) + \frac{h_{e_2}}{2} (\mathbf{n} \times \mathbf{u}|_{e_2}) \\ &\leq C (H \|\operatorname{curl} \mathbf{u}\|_{0;T} + |\vartheta_E|_{1;T} \|\mathbf{u}\|_{0;T} + \|\mathbf{u}\|_{0;t_1} + \|\mathbf{u}\|_{0;t_2}). \end{aligned} \quad (4.8)$$

We next consider the second term on the right hand side of (4.8) in more detail.

To obtain an upper bound for  $|\vartheta_E|_{1;T}$ , we split  $T$  into  $t_1 \cup t_2$  and  $T \setminus (t_1 \cup t_2)$

$$\begin{aligned}
|\vartheta_E|_{1;T}^2 &= \int_{t_1 \cup t_2} |\mathbf{grad} \vartheta_E|^2 dx + \int_{T \setminus (t_1 \cup t_2)} |\mathbf{grad} \vartheta_E|^2 dx \\
&\leq C \left( \int_{t_1 \cup t_2} \frac{1}{h^2} dx + \int_{T \setminus (t_1 \cup t_2)} \frac{1}{r^2} dx \right) \leq C \left( 1 + \int_h^H \int_0^{2\pi} \frac{1}{r} d\phi dr \right) \\
&\leq C \left( 1 + \log \left( \frac{H}{h} \right) \right).
\end{aligned} \tag{4.9}$$

Taking (2.28), (4.8), and (4.9) into account, we find (4.6) by summing over all  $E \subset \partial T$ .  $\square$

**Remark 4.2.1** *We can obtain a similar estimate for the energy norm on the substructure  $T$ . However in this case, the constant also depends on the ratio of the coefficients*

$$\begin{aligned}
\int_T B (\rho_H \mathbf{u}) \cdot (\rho_H \mathbf{u}) dx &\leq C \frac{\gamma_T}{\beta_T} \left( 1 + \log \left( \frac{H}{h} \right) \right) \int_T B \mathbf{u} \cdot \mathbf{u} dx \\
&\quad + C \frac{H_T^2 \gamma_T}{a_T} \int_T a \operatorname{curl} \mathbf{u} \operatorname{curl} \mathbf{u} dx.
\end{aligned}$$

#### 4.2.4 Main result

In this section, we will prove our main result, i.e., a bound for the condition number of the additive Schwarz operator, defined in (2.51), associated to the decomposition (4.3). A bound for the error operator of the corresponding multiplicative operator, defined in (2.52), can also be found using Lemma 2.3.3.

We proceed by first introducing an auxiliary decomposition of the Nédélec space  $X_{0;h}(\Omega)$ , related to the Laplace operator, and prove, in Lemma 4.2.3, that a stable splitting can be found. To do so, we will employ some results for piecewise linear continuous functions. We will then use this result and Lemma 2.3.1 to prove a lower bound for the smallest eigenvalue of the additive method. We conclude this section by showing that there is also a bound that is independent of the the ratio of the coefficients  $B$  and  $a$  in (4.1). As is often the case, a good bound for the

largest eigenvalue is routine and can be obtained by a standard coloring argument; see, e.g. [54, Page 165].

We first consider the following splitting:

$$X_{0;h} = X_{0;H} + \sum_{T \in \mathcal{T}_H} X_T + \sum_{E \in \mathcal{E}_H} \tilde{X}_E. \quad (4.10)$$

For every coarse edge  $E$ , the space  $\tilde{X}_E$  consists of the gradient of functions in  $\mathcal{S}_{0;h}(T_E)$ , which are discrete harmonic with respect to the Laplace operator on  $T_i$  and  $T_j$ , i.e., the extension with smallest  $H^1$  semi-norm of all finite element functions with the given boundary values.

It is then easy to see that

$$X_{0;H} \cap X_T = X_{0;H} \cap \tilde{X}_E = \tilde{X}_E \cap X_T = \{0\}, \quad E \in \mathcal{E}_H, T \in \mathcal{T}_H.$$

Furthermore, for  $T_1 \neq T_2$  and  $E_1 \neq E_2$ , the spaces  $X_{T_1}$  and  $X_{T_2}$  as well as  $\tilde{X}_{E_1}$  and  $\tilde{X}_{E_2}$  have an empty intersection. Counting the degrees of freedom then guarantees that (4.10) is a direct sum.

We remark that  $\tilde{X}_E$  is not defined by solving a homogeneous Maxwell equation with boundary data given by piecewise constant functions, with zero averages over the edges; see below for a discussion of that case.

We will need the following result for continuous, piecewise linear functions. A proof can be found in [59, Lemma 3.3].

**Lemma 4.2.2** *Let  $\phi \in \mathcal{S}_h^1(\Omega)$  and  $\eta := \phi - \Pi_H^{\mathcal{S}^1} \phi$ , where  $\Pi_H^{\mathcal{S}^1} \phi$  is the piecewise linear interpolant on the coarse triangulation. Then the following estimate holds*

$$\sum_{E \subset \partial T} |\eta|_{H^{1/2}(\partial T)}^2 \leq C \left(1 + \log \frac{H}{h}\right)^2 |\phi|_{1;T}^2.$$

We are now ready to prove the following lemma.

**Lemma 4.2.3** *For each  $\mathbf{u} \in X_{0;h}$ , there exists a unique decomposition*

$$\mathbf{u} = \mathbf{u}_H + \sum_{T \in \mathcal{T}_H} \mathbf{u}_T + \sum_{E \in \mathcal{E}_H} \tilde{\mathbf{u}}_E, \quad (4.11)$$

corresponding to (4.10), such that

$$a(\mathbf{u}_H, \mathbf{u}_H) + \sum_{T \in \mathcal{T}_H} a(\mathbf{u}_T, \mathbf{u}_T) + \sum_{E \in \mathcal{E}_H} a(\tilde{\mathbf{u}}_E, \tilde{\mathbf{u}}_E) \leq C \left(1 + \log \left(\frac{H}{h}\right)\right)^2 a(\mathbf{u}, \mathbf{u}),$$

with a constant  $C > 0$ , independent of  $h$ ,  $H$ , and  $\mathbf{u}$ .

*Proof.* We have already proven that the decomposition (4.10) is unique. Because of this uniqueness and  $\rho_H(\mathbf{u} - \mathbf{u}_H) = 0$ , we obtain

$$\mathbf{u}_H = \rho_H \mathbf{u}.$$

Using Lemma 4.2.1, we immediately obtain an upper bound for the first term;

$$a(\mathbf{u}_H, \mathbf{u}_H) \leq C \eta \left(1 + \log \frac{H}{h}\right) a(\mathbf{u}, \mathbf{u}),$$

where  $\eta$  depends on the coefficients. An upper bound for  $\eta$  is given by

$$\max_{T \in \mathcal{T}_H} \max \left( \frac{\gamma_T}{\beta_T}, \frac{H_T^2 \gamma_T}{a_T} \right); \quad (4.12)$$

see Remark 4.2.1.

The upper bound for the remaining terms is established on the substructure level, and the global result is obtained by summing over all substructures.

Let us consider a generic substructure  $T$ . For an upper bound of  $\|\tilde{\mathbf{u}}_E\|_{0;T}$ , we proceed by further decomposing the subspaces  $X_{0;H}$ ,  $X_E$ , and  $X_T$ , restricted to  $T$ , into gradient spaces and orthogonal complements.

We recall that  $X_{0;H}$  restricted to  $T$  is equal to  $\mathcal{R}(T)$  and thus each  $\mathbf{u}_H \in X_{0;H}$  can be written on  $T \in \mathcal{T}_H$  as

$$\mathbf{u}_H|_T = \mathbf{grad} \phi_0 + \alpha_T \begin{pmatrix} y - y_T \\ x_T - x \end{pmatrix} := \mathbf{grad} \phi_0 + \mathbf{u}_0,$$

where  $\phi_0$  is a linear function and  $(x_T, y_T)$  is the center of gravity of the  $T$ . Then, it can be easily seen that this is a  $L^2$ -orthogonal decomposition and that

$$\|\mathbf{u}_0\|_{0;T} \leq CH \|\mathbf{curl} \mathbf{u}_0\|_{0;T}. \quad (4.13)$$

For the local subspace  $X_T = X_{0;h}(T)$ , we use the orthogonal splitting already introduced in (2.41), for  $\Omega = T$ . Each  $\mathbf{u}_T \in X_T = X_{0;h}(T)$  can be written as

$$\mathbf{u}_T = \mathbf{grad} \phi_T + \mathbf{u}_\perp,$$

with  $\phi_T \in \mathcal{S}_{0;h}(T)$  and  $\mathbf{u}_\perp \in \mathcal{N}\mathcal{D}_{0;h}^\perp(T)$ .

By the definition of  $\tilde{X}_E$ , each  $\tilde{\mathbf{u}}_E$  is the gradient of a continuous piecewise linear function  $\phi_E$ .

By defining

$$\psi := \phi_0 + \phi_T + \sum_{E \subset \partial T} \phi_E, \quad \mathbf{w} := \mathbf{u}_0 + \mathbf{u}_\perp,$$

we obtain the following decomposition for  $\mathbf{u}$  on  $T$

$$\mathbf{u} = \mathbf{grad} \psi + \mathbf{w}. \quad (4.14)$$

We remark that this is not an orthogonal decomposition.

It follows, by definition, that  $\phi_0 + \sum_{E \subset \partial T} \phi_E$  is a discrete harmonic function. Applying Lemma 4.2.2, we obtain

$$\sum_{E \subset \partial T} |\phi_E|_{H^{1/2}(\partial T)}^2 \leq C \left(1 + \log \frac{H}{h}\right)^2 \left|\phi_0 + \sum_{E \subset \partial T} \phi_E\right|_{1;T}^2. \quad (4.15)$$

Using (4.15), the equivalence between the  $H^{1/2}$ -semi-norm on  $\partial T$  and the  $H^1$ -semi-norm on  $T$  for discrete harmonic functions, we obtain

$$\sum_{E \subset \partial T} \|\tilde{\mathbf{u}}_E\|_{0;T}^2 \leq C \sum_{E \subset \partial T} |\phi_E|_{H^{1/2}(\partial T)}^2. \quad (4.16)$$

Since  $\mathbf{grad} \phi_T$  and  $\mathbf{grad}(\phi_0 + \sum_{E \subset \partial T} \phi_E)$  are orthogonal in  $L^2$ , (4.15) and (4.16) yield

$$\sum_{E \subset \partial T} \|\tilde{\mathbf{u}}_E\|_{0;T}^2 \leq C \left(1 + \log \frac{H}{h}\right)^2 \|\mathbf{grad} \psi\|_{0;T}^2.$$

In a last step, we have to bound  $\|\mathbf{grad} \psi\|_{0;T}^2$  by  $\|\mathbf{u}\|_{\text{curl};T}^2$ . Using inequality (2.42) for  $\Omega = T$ , applied to  $\mathbf{u}_\perp$ , and (4.13), we obtain

$$\|\mathbf{w}\|_{0;T}^2 \leq C_\perp H^2 (\|\text{curl} \mathbf{u}_\perp\|_{0;T}^2 + \|\text{curl} \mathbf{u}_0\|_{0;T}^2).$$



Since  $\text{curl } \mathbf{u}_H$  is constant and  $\text{curl } \mathbf{u}_\perp$  has mean value zero on  $T$ , they are orthogonal in  $L^2(T)$ , and we finally find

$$\|\mathbf{w}\|_{0;T}^2 \leq C_\perp H^2 \|\text{curl } \mathbf{w}\|_{0;T}^2. \quad (4.17)$$

Using (4.14), we obtain

$$\|\mathbf{u}\|_{\text{curl};T}^2 = |\psi|_{1;T}^2 + \|\mathbf{w}\|_{\text{curl};T}^2 + 2(\mathbf{w}, \mathbf{grad } \psi)_{0;T}.$$

Applying Young's inequality gives

$$2(\mathbf{w}, \mathbf{grad } \psi)_{0;T} \leq \epsilon |\psi|_{1;T}^2 + \frac{1}{\epsilon} \|\mathbf{w}\|_{0;T}^2, \quad \epsilon > 0.$$

Employing (4.17), for  $0 < \epsilon < 1$ , we obtain

$$\|\mathbf{u}\|_{\text{curl};T}^2 \geq (1 - \epsilon) |\psi|_{1;T}^2 + (1 + (1 - \epsilon^{-1}) C_\perp H^2) \|\text{curl } \mathbf{w}\|_{0;T}^2.$$

The choice  $\epsilon = C_\perp H^2 / (C_\perp H^2 + 1)$  gives

$$|\psi|_{1;T}^2 \leq C \|\mathbf{u}\|_{\text{curl};T}^2,$$

and thus

$$\sum_{E \subset \partial T} |\tilde{\mathbf{u}}_E|_{0;T}^2 \leq C \left(1 + \log \frac{H}{h}\right)^2 \|\mathbf{u}\|_{\text{curl};T}^2.$$

The norm of  $\mathbf{u}_T$  on  $T$  is then bounded using the triangle inequality. Summing over all subdomains, we finally get

$$\|\mathbf{u}_H\|_{\text{curl};\Omega}^2 + \sum_{T \in \mathcal{T}_H} \|\mathbf{u}_T\|_{\text{curl};\Omega}^2 + \sum_{E \subset \partial T} \|\tilde{\mathbf{u}}_E\|_{\text{curl};\Omega}^2 \leq C \left(1 + \log \left(\frac{H}{h}\right)\right)^2 \|\mathbf{u}\|_{\text{curl};\Omega}^2.$$

Lemma 4.2.3 is now a consequence of the norm equivalence of the graph norm  $\|\cdot\|_{\text{curl}}$  and the energy norm  $\|\cdot\|_a$ .  $\square$

A detailed analysis of the constant  $C$  shows that it depends on  $\eta$  but not on jumps of the coefficients. In case of time-dependent Maxwell's equations  $\eta$  tends to infinity if the time step tends to zero, and then the constant  $C$  in Lemma 4.2.3 deteriorates. This is due to the fact that the interpolation operator  $\rho_H$  is not

logarithmically stable with respect of the  $L^2$ -norm. As previously remarked, the best bound for the  $L^2$ -norm alone is

$$\|\rho_H \mathbf{u}\|_{0;T} \leq C \frac{H}{h} \|\rho_H \mathbf{u}\|_{0;T}.$$

In contrast to the auxiliary decomposition (4.10), (4.3) is stable with respect to the  $L^2$ -norm, as we will show later.

We will now consider the decomposition given by (4.3).

**Theorem 4.2.1** *For each  $\mathbf{u} \in X_{0;h}$ , there exists a decomposition*

$$\mathbf{u} = \mathbf{u}_H + \sum_{T \in \mathcal{T}_H} \mathbf{u}_T + \sum_{E \in \mathcal{E}_H} \mathbf{u}_E,$$

corresponding to (4.3) such that

$$a(\mathbf{u}_H, \mathbf{u}_H) + \sum_{T \in \mathcal{T}_H} a(\mathbf{u}_T, \mathbf{u}_T) + \sum_{E \in \mathcal{E}_H} a(\mathbf{u}_E, \mathbf{u}_E) \leq C \left(1 + \log \left(\frac{H}{h}\right)\right)^2 a(\mathbf{u}, \mathbf{u}),$$

with a constant  $C > 0$ , independent of  $h$  and  $\mathbf{u}$ .

*Proof.* The proof is based on the stability of the splitting (4.10). Each function in  $\tilde{X}_E$  can be written as the gradient of a piecewise discrete harmonic function  $\phi_E$  with respect to the Laplace operator, while this is not generally true for a function  $\mathbf{u}_E \in X_E$ . However, it can be characterized as the solution of a minimization problem. Choosing  $\mathbf{u}_H = \rho_H \mathbf{u}$ , which ensures that  $\mathbf{u}_E \times \mathbf{n}|_E = \tilde{\mathbf{u}}_E \times \mathbf{n}|_E$ , we obtain

$$a(\mathbf{u}_E, \mathbf{u}_E) = \min_{\substack{\mathbf{v}_E \in X_{0;h}(T_E) \\ \mathbf{v}_E \times \mathbf{n}|_E = \mathbf{u}_E \times \mathbf{n}|_E}} a(\mathbf{v}_E, \mathbf{v}_E) \leq a(\tilde{\mathbf{u}}_E, \tilde{\mathbf{u}}_E).$$

We remark that the coarse space contribution  $\mathbf{u}_H$  is exactly the same as in the direct decomposition of Lemma 4.2.3.  $\square$

Finally, we consider the splitting (4.3) for the limit case  $a = 0$ . In this case, the bilinear form  $a(\cdot, \cdot)$  is just a weighted  $L^2$ -scalar product

$$a(\mathbf{v}, \mathbf{w}) = \int_{\Omega} B \mathbf{w} \mathbf{v} \, dx.$$

Let us, for the moment, decompose  $\mathbf{u}$  in

$$\mathbf{u} = \sum_{T \in \mathcal{T}_H} \hat{\mathbf{u}}_T + \sum_{E \in \mathcal{E}_H} \hat{\mathbf{u}}_E$$

where  $\hat{\mathbf{u}}_E \in X_{0;h}$  with  $\lambda_e(\hat{\mathbf{u}}_E) := \lambda_e(\mathbf{u}_E)$ ,  $e \subset E$  and  $\lambda_e(\hat{\mathbf{u}}_E) = 0$  elsewhere, and  $\mathbf{u}_T \in X_T$ . Then the bound (2.28) guarantees that

$$\sum_{E \in \mathcal{E}_H} \|\hat{\mathbf{u}}_E\|_{0;\Omega}^2 \leq C \|\mathbf{u}\|_{0;\Omega}^2.$$

We remark that  $\hat{\mathbf{u}}_E$  is an extension by zero to the interior of the substructures and in general not contained in  $X_E$ . Considering now the unique decomposition of  $\mathbf{u}$ ,

$$\mathbf{u} = \sum_{T \in \mathcal{T}_H} \mathbf{u}_T + \sum_{E \in \mathcal{E}_H} \mathbf{u}_E$$

where  $\mathbf{u}_T \in X_T$  and  $\mathbf{u}_E \in X_E$ , we get, because of the minimization property of  $\mathbf{u}_E$ ,

$$\sum_{E \in \mathcal{E}_H} \|\tilde{\mathbf{u}}_E\|_{0;\Omega}^2 \leq C \|\mathbf{u}\|_{0;\Omega}^2.$$

This proves the stability of the decomposition of  $\mathbf{u}$  with respect to the  $L^2$ -norm. Thus as  $\eta$  becomes large, we expect an upper bound for the condition number which is independent of the ratio  $H/h$ . We remark that this result cannot be obtained with the splitting (4.10).

In the second limit case,  $B = 0$ , the bilinear form  $a(\cdot, \cdot)$  is no longer positive definite. However, we can still work with a preconditioned cg-iteration in a subspace, if the right hand side  $\mathbf{f}$  is consistent. Then the stability of  $\rho_H$  with respect to the  $L^2$ -norm of the curl, (4.5), gives us optimal results, i.e. a condition number which is independent of the ratio  $H/h$ .

**Remark 4.2.2** *As we have already pointed out in the beginning of Section 4.2, our results and analysis carried out for the space  $H(\mathbf{curl}; \Omega)$  and Nédélec elements are also valid for  $H(\mathbf{div}; \Omega)$  and the lowest-order Raviart–Thomas elements.*

## 4.2.5 Numerical results

In this section, we present some numerical results on the performance of the iterative substructuring method described in the previous sections, when varying the diameters of the coarse and fine meshes, and the coefficients  $a$  and  $B$ . We refer to [54], for a general discussion of practical issues concerning Schwarz methods. Our numerical results are given for a decomposition slightly different than (4.3)

$$X_{0;h} = X_{0;H} + \sum_{E \in \mathcal{E}_H} X_{0;h}(T_E).$$

Because of the orthogonality between the spaces  $\{X_T\}$  and  $\{X_E\}$ , this decomposition is stable if and only if (4.3) is. The corresponding preconditioner is

$$B = R_H^T A_H^{-1} R_H + \sum_{E \in \mathcal{E}_H} (R_E^T A_E^{-1} R_E),$$

where the extension matrices  $R_H^T$  and  $\{R_E^T\}$  map the degrees of freedom of the coarse and local spaces, respectively, into the the global ones, and  $A_H$  and  $\{A_E\}$  are the matrices relative to Dirichlet problems on the coarse mesh and on the regions  $T_E$ ; see Section 2.3.

We have considered the domain  $\Omega = (0, 1)^2$  and a uniform rectangular triangulations  $\mathcal{T}_h$  and  $\mathcal{T}_H$ . The fine triangulation  $\mathcal{T}_h$  consists of  $n^2$  square elements, with  $h = 1/n$ . The matrix  $B$  is given by

$$B = \text{diag}\{b, b\}.$$

In Table 4.1, we show the estimated condition number and the number of iterations in order to obtain a reduction of the residual norm by a factor  $10^{-6}$ , as a function of the dimensions of the fine and coarse meshes. For fixed ratios  $H/h$ , the condition number is quite insensitive to the dimension of the fine mesh. The number of iterations varies slowly with  $H/h$  and our results compare well with those for finite element approximations in  $H^1$  of Laplace's equation; see, e.g. [54]. We remark that the largest eigenvalue is bounded by 5 in all the cases in Table 4.1, except for  $(n = 32, H/h = 16)$  and  $(n = 64, H/h = 32)$ ; the latter cases correspond to a partition of 2 by 2 subregions and, consequently, the bound for

Table 4.1: Estimated condition number and number of CG iterations for a residual norm reduction of  $10^{-6}$  (in parentheses), versus  $H/h$  and  $n$ . Case of  $a = 1$ ,  $b = 1$ .

$H/h$	32	16	8	4	2
n=32	-	20.23 (11)	26.50 (20)	19.10 (20)	12.86 (17)
n=64	26.27 (11)	35.94 (20)	27.16 (21)	19.00 (17)	12.90 (16)
n=128	46.83 (20)	36.68 (18)	27.06 (17)	18.92 (16)	x
n=192	-	36.71 (17)	27.00 (17)	18.90 (16)	x
n=256	47.80 (18)	36.66 (17)	26.97 (16)	18.89 (16)	x

the largest eigenvalue is 3.

In Figure 4.1, we plot the results of Table 4.1, together with the best second order logarithmic polynomial least-square fit. The relative fitting error is about 1.8 per cent. Our numerical results are therefore in good agreement with the theoretical bound obtained in the previous section and confirm that our bound is sharp.

In Table 4.2, we show some results when the ratio of the coefficients  $b$  and  $a$  is changed. For a fixed value of  $n = 128$  and  $a = 1$ , the estimated condition number and the number of iterations are shown as functions of  $H/h$  and  $b$ . The numerical results also confirm the theoretical results in the limit cases  $b = 0$  and  $b = \infty$ . More precisely, we remark that the condition number tends to be independent of the ratio  $H/h$  when the ratio  $b/a$  is very small or very large. We recall that when Maxwell's equations are discretized with an implicit time-scheme, the time step is related to the ratio  $b/a$ . The iterative substructuring method presented in this chapter therefore appears very attractive for the solution of linear systems arising from the finite element approximation of time-dependent Maxwell's equations.

In Table 4.3, we show some results when the coefficient  $b$  has jumps across the substructures. We consider the checkerboard distribution shown in Figure 4.2, where  $b$  is equal to  $b_1$  in the shaded area and to  $b_2$  elsewhere. For a fixed value of  $n = 128$ ,  $b_1 = 100$ , and  $a = 1$ , the estimated condition number and the number of iterations are shown as functions of  $H/h$  and  $b_2$ . For  $b_2 = 100$ , the

Table 4.2: Estimated condition number and number of CG iterations for a residual norm reduction of  $10^{-6}$  (in parentheses), versus  $H/h$  and  $b$ . Case of  $n = 128$  and  $a = 1$ .

$H/h$	32	16	8	4
$b = 1e - 5$	3.87 (10)	4.68 (13)	4.86 (13)	4.92 (13)
$b = 1e - 4$	3.87 (10)	36.3 (16)	26.2 (16)	13 (15)
$b = 1e - 3$	16.9 (11)	36.5 (16)	27 (16)	18.7 (16)
$b = 1e - 2$	46.9 (14)	36.7 (17)	27.1 (16)	18.9 (16)
$b = 1e - 1$	46.9 (14)	36.7 (17)	27.1 (17)	18.9 (16)
$b = 1$	46.8 (20)	36.7 (18)	27.1 (17)	18.9 (16)
$b = 1e + 1$	45.3 (22)	36.4 (22)	27 (18)	18.9 (17)
$b = 1e + 2$	40.8 (25)	34.8 (23)	26.7 (20)	18.9 (19)
$b = 1e + 3$	29.8 (24)	28.4 (23)	24.5 (21)	18.4 (19)
$b = 1e + 4$	17.4 (18)	17.3 (17)	16.8 (18)	15.3 (17)
$b = 1e + 5$	9.41 (14)	9.37 (14)	9.3 (14)	9.15 (14)

coefficient  $b$  has a uniform distribution, and this corresponds to a minimum for the condition number and the number of iterations. When  $b_2$  decreases or increases, the condition number and the number of iterations also increase, but they can still be bounded independently of  $b_2$ .

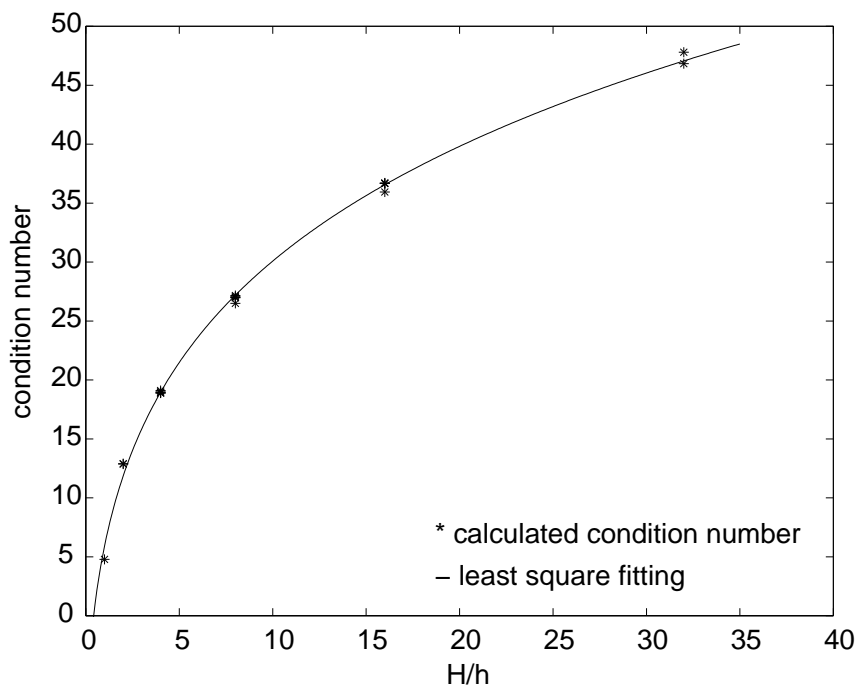


Figure 4.1: Estimated condition number from Table 4.1 (asterisk) and least-square second order logarithmic polynomial (solid line), versus  $H/h$ ; relative fitting error about 1.8 per cent.

Table 4.3: Checkerboard distribution for  $b$ :  $(b_1, b_2)$ . Estimated condition number and number of CG iterations for a residual norm reduction of  $10^{-6}$  (in parentheses), versus  $H/h$  and  $b_2$ . Case of  $n = 128$ ,  $a = 1$ , and  $b_1 = 100$ .

$H/h$	4	8	16
$b_2 = 1e - 3$	18.9708 (25)	25.2740 (27)	29.2245 (30)
$b_2 = 1e - 2$	18.9700 (25)	25.2707 (27)	29.2087 (30)
$b_2 = 1e - 1$	18.9630 (25)	25.2432 (27)	29.0817 (30)
$b_2 = 1$	18.9343 (25)	25.1751 (27)	28.9695 (30)
$b_2 = 1e + 1$	18.8344 (24)	25.0193 (28)	28.7278 (29)
$b_2 = 1e + 2$	18.0958 (19)	23.9682 (19)	28.0473 (21)
$b_2 = 1e + 3$	17.1748 (25)	21.0009 (28)	28.2490 (28)
$b_2 = 1e + 4$	17.0405 (23)	24.8333 (24)	30.4664 (23)
$b_2 = 1e + 5$	18.0374 (18)	25.7533 (18)	30.7846 (17)
$b_2 = 1e + 6$	18.2865 (15)	25.7317 (14)	5.4293 (11)

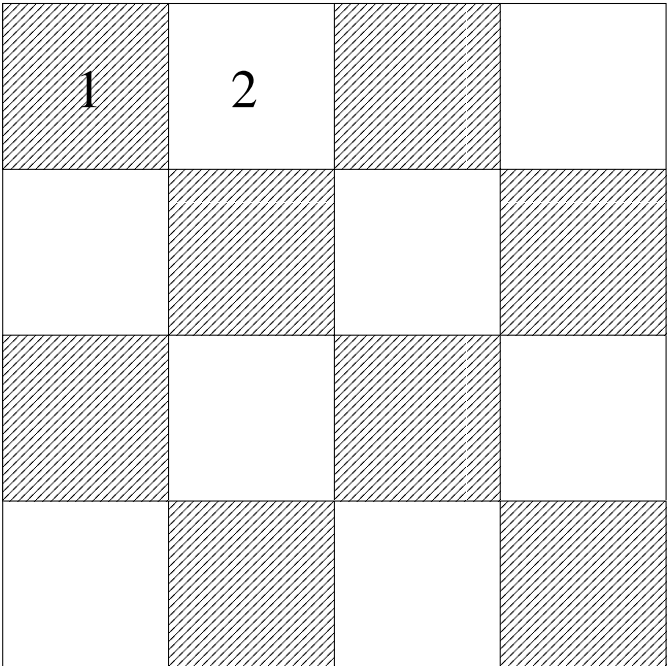


Figure 4.2: Checkerboard distribution of the coefficients in the unit square.



## 4.3 A face space method in three dimensions

In this section, we will present some results for the space  $H(\operatorname{div}; \Omega)$  in three dimensions. The algorithm presented here is the generalization to the three-dimensional case of the edge space method described in Section 4.2. But, as opposed to the two-dimensional case, it has no direct generalization to  $H(\mathbf{curl}; \Omega)$  in three dimensions, since, in this case, the Raviart–Thomas and Nédélec spaces are completely different; see Section 2.2.

### 4.3.1 Discrete problem and finite element spaces

Let  $\Omega$  be a bounded Lipschitz polyhedron in  $\mathbb{R}^3$ . We will consider problems involving the bilinear form

$$a(\mathbf{u}, \mathbf{v}) := \int_{\Omega} (a \operatorname{div} \mathbf{u} \operatorname{div} \mathbf{v} + B \mathbf{u} \cdot \mathbf{v}) \, dx, \quad \mathbf{u}, \mathbf{v} \in H(\operatorname{div}; \Omega). \quad (4.18)$$

As in the two-dimensional case, the coefficient matrix  $B$  is a symmetric uniformly positive definite matrix-valued function with  $b_{i,j} \in L^\infty(\Omega)$ ,  $1 \leq i, j \leq n$ , and  $a \in L^\infty(\Omega)$  is a positive function bounded away from zero.

Let  $\mathcal{T}_H$  be a triangulation of  $\Omega$ , of maximum diameter  $H$ , consisting of tetrahedra or hexahedra, and let  $\mathcal{T}_h$  be *shape-regular* and *quasi-uniform* refinement of  $\mathcal{T}_H$ , with characteristic diameter  $h$ . A generic element of  $\mathcal{T}_h$  and  $\mathcal{T}_H$  will be denoted by  $t$  and  $T$ , respectively. The sets of faces and edges of the triangulations  $\mathcal{T}_h$  and  $\mathcal{T}_H$ , are denoted by  $\mathcal{F}_h, \mathcal{F}_H$  and  $\mathcal{E}_h, \mathcal{E}_H$ , respectively. A generic face will be denoted by  $f$  and  $F$ , and a generic edge by  $e$  and  $E$ , respectively. As before, the elements of the coarse triangulation are called substructures. For each interior face  $F \in \mathcal{F}_H$ , there are two elements  $T_i, T_j \in \mathcal{T}_H$  such that  $\bar{F} := \partial T_i \cap \partial T_j$ , and we set

$$\bar{T}_F := \bar{T}_i \cup \bar{T}_j.$$

We also suppose that the coefficients  $a$  and  $B$  are constant on each substructure  $T$  and equal to  $a_T$  and  $B_T$ , respectively. They may have arbitrary jumps across the inner faces of the substructures. In addition, the matrices  $\{B_T\}$  satisfy

$$\beta_T \eta^T \eta \leq \eta^T B_T \eta \leq \gamma_T \eta^T \eta, \quad \forall \eta \in \mathbb{R}^3,$$

where  $\beta_T$  and  $\gamma_T$  are positive constants, which can depend on the substructure  $T$ .

In this section, we only consider, in full detail, triangulations based on hexahedra, but our results are equally valid for finite element spaces built on tetrahedra. Much of the analysis is carried out on a cubic substructure divided into cubic elements but the results remain equally valid if the elements and substructures are images of a reference cube under sufficiently benign mappings, which effectively means that their aspect ratios have to remain uniformly bounded. We remark that our analysis is carried out locally for one substructure at a time. We can therefore interpret the factor  $H/h$ , which appears in our the estimates, as

$$\max_{T \in \mathcal{T}_H} \max_{\substack{t \in \mathcal{T}_h \\ t \subset T}} \frac{H_T}{H_t}.$$

We consider the lowest order Raviart–Thomas elements defined on the fine and coarse meshes, respectively,

$$\begin{aligned} X_{0;h} &:= \mathcal{RT}_{0;h}^1(\Omega) = \mathcal{RT}_{0;h}(\Omega), \\ X_{0;H} &:= \mathcal{RT}_{0;H}^1(\Omega) = \mathcal{RT}_{0;H}(\Omega), \end{aligned}$$

conforming in  $H_0(\operatorname{div}; \Omega)$ ; see Section 2.2.1. We will also need the the finite element space  $X_{0;h}(\mathcal{D}) \subset H_0(\operatorname{div}; \mathcal{D})$ , when  $\mathcal{D}$  is a substructure or the union of two substructures that have a common face, and  $X_h(\mathcal{D}) := \mathcal{RT}_h^1(\mathcal{D})$ , when  $\mathcal{D}$  is an arbitrary Lipschitz polyhedron. We will introduce some finite element spaces defined on the boundaries of the substructures in Section 4.3.3.

### 4.3.2 Description of the algorithm

We will consider the approximate problem:

Find  $\mathbf{u} \in X_{0;h}$  such that

$$a(\mathbf{u}, \mathbf{v}) = (\mathbf{f}, \mathbf{v}) \quad \forall \mathbf{v} \in X_{0;h}, \tag{4.19}$$

where  $\mathbf{f} \in L^2(\Omega)^3$ . The generalization to the case of the  $\mathcal{RT}_h(\Omega)$  (Neumann boundary conditions) does not present any particular difficulty.

We decompose  $X_{0;h}$  into the coarse space  $X_{0;H}$ , the interior spaces  $\{X_T, T \in \mathcal{T}_H\}$

$$X_T := X_{0;h}(T), \quad T \in \mathcal{T}_H,$$

and the face spaces  $\{X_F, F \in \mathcal{F}_H\}$

$$X_F := \{\mathbf{v} \in X_{0;h} \mid a(\mathbf{v}, \mathbf{w}) = 0, \mathbf{w} \in X_{T_i} \cup X_{T_j}, \text{supp } \mathbf{v} \subset \overline{T}_F\}.$$

We note that any element  $\mathbf{v} \in X_F$  is the harmonic extension of a function defined on the face  $F$  to  $T_F$ , and that it is defined uniquely by its value of  $\mathbf{n} \cdot \mathbf{v}$  on  $F$ . In addition, the coarse space  $X_{0;H}$  is contained in the union of the face and interior spaces, and, consequently, the decomposition

$$X_{0;h} = X_{0;H} + \sum_{T \in \mathcal{T}_H} X_T + \sum_{F \in \mathcal{F}_H} X_F, \quad (4.20)$$

is not a direct sum.

We will use the original bilinear form  $a(\cdot, \cdot)$  on all the subspaces  $X_{0;h}$ ,  $X_F$ , and  $X_T$ .

### 4.3.3 Technical tools

#### A stability estimate for the interpolation operator

As in the two-dimensional case, we need a stability estimate for the interpolation operator onto the coarse space

$$\rho_H : X_{0;h} \longrightarrow X_{0;H}.$$

In particular, this interpolant will be logarithmically stable in the  $\|\cdot\|_{\text{div}}$  norm. We note that the best bound for the  $L^2$ -norm alone involves a factor of  $H/h$ , as can easily be seen by considering an element  $\mathbf{u}$ , for which all the interior degrees of freedom vanish.

The interpolation operator has already been defined in Section 2.2.1. In particular, we recall that  $\rho_H$  is defined in terms of the degrees of freedom of the coarse space  $X_{0;H}$ , i.e.

$$\lambda_F(\rho_H \mathbf{u}) := \frac{1}{|F|} \int_F \mathbf{n} \cdot \mathbf{u} \, ds, \quad F \in \mathcal{F}_H. \quad (4.21)$$

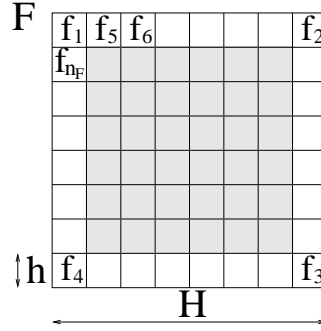


Figure 4.3: Decomposition of the face  $F$ .

**Lemma 4.3.1** *Let  $T$  be a substructure. Then, there exists a constant  $C > 0$ , which depends only on the aspect ratios of  $T$  and the elements in  $\mathcal{T}_h$ , such that for all  $\mathbf{u} \in X_{0;h}$ ,*

$$\|\operatorname{div}(\rho_H \mathbf{u})\|_{0;T}^2 \leq \|\operatorname{div} \mathbf{u}\|_{0;T}^2, \quad (4.22)$$

$$\|\rho_H \mathbf{u}\|_{0;T}^2 \leq C \left( \left(1 + \log \left(\frac{H}{h}\right)\right) \|\mathbf{u}\|_{0;T}^2 + H_T^2 \|\operatorname{div} \mathbf{u}\|_{0;T}^2 \right). \quad (4.23)$$

*Proof.* By (2.39) in Proposition 2.2.1, we have that

$$(\operatorname{div}(\rho_H \mathbf{u}))|_T = (Q_H \operatorname{div}(\mathbf{u}))|_T, \quad (4.24)$$

where  $Q_H$  is the  $L^2$ -projection operator onto the space of constants on  $T \in \mathcal{T}_H$ . Inequality (4.22) follows immediately.

The proof of (4.23) is similar to the one of the analogous estimate in Lemma 4.2.1, and uses Green's formula, (2.28), and a partition of unity very similar to one given in [22] for the simplex case. We consider a face  $F \subset \partial T$ , and note that it is partitioned into  $N_F$  non-overlapping faces  $f \in \mathcal{F}_h$ ; see Figure 4.3 depicting, for simplicity, just a very regular case. We then number these faces so that  $f_i$ ,  $1 \leq i \leq n_F$  have at least one vertex on an edge of  $F$ , (see Fig 4.3), and  $\{f_1, f_2, f_3, f_4\}$  are the faces that contain a corner point. Let  $t_i \subset T$ , be the associated elements. We note that since, by assumption, the triangulation of the face is quasi-uniform,  $n_F \leq C(H/h)$ .

Let  $\vartheta_F$  be a continuous, piecewise trilinear function defined on  $T$ . It vanishes on  $\partial T \setminus F$  and is equal to one at all the interior mesh points of  $F$ . The extension of

$\vartheta_F$  to the interior of  $T$  has values between zero and one, and the absolute value of its gradient is bounded by  $C/\max(r, h)$  where  $r$  denotes the distance to the wire-basket of  $T$ . We refer to [22] for an explicit construction of such a function for a simplex; this construction can easily be adapted to the cubic case. It is proved in [22] that

$$|\vartheta_F|_{1;T}^2 \leq C(1 + \log H/h)H, \quad \|\vartheta_F\|_{0;T}^2 \leq CH^3. \quad (4.25)$$

Because of (2.28), it is sufficient to bound  $\lambda_F(\rho_H \mathbf{u})$ , for each face  $F \subset \partial T$ . Applying Green's formula, we obtain

$$\begin{aligned} |F| \lambda_F(\rho_H \mathbf{u}) &= \int_F (\mathbf{u} \cdot \mathbf{n}) ds \\ &= \int_{\partial T} \vartheta_F (\mathbf{u} \cdot \mathbf{n}) ds + \frac{3}{4} \sum_{i=1}^4 |f_i| (\mathbf{u} \cdot \mathbf{n}|_{f_i}) + \frac{1}{2} \sum_{i=5}^{n_F} |f_i| (\mathbf{u} \cdot \mathbf{n}|_{f_i}) \\ &= \int_{\partial T} (\vartheta_F \operatorname{div} \mathbf{u} + \mathbf{grad} \vartheta_F \cdot \mathbf{u}) + \frac{3}{4} \sum_{i=1}^4 |f_i| \lambda_{f_i}(\mathbf{u}) + \frac{1}{2} \sum_{i=5}^{n_F} |f_i| \lambda_{f_i}(\mathbf{u}). \end{aligned}$$

By using (2.28), the absolute values of the last two terms can be bounded by

$$C \sum_{i=1}^{n_F} h^{1/2} \|\mathbf{u}\|_{0;t_i} \leq C n_F^{1/2} h^{1/2} \left( \sum_{i=1}^{n_F} \|\mathbf{u}\|_{0;t_i}^2 \right)^{1/2} \leq CH^{1/2} \|\mathbf{u}\|_{0;T},$$

and, by using (4.25), we find the following bound for  $|F| |\lambda_F(\rho_H \mathbf{u})|$

$$C \left( H^{3/2} \|\operatorname{div} \mathbf{u}\|_{0;T} + (H(1 + \log H/h))^{1/2} \|\mathbf{u}\|_{0;T} + H^{1/2} \|\mathbf{u}\|_{0;T} \right). \quad (4.26)$$

Observing that

$$\left( \sum_{i=1}^{n_F} h^{1/2} \|\mathbf{u}\|_{0;t_i} \right)^2 \leq n_F \sum_{i=1}^{n_F} h \|\mathbf{u}\|_{0;t_i}^2 \leq CH \|\mathbf{u}\|_{0;T}^2,$$

and summing over all  $F \subset \partial T$ , (4.26) finally gives

$$\|\rho_H \mathbf{u}\|_{0;T}^2 \leq CH^2 \|\operatorname{div} \mathbf{u}\|_{0;T}^2 + C \left( 1 + \log \left( \frac{H}{h} \right) \right) \|\mathbf{u}\|_{0;T}^2.$$

□

**Remark 4.3.1** *We can obtain a similar estimate for the energy norm on each substructure  $T$ :*

$$\begin{aligned} \int_T B (\rho_H \mathbf{u}) \cdot (\rho_H \mathbf{u}) dx &\leq C \frac{\gamma_T}{\beta_T} \left(1 + \log \left(\frac{H}{h}\right)\right) \int_T B \mathbf{u} \cdot \mathbf{u} dx \\ &\quad + C \frac{H_T^2 \gamma_T}{a_T} \int_T a \operatorname{div} \mathbf{u} \operatorname{div} \mathbf{u} dx. \end{aligned}$$

### Trace spaces

In this subsection, we will introduce some discrete trace spaces, together with an equivalent norm defined on them, and prove a decomposition lemma for these spaces. We recall that the normal component of a vector in  $H(\operatorname{div}; \Omega)$  on the boundary belongs to  $H^{-\frac{1}{2}}(\partial\Omega)$ , and a stability estimate was given in (2.4).

Given a substructure  $T$ , define  $S_H(\partial T)$  as the space of functions which are constant on each face  $F \subset \partial T$ ; its dimension is six. We also define  $S_h(\partial T)$  as the space of functions that are constant on each fine face  $f \in \mathcal{F}_h$ ,  $f \subset \partial T$ , and its subspace  $S_{0,h}(\partial T)$ , of functions that have mean value zero on  $\partial T$ . It is immediate to check that the normal component of a vector in  $X_h(T)$  belongs to  $S_h(\partial T)$ .

We will first introduce some norms in  $S_h(\partial T)$  and  $S_{0,h}(\partial T)$  that are equivalent to the  $H^{-\frac{1}{2}}$ -norm. The following lemma is valid for functions in  $H^{-\frac{1}{2}}(\partial\Omega)$ .

**Lemma 4.3.2** *There exists a constant  $c$ , which is independent of the diameter of  $\mathcal{D}$ , such that for each  $\psi \in H^{-\frac{1}{2}}(\partial\mathcal{D})$  with  $\langle \psi, 1 \rangle = 0$*

$$c \sup_{\substack{\phi \in H^{\frac{1}{2}}(\partial\mathcal{D}) \\ \phi \neq \text{const}}} \frac{\langle \psi, \phi \rangle}{|\phi|_{\frac{1}{2}; \partial\mathcal{D}}} \leq \|\psi\|_{-\frac{1}{2}; \partial\mathcal{D}} \leq \sup_{\substack{\phi \in H^{\frac{1}{2}}(\partial\mathcal{D}) \\ \phi \neq \text{const}}} \frac{\langle \psi, \phi \rangle}{|\phi|_{\frac{1}{2}; \partial\mathcal{D}}}. \quad (4.27)$$

*Proof.* The upper bound in (4.27) is an immediate consequence of the definition of the  $H^{-1/2}$ -norm. The proof of the lower bound in (4.27) is based on the following norm equivalence

$$c \|\phi\|_{\frac{1}{2}; \partial\mathcal{D}}^2 \leq |\phi|_{\frac{1}{2}; \partial\mathcal{D}}^2 + \frac{1}{H_{\mathcal{D}}^3} \left( \int_{\partial\mathcal{D}} \phi ds \right)^2 \leq C \|\phi\|_{\frac{1}{2}; \partial\mathcal{D}}^2. \quad (4.28)$$

This is a Poincaré-type inequality; see, e.g. [46, Chap. 2.7] for a classical introduction to such inequalities. We note that the scale factor results from writing down the result for a region of diameter one and using dilation. Then, the definition of the  $H^{-\frac{1}{2}}$ -norm and the assumption that  $\langle \psi, 1 \rangle = 0$  yield, for all real  $\alpha$ ,

$$\|\psi\|_{-\frac{1}{2};\partial\mathcal{D}} = \sup_{\substack{\phi \in H^{\frac{1}{2}}(\partial\mathcal{D}) \\ \phi \neq \text{const.}}} \frac{\langle \psi, \phi \rangle}{\|\phi - \alpha\|_{\frac{1}{2};\partial\mathcal{D}}}.$$

The lower bound is obtained by using (4.28) and choosing  $\alpha = \int_{\partial\mathcal{D}} \phi \, ds$ .  $\square$

As a second step, we replace the supremum over the whole space  $H^{\frac{1}{2}}(\partial T)$  by the supremum over a finite dimensional space, in the definition of the  $H^{-\frac{1}{2}}$ -norm. In order to do so, we have to introduce a suitable approximation of the space  $H^{\frac{1}{2}}(\partial T)$ . Our approximation  $V_h(\partial T)$  of  $H^{\frac{1}{2}}(\partial T)$  is given as a direct sum

$$V_h(\partial T) := Q_h(\partial T) + B_h(\partial T).$$

Here  $Q_h(\partial T)$  is the space of all continuous piecewise bilinear functions and  $B_h(\partial T)$  a space of bubble functions vanishing on the faces  $f \in \mathcal{F}_h$ ,  $f \subset \partial T$ :

$$\begin{aligned} Q_h(\partial T) &:= \{\phi \in C^0(\partial T), \phi|_f \in \mathbb{Q}_1(f), f \subset \partial T, f \in \mathcal{F}_h\}, \\ B_h(\partial T) &:= \{\phi \in C^0(\partial T), \phi|_f = \alpha_f \varphi_1 \varphi_2 \varphi_3 \varphi_4, f \subset \partial T, f \in \mathcal{F}_h, \alpha_f \in \mathbb{R}\}, \end{aligned}$$

where  $\varphi_i$ ,  $1 \leq i \leq 4$ , are the nodal basis functions that span  $\mathbb{Q}_1(f)$  on the face  $f$ . The support of any such bubble basis function is exactly one element. This property is often exploited, e.g., in local a posteriori analysis [58]. The following lemma shows that the  $H^{\frac{1}{2}}$ -seminorm of an element  $\phi = \phi_Q + \phi_B$  in  $V_h(\partial T)$ , with  $\phi_Q \in Q_h(\partial T)$  and  $\phi_B \in B_h(\partial T)$ , is equivalent to the sum of the seminorms of  $\phi_B$  and  $\phi_Q$ .

**Lemma 4.3.3** *There exists a constant  $C$ , which depends only on the aspect ratio of  $T$ , such that for each  $\phi = \phi_Q + \phi_B$ , with  $\phi_Q \in Q_h(\partial T)$  and  $\phi_B \in B_h(\partial T)$ , the following equivalence holds*

$$|\phi|_{\frac{1}{2};\partial T} \leq |\phi_Q|_{\frac{1}{2};\partial T} + |\phi_B|_{\frac{1}{2};\partial T} \leq C|\phi|_{\frac{1}{2};\partial T}. \quad (4.29)$$

*Proof.* The lower bound follows from the triangle inequality. To prove the upper one, we consider one element at a time and note that the restriction of the two subspaces to a face  $f$  of an element are of fixed dimension. It then follows immediately from the linear independence of the basis functions the fact that  $\|\phi_Q\|_{0,f} \leq C\|\phi\|_{0,f}$  and  $|\phi_Q|_{1,f} \leq C|\phi|_{1,f}$ . Squaring these inequalities and adding, gives the same inequalities for  $\partial T$ . An interpolation argument then gives a bound in  $H^{\frac{1}{2}}$  from which (4.29) follows directly.  $\square$

We now introduce the operator

$$P_h : H^{\frac{1}{2}}(\partial T) \rightarrow V_h(\partial T),$$

defined by

$$P_h := P_Q + P_B.$$

Here,  $P_Q$  is the  $L^2$ -projection onto  $Q_h(\partial T)$  and  $P_B$  a projection onto  $B_h(\partial T)$ , defined by

$$\int_f P_B \phi \, ds = \int_f (\phi - P_Q \phi) \, ds, \quad f \in \mathcal{F}_h, \quad f \subset \partial T.$$

We note that the operator  $P_h$  preserves integrals over each face  $f$ .

**Lemma 4.3.4** *The operator  $P_h$  is bounded uniformly in  $L_2(\partial T)$  as well as in  $H^{\frac{1}{2}}(\partial T)$ .*

*Proof.* It is well known that  $P_Q$  is  $L^2$ - and  $H^1$ -stable, since  $\mathcal{T}_h$  is quasi-uniform; see, e.g. [12]. We then obtain the  $H^{\frac{1}{2}}$ -stability of  $P_Q$  by an interpolation argument. To prove the  $H^{\frac{1}{2}}$ -stability of  $P_h$ , we also have to consider  $P_B$ . The proof of its  $L^2$ -stability is quite elementary. By using the inverse inequality

$$|\phi_B|_{\frac{1}{2}, \partial T}^2 \leq \frac{C}{h} \|\phi_B\|_{0, \partial T}^2, \quad \phi_B \in B_h(\partial T),$$

and the approximation property of  $P_Q$ , see [12], we find that

$$\begin{aligned} \|P_B \phi\|_{\frac{1}{2}, \partial T}^2 &\leq \frac{C}{h} \|P_B \phi\|_{0, \partial T}^2 \leq \frac{C}{h^3} \sum_{\substack{f \subset \partial T \\ f \in \mathcal{F}_h}} \left( \int_f (\phi - P_Q \phi) \, d\sigma \right)^2 \\ &\leq \frac{C}{h} \|\phi - P_Q \phi\|_{0, \partial T}^2 \leq C |\phi|_{\frac{1}{2}, \partial T}^2. \end{aligned}$$



We recall that we use a rescaled norm for the space  $H^{\frac{1}{2}}(\partial T)$ ; see Section 2.1.  $\square$

We are now ready to prove an important lemma. It establishes the equivalence of a discrete norm and the  $H^{-\frac{1}{2}}$ -norm for functions in  $S_h(\partial T)$ . Its proof employs the stability of  $P_h$  in  $H^{\frac{1}{2}}$  and the fact that this operator preserves the integrals over the faces  $f$ . This latter property is not satisfied by  $P_Q$  alone.

**Lemma 4.3.5** *There exist constants,  $c$  and  $C$ , such that, for any  $\psi \in S_h(\partial T)$ ,*

$$c \sup_{\substack{\phi \in V_h(\partial T) \\ \phi \neq 0}} \frac{\langle \psi, \phi \rangle}{\|\phi\|_{\frac{1}{2}; \partial T}} \leq \|\psi\|_{-\frac{1}{2}; \partial T} \leq C \sup_{\substack{\phi \in V_h(\partial T) \\ \phi \neq 0}} \frac{\langle \psi, \phi \rangle}{\|\phi\|_{\frac{1}{2}; \partial T}}. \quad (4.30)$$

Furthermore, if  $\langle \psi, 1 \rangle = 0$ , the  $\|\cdot\|_{-\frac{1}{2}; \partial T}$ -norm in (4.30) can be replaced by the seminorm and the supremum can be taken over the non-constant functions  $\phi$ .

*Proof.* The lower bound follows directly from the definition of the  $\|\cdot\|_{-\frac{1}{2}; \partial T}$  norm. For the upper bound, let  $\psi \in S_h(\partial T)$ . There then exists a  $\tilde{\phi} \in H^{\frac{1}{2}}(\partial T)$  such that

$$\|\psi\|_{-\frac{1}{2}; \partial T} \leq 2 \frac{\langle \psi, \tilde{\phi} \rangle}{\|\tilde{\phi}\|_{\frac{1}{2}; \partial T}}.$$

Recalling the definition of  $P_h$  and the fact that  $\psi$  is constant on each element, and using Lemma 4.3.4, we find that

$$\|\psi\|_{-\frac{1}{2}; \partial T} \leq 2 \frac{\langle \psi, P_h \tilde{\phi} \rangle}{\|\tilde{\phi}\|_{\frac{1}{2}; \partial T}} \leq C \frac{\langle \psi, P_h \tilde{\phi} \rangle}{\|P_h \tilde{\phi}\|_{\frac{1}{2}; \partial T}}.$$

The proof is now completed by proceeding as in the proof of Lemma 4.3.2.  $\square$

We are now ready to prove a decomposition lemma for the traces of Raviart–Thomas functions on a substructure.

**Lemma 4.3.6** *Let  $T$  be in  $\mathcal{T}_H$  and let  $\{\mu_F, F \subset \partial T\}$  be functions in  $S_{0;h}(\partial T)$ , which vanish on  $\partial T \setminus F$ . Let  $\mu := \sum_{F \subset \partial T} \mu_F$ . Then there exists a constant  $C$ , independent of  $h$  and  $\mu_H$ , such that,  $\forall \mu_H \in S_H(\partial T)$ ,*

$$\|\mu_F\|_{-\frac{1}{2}; \partial T}^2 \leq C(1 + \log H/h) \left( (1 + \log H/h) \|\mu + \mu_H\|_{-\frac{1}{2}; \partial T}^2 + \|\mu\|_{-\frac{1}{2}; \partial T}^2 \right).$$

*Proof.* Since  $\mu_F \in S_{0;h}(\partial T)$ , we obtain

$$\|\mu_F\|_{-\frac{1}{2};\partial T} \leq C \sup_{\substack{\phi \in V_h(\partial T) \\ \phi \neq \text{const.}}} \frac{\langle \mu_F, \phi \rangle}{|\phi|_{\frac{1}{2};\partial T}},$$

by applying Lemma 4.3.5.

Now, any  $\phi \in V_h(\partial T)$  can be split uniquely into  $\phi_Q + \phi_B$ ,  $\phi_Q \in Q_h(\partial T)$ ,  $\phi_B \in B_h(\partial T)$  and by using Lemma 4.3.3, we find that

$$\|\mu_F\|_{-\frac{1}{2};\partial T} \leq C \left( \sup_{\substack{\phi_Q \in Q_h(\partial T) \\ \phi_Q \neq \text{const.}}} \frac{\langle \mu_F, \phi_Q \rangle}{|\phi_Q|_{\frac{1}{2};\partial T}} + \sup_{\substack{\phi_B \in B_h(\partial T) \\ \phi_B \neq 0}} \frac{\langle \mu_F, \phi_B \rangle}{|\phi_B|_{\frac{1}{2};\partial T}} \right). \quad (4.31)$$

For any  $\phi_Q \in Q_h(\partial T)$ , we now define a weighted average  $c_{\phi_Q}$  by

$$c_{\phi_Q} := \frac{\int I_h(\vartheta_F \phi_Q) ds}{\int \vartheta_F ds}.$$

Here,  $\vartheta_F$  is given in the proof of Lemma 4.3.1 and  $I_h$  is the nodal interpolation operator onto  $Q_h(\partial T)$ . Then, the first term on the right in (4.31) can be replaced by

$$\sup_{\substack{\phi_Q \in Q_h(\partial T) \\ \phi_Q \neq \text{const.}}} \frac{\langle \mu_F, \phi_Q - c_{\phi_Q} \rangle}{|\phi_Q - c_{\phi_Q}|_{\frac{1}{2};\partial T}} = \sup_{\substack{\phi_Q \in Q_h(\partial T) \\ \phi_Q \neq 0, c_{\phi_Q} = 0}} \frac{\langle \mu_F, \phi_Q \rangle}{|\phi_Q|_{\frac{1}{2};\partial T}}, \quad (4.32)$$

i.e., we need only consider functions  $\phi_Q$  which have a zero weighted average. The following norm equivalence is similar to (4.28) and can be proved by the same standard techniques

$$c(|\phi_Q|_{\frac{1}{2};\partial T}^2 + Hc_{\phi_Q}^2) \leq \|\phi_Q\|_{\frac{1}{2};\partial T}^2 \leq C(|\phi_Q|_{\frac{1}{2};\partial T}^2 + Hc_{\phi_Q}^2). \quad (4.33)$$

We remark that, because of (4.33), in the last term of (4.32), the  $H^{\frac{1}{2}}$ -seminorm can be replaced by the full norm.

We next decompose  $\phi_B$  into the sum of terms  $\phi_{B;F}$  supported on individual faces  $F \subset \partial T$

$$\phi_B = \sum_{\substack{F \in \mathcal{F}_H \\ F \subset \partial T}} \phi_{B;F}. \quad (4.34)$$

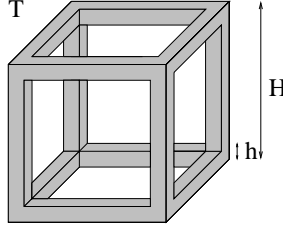


Figure 4.4: Neighborhood of the wire-basket.

Similarly, we decompose  $\phi_Q$  into a sum of contributions  $\phi_{Q;F}$ , supported on individual faces  $F \subset \partial T$  and  $\phi_{Q;w}$  supported in a neighborhood of the wire-basket which is one element wide; see Figure 4.4. Thus,

$$\phi_Q = \sum_{\substack{F \in \mathcal{F}_H \\ F \subset \partial T}} \phi_{Q;F} + \phi_{Q;w}. \quad (4.35)$$

Local inverse estimates combined with interpolation arguments easily give

$$|\phi_{B;F}|_{\frac{1}{2};\partial T}^2 \leq C |\phi_B|_{\frac{1}{2};\partial T}^2. \quad (4.36)$$

Similar arguments give

$$|\phi_{Q;w}|_{\frac{1}{2};\partial T}^2 \leq C \frac{1}{h} \|\phi_{Q;w}\|_{0;\partial T}^2 \leq C \|\phi_{Q;w}\|_{0;W}^2, \quad (4.37)$$

where  $W$  is the wire-basket of  $T$ . We note that  $\|\phi_{Q;w}\|_{0;W}^2$  is defined by a line integral and that, as usual, we use rescaled norms. By using the inequality  $\|u^h\|_{1;T} \leq C \|u^h\|_{1/2;\partial T}^2$ , which is valid for discrete harmonic functions, and [22, Lemma 4.3 and Lemma 4.5], we can prove

$$\|\phi_{Q;w}\|_{0;W}^2 \leq C(1 + \log H/h) \|\phi_Q\|_{\frac{1}{2};\partial T}^2, \quad (4.38)$$

$$|\phi_{Q;F}|_{\frac{1}{2};\partial T}^2 \leq C(1 + \log H/h)^2 \|\phi_Q\|_{\frac{1}{2};\partial T}^2. \quad (4.39)$$

The proofs in [22] are for the simplicial case; they can be carried out in exactly the same way for the case of cubes and are therefore omitted. Combining (4.37) and (4.38), we find

$$\|\phi_{Q;w}\|_{\frac{1}{2};\partial T}^2 \leq C(1 + \log H/h) \|\phi_Q\|_{\frac{1}{2};\partial T}^2. \quad (4.40)$$

We find, by using the splitting (4.35), that

$$\begin{aligned}\langle \mu_F, \phi_Q \rangle &= \sum_{\hat{F} \subset \partial T} \langle \mu_F, \phi_{Q;\hat{F}} \rangle + \langle \mu_F, \phi_{Q;w} \rangle \\ &= \langle \mu, \phi_{Q;F} \rangle + \langle \mu_F, \phi_{Q;w} \rangle.\end{aligned}\tag{4.41}$$

Since  $I_h(\vartheta_F \phi_Q) = \phi_{Q;F} = I_h(\vartheta_F \phi_{Q;F})$  and since we can always assume that  $c_{\phi_Q} = 0$ , we obtain

$$\langle \mu_H, \phi_{Q;F} \rangle = 0, \quad \forall \mu_H \in S_H(\partial T),$$

and  $c_{\phi_{Q;F}} = 0$ . The first term on the right side of (4.41) can be bounded by means of (4.39)

$$|\langle \mu, \phi_{Q;F} \rangle| = |\langle \mu + \mu_H, \phi_{Q;F} \rangle| \leq C(1 + \log H/h) \|\phi_Q\|_{\frac{1}{2}, \partial T} \|\mu + \mu_H\|_{-\frac{1}{2}, \partial T}.\tag{4.42}$$

For each  $\phi_{Q;w}$  there is a unique  $\tilde{\phi}_{B;F} \in B_h(\partial T)$  such that

$$\int_f \phi_{Q;w} ds = \int_f \tilde{\phi}_{B;F} ds, \quad f \in \mathcal{F}_h, f \subset F,$$

with  $\tilde{\phi}_{B;F} = 0$  on  $\partial T \setminus F$ . Moreover, this mapping is continuous

$$\|\tilde{\phi}_{B;F}\|_{\frac{1}{2}, \partial T}^2 \leq C \frac{1}{h} \|\tilde{\phi}_{B;F}\|_{0, \partial T}^2 \leq C \frac{1}{h} \|\phi_{Q;w}\|_{0, \partial T}^2 \leq C \|\phi_{Q;w}\|_{\frac{1}{2}, \partial T}^2.$$

By means of this bound and (4.40), we finally obtain

$$\begin{aligned}|\langle \mu_F, \phi_{Q;w} \rangle| &= |\langle \mu_F, \tilde{\phi}_{B;F} \rangle| = |\langle \mu, \tilde{\phi}_{B;F} \rangle| \leq C \|\mu\|_{-\frac{1}{2}, \partial T} \|\phi_{Q;w}\|_{\frac{1}{2}, \partial T} \\ &\leq C(1 + \log H/h)^{1/2} \|\mu\|_{-\frac{1}{2}, \partial T} \|\phi_Q\|_{\frac{1}{2}, \partial T}.\end{aligned}\tag{4.43}$$

Using (4.36), we find for the second term on the right hand side of (4.31)

$$\begin{aligned}\frac{|\langle \mu_F, \phi_B \rangle|}{|\phi_B|_{\frac{1}{2}, \partial T}} &= \frac{|\langle \mu, \phi_{B;F} \rangle|}{|\phi_B|_{\frac{1}{2}, \partial T}} \leq \frac{\|\mu\|_{-\frac{1}{2}, \partial T} \|\phi_{B;F}\|_{\frac{1}{2}, \partial T}}{|\phi_B|_{\frac{1}{2}, \partial T}} \\ &\leq C \frac{\|\mu\|_{-\frac{1}{2}, \partial T} |\phi_{B;F}|_{\frac{1}{2}, \partial T}}{|\phi_B|_{\frac{1}{2}, \partial T}} \leq C \|\mu\|_{-\frac{1}{2}, \partial T}.\end{aligned}\tag{4.44}$$

The proof is completed by combining (4.31), (4.32), (4.33), (4.35), (4.42), (4.43), and (4.44).  $\square$

## An extension operator

An important step in finding a stable decomposition of  $X_{0;h}(\Omega)$  involves a discrete extension operator from the boundary of a substructure to its interior. The stable extension operator, defined in the next lemma, provides a divergence-free extension of the boundary data given on  $\partial T$ . This fact ensures that the stability constant will be independent of the diameter of  $T$ . This will not be true for some other extension procedures, as can be easily checked using a rescaling argument.

**Lemma 4.3.7** *There exists an extension operator  $\widetilde{\mathcal{H}}_T : S_{0;h}(\partial T) \rightarrow X_h(T)$ , such that, for any  $\mu \in S_{0;h}(\partial T)$ ,*

$$\operatorname{div} \widetilde{\mathcal{H}}_T \mu = 0,$$

and

$$\|\widetilde{\mathcal{H}}_T \mu\|_{0;T} \leq C \|\mu\|_{-\frac{1}{2};\partial T}. \quad (4.45)$$

Here  $C$  is independent of  $h$ ,  $H$ , and  $\mu$ .

*Proof.* The proof is similar to one given in [29, Lemma 2.47]. We will first prove the result for a substructure  $T$  of unit diameter. Consider a Neumann problem

$$\begin{aligned} \Delta \phi &= 0, & \text{in } T, \\ \frac{\partial \phi}{\partial n} &= \mu, & \text{on } \partial T. \end{aligned}$$

Here,  $\partial/\partial n$  is the derivative in the direction of the outward normal of  $\partial T$ . This problem is solvable, since the boundary data  $\mu$  has mean value zero on  $\partial T$ . We can select any solution, e.g., that with mean value zero on  $T$ . Our extension operator  $\widetilde{\mathcal{H}}_T$  is defined by  $\widetilde{\mathcal{H}}_T \mu := \Pi_h^{\mathcal{RT}^1} \mathbf{u}$ , where  $\mathbf{u} = \mathbf{grad} \phi$ , and  $\Pi_h^{\mathcal{RT}^1}$  is the interpolant onto the Raviart–Thomas space; we will show below that  $\Pi_h^{\mathcal{RT}^1} \mathbf{u}$  is well defined.

An elementary variational argument shows that  $\|\mathbf{u}\|_{0;T} = |\phi|_{1;T} \leq C \|\mu\|_{-\frac{1}{2};\partial T}$ . In order to estimate  $\|\Pi_h^{\mathcal{RT}^1} \mathbf{u}\|_{0;T}$ , we will now estimate  $\|\mathbf{u} - \Pi_h^{\mathcal{RT}^1} \mathbf{u}\|_{0;T}$ . This requires the use of a regularity result and a finite element error bound. Since  $\mu$  is piecewise constant on  $\partial T$ , it belongs to  $H^s(\partial T)$ , for all  $s < 1/2$ . Using the surjectivity of the map  $\phi \mapsto \partial\phi/\partial n$  from  $H^{3/2+s}(T)$  onto  $H^s(\partial T)$  and a regularity result given in [17, Corollary 23.5], we deduce

$$\|\phi\|_{\frac{3}{2}+s;T} \leq C \|\mu\|_{s;\partial T}, \quad s < \epsilon_T. \quad (4.46)$$

Here  $\epsilon_T$  is strictly positive and depends on  $T$ .

The  $\{\lambda_f(\mathbf{u}), f \in \mathcal{F}_h\}$  are well-defined, since  $\mathbf{u} \in H^{\frac{1}{2}+s}(T)$ , with  $s > 0$ ; see the discussion at the end of Section 2.2.1. Equation (2.39) ensures that

$$\operatorname{div} \left( \Pi_h^{\mathcal{RT}^1} \mathbf{u} \right) = Q_h (\operatorname{div} \mathbf{u}) = 0,$$

where  $Q_h$  is the  $L^2$  projection onto the space of constant functions on each fine element  $t \subset T$ .

Employing the error estimate (2.30) with  $r = 1/2 + s$ , (4.46) and an inverse inequality, we find that, for  $s < \epsilon_T$ ,

$$\|\mathbf{u} - \Pi_h^{\mathcal{RT}^1} \mathbf{u}\|_{0;T} \leq Ch^{\frac{1}{2}+s} \|\phi\|_{\frac{3}{2}+s;T} \leq C \|\mu\|_{-\frac{1}{2};\partial T}. \quad (4.47)$$

The bound for the  $L_2$ -norm of  $\Pi_h^{\mathcal{RT}^1} \mathbf{u}$  is then obtained by applying the triangle inequality.

We now consider a substructure  $T$  of diameter  $H$ , obtained by dilation from the substructure of unit diameter. Using the previous result and a scaling argument, we obtain

$$\begin{aligned} \operatorname{div} \widetilde{\mathcal{H}}_T \mu &= 0, \\ \|\widetilde{\mathcal{H}}_T \mu\|_{0;T} &\leq C \|\mu\|_{-\frac{1}{2};\partial T}, \end{aligned}$$

where  $C$  is independent of the diameter of  $T$ .  $\square$

#### 4.3.4 Main result

In this section, we will prove our main result, i.e., a bound for the condition number of the additive Schwarz operator, defined in (2.51), associated with the decomposition (4.20). A bound for the error operator of the corresponding multiplicative operator, defined in (2.52), can be then found using Lemma 2.3.3.

As for the two-dimensional case, we will first prove a stability result for an auxiliary decomposition. We will need the spaces  $\{\widetilde{X}_F\}$ , which are divergence free subspaces of  $X_{0;h}$ , and are built in the following way:

Consider a face  $F \in \mathcal{F}_H$  and any function  $\mu$  on  $F$ , that is piecewise constant and has mean-value zero on  $F$ . Then,  $\mu$  can be extended by zero to all of  $\partial T_i$ , to obtain

a function of  $S_{0,h}(\partial T_i)$ , still denoted by  $\mu$ . Let  $\mathbf{u}_i := \widetilde{\mathcal{H}}_{T_i} \mu$ . In a similar way, we can extend  $-\mu$  by zero on  $\partial T_j \setminus F$ , and construct a function  $\mathbf{u}_j = \widetilde{\mathcal{H}}_{T_j}(-\mu)$ , on  $T_j$ . The minus sign has to be chosen, since the elements  $T_i$  and  $T_j$  have outward normals in opposite directions. We define  $\widetilde{X}_F$  as the space of functions  $\mathbf{u}$ , the restriction of which to  $T_i$  and  $T_j$  are equal to  $\mathbf{u}_i$  and  $\mathbf{u}_j$ , respectively, and that are zero outside  $\bar{T}_F$ . Thus, each element in  $\widetilde{X}_F$  is uniquely defined by its normal component on  $F$ , and its dimension is equal to the number of fine faces in  $F$  minus one.

We are now ready to prove our main result.

**Theorem 4.3.1** *For each  $\mathbf{u} \in X_{0,h}$ , there exists a decomposition*

$$\mathbf{u} = \mathbf{u}_H + \sum_{T \in \mathcal{T}_H} \mathbf{u}_T + \sum_{F \in \mathcal{F}_H} \mathbf{u}_F,$$

corresponding to (4.20), such that

$$a(\mathbf{u}_H, \mathbf{u}_H) + \sum_{T \in \mathcal{T}_H} a(\mathbf{u}_T, \mathbf{u}_T) + \sum_{F \in \mathcal{F}_H} a(\mathbf{u}_F, \mathbf{u}_F) \leq C \left(1 + \log \left(\frac{H}{h}\right)\right)^2 a(\mathbf{u}, \mathbf{u}),$$

with a constant  $C$ , independent of  $h$ ,  $H$ , and  $\mathbf{u}$ .

*Proof.* We remark that, because of the equivalence of the graph and energy norms, we only have to prove the stability of the decomposition (4.20) with respect to the graph norm.

We will first prove the stability of the decomposition

$$X_{0,h} = X_{0,H} + \sum_{T \in \mathcal{T}_H} X_T + \sum_{F \in \mathcal{F}_H} \widetilde{X}_F, \quad (4.48)$$

and we will then employ the energy-minimizing property of the harmonic extensions  $\{\mathbf{u}_F\}$ . We also consider one subdomain  $T$  at a time; the global result is obtained by summing over all subdomains.

Counting the degrees of freedom shows that (4.48) is a direct sum, and consequently for each  $\mathbf{u}$ , (4.48) defines a unique  $\mathbf{u}_H$ . In particular,  $\rho_H(\mathbf{u} - \mathbf{u}_H) = 0$  yields  $\mathbf{u}_H = \rho_H \mathbf{u}$ . Using Lemma 4.3.1, we immediately obtain an upper bound for the first term

$$\|\mathbf{u}_H\|_{\text{div};T}^2 \leq C \left(1 + \log \frac{H}{h}\right) \|\mathbf{u}\|_{\text{div};T}^2.$$

For each face  $F \subset \partial T$  there is a unique  $\mu_F \in S_{0;h}(\partial T)$  which is zero on  $\partial T \setminus F$ , such that  $(\mathbf{u} - \mathbf{u}_H) \cdot \mathbf{n}|_F = \mu_F$ . By means of the definition of  $\widetilde{X}_F$ , we obtain  $\tilde{\mathbf{u}}_F = \widetilde{\mathcal{H}}_T \mu_F$ , in  $T$ . Combining (4.45) and Lemma 4.3.6, we obtain, for any  $\mu_H \in S_H(\partial T)$ ,

$$\begin{aligned} \|\tilde{\mathbf{u}}_F\|_{\text{div};T}^2 &\leq C(1 + \log H/h) \|(\mathbf{u} - \mathbf{u}_H) \cdot \mathbf{n}\|_{-\frac{1}{2};\partial T}^2 \\ &\quad + C(1 + \log H/h)^2 \|(\mathbf{u} - \mathbf{u}_H) \cdot \mathbf{n} + \mu_H\|_{-\frac{1}{2};\partial T}^2. \end{aligned} \quad (4.49)$$

The trace formula (2.4), the triangle inequality, and Lemma 4.3.1 yield

$$\|(\mathbf{u} - \mathbf{u}_H) \cdot \mathbf{n}\|_{-\frac{1}{2};\partial T}^2 \leq C(1 + \log H/h) \|\mathbf{u}\|_{\text{div};T}^2,$$

and the choice  $\mu_H = \mathbf{u}_H \cdot \mathbf{n}$ , finally, gives

$$\|\tilde{\mathbf{u}}_F\|_{\text{div};T}^2 \leq C(1 + \log H/h)^2 \|\mathbf{u}\|_{\text{div};T}^2.$$

An upper bound for  $\|\mathbf{u}_T\|_{\text{div};T}^2$  is now an easy consequence of the triangle inequality.

The stability of (4.48) with respect to the energy norm  $\|\cdot\|_a$  is a consequence of the norm equivalence of the graph norm  $\|\cdot\|_{\text{div}}$  and the energy norm. More precisely, the multiplicative constant in the upper bounds is proportional to

$$\max_{T \in \mathcal{T}_H} \max \left( \frac{\gamma_T}{\beta_T}, \frac{h_T^2 \gamma_T}{a_T} \right); \quad (4.50)$$

see Remark 4.3.1.

In order to prove the stability of the decomposition (4.20), we set  $\mathbf{u}_H := \rho_H \mathbf{u}$  and extend the trace  $\mu_F = (\mathbf{u} - \mathbf{u}_H) \cdot \mathbf{n}|_F$ , harmonically in  $T_i$  and  $T_j$  to obtain a function  $\mathbf{u}_F \in X_F$ . The energy-minimizing property of the harmonic extension yields

$$a(\mathbf{u}_F, \mathbf{u}_F) \leq a(\tilde{\mathbf{u}}_F, \tilde{\mathbf{u}}_F) \leq C \left(1 + \log \frac{H}{h}\right)^2 a(\mathbf{u}, \mathbf{u}).$$

The remainder  $\mathbf{u} - \mathbf{u}_H - \sum_{F \in \mathcal{F}_H} \mathbf{u}_F$  is a sum of elements belonging to the interior spaces, the contributions of which can be bounded using the triangle inequality.  $\square$

Finally, we consider the splitting (4.20) for the limit case  $a = 0$ . In this case, the bilinear form  $a(\cdot, \cdot)$  is just a weighted  $L^2$ -scalar product

$$a(\mathbf{v}, \mathbf{w}) = \int_{\Omega} B \mathbf{v} \cdot \mathbf{w} \, dx.$$



Let us first decompose  $\mathbf{u}$  as follows

$$\mathbf{u} = \sum_{T \in \mathcal{T}_H} \bar{\mathbf{u}}_T + \sum_{F \in \mathcal{F}_H} \bar{\mathbf{u}}_F,$$

where  $\bar{\mathbf{u}}_F \in X_{0;h}$  with  $\lambda_f(\bar{\mathbf{u}}_F) := \lambda_f(\mathbf{u})$ ,  $f \subset F$ ,  $f \in \mathcal{F}_h$  and  $\lambda_f(\bar{\mathbf{u}}_F) = 0$  elsewhere, and  $\mathbf{u}_T \in X_T$ . Then, (2.28) guarantees that

$$\sum_{F \in \mathcal{F}_H} \|\bar{\mathbf{u}}_F\|_0^2 \leq C \|\mathbf{u}\|_0^2.$$

We remark that  $\bar{\mathbf{u}}_F$  is an extension by zero to the interior of the substructures and, therefore, in general not contained in  $X_F$ . Let us now consider the unique decomposition

$$\mathbf{u} = \sum_{T \in \mathcal{T}_H} \mathbf{u}_T + \sum_{F \in \mathcal{F}_H} \mathbf{u}_F,$$

where  $\mathbf{u}_T \in X_T$  and  $\mathbf{u}_F \in X_F$ . By using the minimization property of  $\mathbf{u}_F$  and the fact that  $\mathbf{u}_F \cdot \mathbf{n}|_F = \bar{\mathbf{u}}_F \cdot \mathbf{n}|_F$ , we obtain

$$\sum_{F \in \mathcal{F}_H} \|\mathbf{u}_F\|_0^2 \leq \sum_{F \in \mathcal{F}_H} \|\bar{\mathbf{u}}_F\|_0^2 \leq C \|\mathbf{u}\|_0^2.$$

This proves the stability of the decomposition of  $\mathbf{u}$  with respect to the  $L^2$ -norm. Thus, as the ratio between the coefficients  $B$  and  $a$  becomes large, we expect an upper bound for the condition number which is independent of  $H/h$ . We remark that this result cannot be obtained with the splitting (4.48).

In the second limit case,  $B = 0$ , the bilinear form  $a(\cdot, \cdot)$  is no longer positive definite. However, we can still work with the preconditioned conjugate gradient in a subspace, if the right hand side  $\mathbf{f}$  is consistent. Then, the stability of  $\rho_H$  with respect to the  $L^2$ -norm of the divergence, (4.22), gives us an optimal result, i.e., we obtain a condition number which is independent of  $H/h$ .

### 4.3.5 Numerical results

In this section, we present some numerical results on the performance of the iterative substructuring method described in the previous sections, when varying the diameters of the coarse and fine meshes, and the coefficients  $a$  and  $B$ . As before,

Table 4.4: Estimated condition number and number of conjugate gradient iterations for a residual norm reduction of  $10^{-6}$  (in parentheses), versus  $H/h$  and  $n$ . Case of  $a = 1$ ,  $b = 1$ .

$H/h$	8	4	2
n=8	-	13.28 (14)	15.15 (22)
n=16	19.46 (16)	23.26 (24)	17.37 (24)
n=24	32.78 (27)	25.55 (26)	17.43 (21)
n=32	33.48 (27)	26.01 (26)	17.42 (21)
n=40	35.50 (27)	26.08 (25)	x
n=48	36.47 (28)	25.91 (22)	x

we refer to [54], for a general discussion of practical issues concerning Schwarz methods. Our numerical results are given for a slightly different decomposition than (4.20)

$$X_{0;h} = X_{0;H} + \sum_{F \in \mathcal{F}_H} X_{0;h}(T_F).$$

Because of the orthogonality between the spaces  $\{X_T\}$  and  $\{X_F\}$ , this decomposition is stable if and only if (4.20) is. As for the two-dimensional method, the corresponding preconditioner is

$$B = R_H^T A_H^{-1} R_H + \sum_{F \in \mathcal{F}_H} (R_F^T A_F^{-1} R_F),$$

where the extension matrices  $R_H^T$  and  $\{R_F^T\}$  map the degrees of freedom of the coarse and local spaces, respectively, into the the global ones, and  $A_H$  and  $\{A_F\}$  are the matrices relative to Dirichlet problems on the coarse mesh and on the regions  $T_F$ ; see Sections 2.3 and 4.2.5.

We have considered the domain  $\Omega = (0, 1)^3$  and uniform triangulations  $\mathcal{T}_h$  and  $\mathcal{T}_H$ . The fine triangulation  $\mathcal{T}_h$  consists of  $n^3$  cubical elements, with  $h = 1/n$ . The matrix  $B$  is given by

$$B = \text{diag}\{b, b, b\}.$$

Table 4.4 shows the estimated condition number and the number of iterations to obtain a reduction of the residual norm by a factor  $10^{-6}$ , as a function of the

Table 4.5: Estimated condition number and number of conjugate gradient iterations for a residual norm reduction of  $10^{-6}$  (in parentheses), versus  $H/h$  and  $b$ . Case of  $n = 24$  and  $a = 1$ .

$H/h$	8	4	2
b=1e-09	4.00 (10)	5.81 (16)	6.29 (15)
b=1e-08	4.00 (10)	5.81 (16)	6.29 (15)
b=1e-07	4.00 (10)	5.82 (16)	6.29 (15)
b=1e-06	4.00 (10)	21.0 (18)	6.29 (15)
b=1e-05	17.5 (11)	25.0 (19)	16.1 (18)
b=0.0001	29.5 (12)	25.0 (19)	17.1 (18)
b=0.001	30.9 (15)	25.3 (21)	17.2 (18)
b=0.01	32.3 (20)	25.4 (22)	17.2 (18)
b=0.1	32.6 (22)	25.5 (25)	17.4 (20)
b= 1	32.8 (27)	25.6 (26)	17.4 (21)
b= 10	30.0 (29)	23.4 (26)	17.1 (23)
b=1e+02	23.6 (26)	20.4 (25)	15.1 (22)
b=1e+03	14.4 (21)	14.1 (22)	12.6 (19)
b=1e+04	8.42 (16)	8.57 (17)	9.43 (17)
b=1e+05	6.75 (14)	6.98 (15)	7.92 (17)
b=1e+06	6.72 (14)	6.91 (15)	7.80 (16)

dimensions of the fine and coarse meshes. The estimate of the condition number is obtained from the parameters calculated during the conjugate gradient iteration, using the method described in [47]. For a fixed  $H/h$ , the condition number appears to remain bounded independently of the number of fine mesh points  $n$ . The number of iterations varies slowly with  $H/h$  and  $n$ .

We remark that the supports of the face spaces, consisting of the union of two substructures, can be colored in such a way that spaces with the same color do not intersect and that the largest eigenvalue of the additive Schwarz operator  $T_{as}$  is bounded by the number of colors plus one; see [54, p. 165]. The largest eigenvalue is 7 in all the cases in Table 4.4, except for  $(n = 8, H/h = 4)$  and  $(n = 16, H/h = 8)$ ; the latter cases correspond to a partition into 2 by 2 by 2 subregions and, consequently, the largest eigenvalue is bounded by 4.

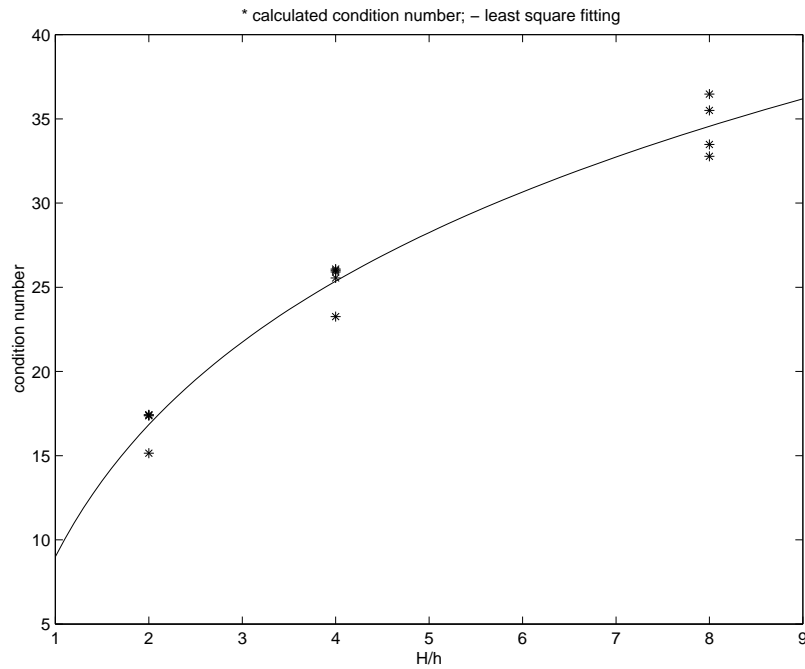


Figure 4.5: Estimated condition number from Table 4.4 (asterisk) and least-square second order logarithmic polynomial (solid line), versus  $H/h$ ; the relative fitting error is about 4.5 per cent.

In Figure 4.5, we plot the results of Table 4.4, together with the best second order logarithmic polynomial least-square fit. Our numerical results are in good agreement with the theoretical bound obtained in the previous section and they suggest that our bound is sharp.

In Table 4.5, we show some results when the ratio of the coefficients  $b$  and  $a$  is changed. For a fixed value of  $n = 24$  and  $a = 1$ , the estimated condition number and the number of iterations are shown as functions of  $H/h$  and  $b$ . These numerical results also confirm the theoretical results in the limit cases  $b = 0$  and  $b = \infty$ , as given in the previous section, since we find that the condition number appears to be bounded independently of the ratio  $H/h$  when the ratio  $b/a$  is very small or very large.

# Chapter 5

## Iterative substructuring methods: Neumann–Neumann methods

### 5.1 Introduction

In this chapter, we will introduce and analyze some Neumann–Neumann preconditioners. We will apply them to the same problems considered in Chapter 4 in  $H(\mathbf{curl}; \Omega)$  and  $H(\mathbf{div}; \Omega)$  in two dimensions, and in  $H(\mathbf{div}; \Omega)$  in three dimensions.

In a substructuring method, the local spaces are related to a partition of the original domain  $\Omega$  into non-overlapping subdomains, called *substructures*. In a Neumann–Neumann method, the degrees of freedom of the local spaces are related to the entire boundaries of the substructures; see [11, 19, 34, 37, 16, 24, 51, 22, 38, 54]. For an introduction to iterative substructuring methods, we refer to Section 4.1 and to the references therein.

An important element in the definition of a Neumann–Neumann method is a set of scaling functions defined on the boundaries of the substructures, which involve the values of the coefficients of the partial differential equation. The use of these functions can ensure that the condition number of the corresponding preconditioned system be independent of the jumps of the coefficients across the substructures. Here, we propose a set of scaling functions, which involve only the values of one coefficient of the bilinear form (5.1). An important feature of our method is that it is independent of jumps of both coefficients.

In order to analyze our methods, we will need the tools described in Section 4.3.3, and which were developed for three-dimensional problems. In Section 5.5, we will modify them for the two-dimensional case and then carry out the analysis of our Neumann–Neumann algorithms in full detail only for  $H(\operatorname{div}; \Omega)$ . For problems in  $H(\mathbf{curl}; \Omega)$  in two dimensions, the result follows from that in  $H(\operatorname{div}; \Omega)$  and the observation that the functions in  $H(\operatorname{div}; \Omega)$  and in the Raviart–Thomas spaces are obtained from those in  $H(\mathbf{curl}; \Omega)$  and in the Nédélec spaces, respectively, by a rotation of ninety degrees; see Sections 2.1.2 and 2.2.2.

## 5.2 Finite element spaces and operators

Let  $\Omega$  be a bounded polygon or polyhedron in  $\mathbb{R}^n$ ,  $n = 2, 3$ . For any  $\mathcal{D} \subset \Omega$ , we define the bilinear form

$$a_{\mathcal{D}}(\mathbf{u}, \mathbf{v}) := \int_{\mathcal{D}} (a \operatorname{div} \mathbf{u} \operatorname{div} \mathbf{v} + B \mathbf{u} \cdot \mathbf{v}) \, dx, \quad \mathbf{u}, \mathbf{v} \in H(\operatorname{div}; \Omega). \quad (5.1)$$

In case  $\mathcal{D} = \Omega$ , we set

$$a(\cdot, \cdot) := a_{\Omega}(\cdot, \cdot).$$

As in the previous chapter, the coefficient matrix  $B$  is a symmetric uniformly positive definite matrix-valued function with  $b_{i,j} \in L^{\infty}(\Omega)$ ,  $1 \leq i, j \leq n$ , and  $a \in L^{\infty}(\Omega)$  is a positive function bounded away from zero.

The results presented in this chapter are equally valid for  $n = 2$  and the bilinear form

$$\int_{\mathcal{D}} (a \operatorname{curl} \mathbf{u} \operatorname{curl} \mathbf{v} + B \mathbf{u} \cdot \mathbf{v}) \, dx, \quad \mathbf{u}, \mathbf{v} \in H(\mathbf{curl}; \Omega).$$

Let  $\mathcal{T}_H$  be a shape-regular triangulation of  $\Omega$ , of maximum diameter  $H$ , consisting of triangles or rectangles, for  $n = 2$ , and of tetrahedra or parallelepipeds, for  $n = 3$ . Let also  $\mathcal{T}_h$  be a *shape-regular* and *quasi-uniform* triangulation, with characteristic diameter  $h$ , obtained by refining the elements of  $\mathcal{T}_H$ , in such a way that  $\mathcal{T}_h$  is conforming in  $\Omega$ . We will use some of the notations in Sections 4.2.1 and 4.3.1, but will change others, in order to unify our analysis for the cases  $n = 2, 3$ . A generic element of  $\mathcal{T}_h$  and  $\mathcal{T}_H$  will be denoted by  $t$  and  $T$ , respectively. For

$n = 3$ , the sets of faces of the triangulations  $\mathcal{T}_h$  and  $\mathcal{T}_H$ , are denoted by  $\mathcal{F}_h$  and  $\mathcal{F}_H$ , respectively. For  $n = 2$ , the sets of edges of the triangulations  $\mathcal{T}_h$  and  $\mathcal{T}_H$ , are also denoted by  $\mathcal{F}_h$  and  $\mathcal{F}_H$ , respectively. A generic face (or edge, for  $n = 2$ ) will be denoted by  $f$  or  $F$ . The elements of the coarse triangulation are called substructures. The interface  $\Gamma$  is the union of the parts of the boundaries of the substructures that do not belong to  $\partial\Omega$ ,

$$\Gamma := \bigcup_{T \in \mathcal{T}_H} \partial T \setminus \partial\Omega. \quad (5.2)$$

We also suppose that the coefficients  $a$  and  $B$  are constant on each substructure  $T$  and equal to  $a_T$  and  $B_T$ , respectively. They may have arbitrary jumps across the interface. In addition, the matrices  $\{B_T\}$  satisfy

$$\beta_T \eta^T \eta \leq \eta^T B_T \eta \leq \gamma_T \eta^T \eta, \quad \forall \eta \in \mathbb{R}^n, \quad (5.3)$$

where  $\beta_T$  and  $\gamma_T$  are positive constants, which can depend on the substructure  $T$ .

In the following, we will only consider, in full detail, triangulations based on rectangles and parallelepipeds, but our results are equally valid for finite element spaces built on triangles and tetrahedra. Much of the analysis is carried out on a square or cubic substructure divided into square or cubic elements, but the results remain equally valid if the elements and substructures are images of a reference square or cube under sufficiently benign mappings, which effectively means that their aspect ratios have to remain uniformly bounded. We remark that, as in the previous chapter, our analysis is carried out locally for one substructure at a time. We can therefore interpret the factor  $H/h$ , which appears in our the estimates, as

$$\max_{T \in \mathcal{T}_H} \max_{\substack{t \in \mathcal{T}_h \\ t \subset T}} \frac{H_T}{H_t}.$$

We consider the lowest order Raviart–Thomas elements defined on the fine and coarse meshes, respectively,

$$\begin{aligned} X_{0;h} &:= \mathcal{RT}_{0;h}^1(\Omega) = \mathcal{RT}_{0;h}(\Omega), \\ X_{0;H} &:= \mathcal{RT}_{0;H}^1(\Omega) = \mathcal{RT}_{0;H}(\Omega), \end{aligned}$$

which are conforming in  $H_0(\text{div}; \Omega)$ ; see Section 2.2.1. For a generic substructure  $T$ , we will also need the finite element spaces

$$\begin{aligned} X_h(T) &:= \mathcal{RT}_h^1(T), \\ X_{0;h}(T) &:= \mathcal{RT}_{0;h}^1(T). \end{aligned}$$

We will now define some finite element spaces on the boundaries of the substructures; see Section 4.3.3. Given a substructure  $T$ , define  $S_H(\partial T)$  as the space of functions which are constant on each face (edge, for  $n = 2$ )  $F \subset \partial T$

$$S_H(\partial T) := \{\psi : \partial T \rightarrow \mathbb{R} \mid \psi|_F \text{ constant}, F \in \mathcal{F}_H, F \subset \partial T\};$$

its dimension is six, for  $n = 3$ , and four, for  $n = 2$ . We also define  $S_h(\partial T)$  as the space of functions that are constant on each fine face (edge)  $f \in \mathcal{F}_h, f \subset \partial T$ :

$$S_h(\partial T) := \{\psi : \partial T \rightarrow \mathbb{R} \mid \psi|_f \text{ constant}, f \in \mathcal{F}_h, f \subset \partial T\},$$

and its subspace  $S_{0;h}(\partial T)$ , of functions that have mean value zero on  $\partial T$

$$S_{0;h}(\partial T) := \left\{ \psi \in S_h(\partial T) \mid \int_{\partial T} \psi \, dx = 0 \right\}.$$

It is immediate to check that the normal component of a vector in  $X_h(T)$  belongs to  $S_h(\partial T)$ . Finally let  $S_h(\Gamma)$  be the global space of piecewise constant functions on  $\Gamma$ , such that their restriction to the boundary of a substructure  $T$  belongs to  $S_h(\partial T)$

$$S_h(\Gamma) := \{\psi : \Gamma \rightarrow \mathbb{R} \mid \psi|_{\partial T} \in S_h(\partial T)\}.$$

We will now define some extension and interpolation operators. For each substructure  $T$  and each function  $\psi \in S_h(\partial T)$ , the harmonic extension operator

$$\mathcal{H}_T : S_h(\partial T) \longrightarrow X_h(T),$$

is the vector  $\mathbf{u} := \mathcal{H}_T \psi$  which satisfies

$$a_T(\mathbf{u}, \mathbf{v}) = 0, \quad \mathbf{v} \in X_{0;h}(T). \tag{5.4}$$



The corresponding global operator

$$\mathcal{H} : S_h(\Gamma) \longrightarrow X_{0;h},$$

satisfies

$$a(\mathcal{H}\psi, \mathbf{v}) = 0, \quad \mathbf{v} \in X_{0;h}(T), \quad T \in \mathcal{T}_H, \quad (5.5)$$

or, equivalently,

$$(\mathcal{H}\psi)|_T = \mathcal{H}_T(\psi|_{\partial T}).$$

The space of the harmonic extensions on the substructures is denoted by  $\widetilde{X}_{0;h} \subset X_{0;h}$ , and  $\mathbf{u} \in \widetilde{X}_{0;h}$  if and only if  $\mathbf{u}$  verifies (5.4).

We will also need the space of the coarse harmonic extensions,  $\widetilde{X}_{0;H} \subset \widetilde{X}_{0;h}$ :  $\widetilde{X}_{0;H}$  is the space of harmonic functions, the normal component of which is constant on each coarse face (edge, if  $n = 2$ )  $F \in \mathcal{F}_H$ , i.e.,  $\mathbf{u} \in \widetilde{X}_{0;H}$  if and only if

$$\mathbf{u} \cdot \mathbf{n}|_{\partial T} \in S_H(\partial T), \quad T \in \mathcal{T}_H.$$

We remark that the functions in the spaces  $X_{0;H}$  and  $\widetilde{X}_{0;H}$  have the same normal traces on the boundaries of the substructures.

The interpolation operator  $\rho_H$  onto the coarse space  $X_{0;H}$ ,

$$\rho_H : X_{0;h} \longrightarrow X_{0;H},$$

has already been defined in Section 2.2.1. In particular, we recall that  $\rho_H$  is defined in terms of the degrees of freedom of the coarse space

$$\lambda_F(\rho_H \mathbf{u}) := \frac{1}{|F|} \int_F \mathbf{n} \cdot \mathbf{u} \, ds, \quad F \in \mathcal{F}_H. \quad (5.6)$$

In a similar fashion, the degrees of freedom (5.6) define a unique interpolation operator  $\Pi_H$

$$\Pi_H : X_{0;h} \longrightarrow \widetilde{X}_{0;H}.$$

Here, for any vector  $\mathbf{u} \in X_{0;h}$ ,  $\Pi_H \mathbf{u}$  is the unique function in  $\widetilde{X}_{0;H}$ , such that

$$(\Pi_H \mathbf{u}) \cdot \mathbf{n}|_{\partial T} = (\rho_H \mathbf{u}) \cdot \mathbf{n}|_{\partial T}, \quad T \in \mathcal{T}_H.$$

### 5.3 Discrete problem and Schur complement system

We will consider the approximate problem:

Find  $\mathbf{u} \in X_{0;h}$  such that

$$a(\mathbf{u}, \mathbf{v}) = (\mathbf{f}, \mathbf{v}) \quad \forall \mathbf{v} \in X_{0;h}, \quad (5.7)$$

where  $\mathbf{f} \in L^2(\Omega)^n$ . The generalization to the case of the  $\mathcal{RT}_h(\Omega)$  (Neumann boundary conditions) does not present any particular difficulty. In particular, we remark that if Neumann conditions are considered on some part of the boundary  $\partial\Omega_N \subset \partial\Omega$ ,  $\partial\Omega_N$  has to be added to  $\Gamma$ ; see definition (5.2) and, e.g., [24].

We will now introduce a Schur complement formulation of problem (5.7). We refer to [54, Ch. 4] and to the references therein, for a general discussion and some implementation issues related to Schur complement methods.

Let  $T_i$  be a substructure. Let  $A$  and  $A^{(i)}$  be the matrices of the bilinear forms  $a(\cdot, \cdot)$  and  $a_{T_i}(\cdot, \cdot)$ . Given two functions  $\mathbf{u} \in X_{0;h}$  and  $\mathbf{u}^{(i)} \in X_h(T_i)$ , the column vectors of the corresponding degrees of freedom are denoted by  $U$  and  $U^{(i)}$ , respectively. If  $\{\mathbf{w}_k\}$  and  $\{\mathbf{w}_j^{(i)}\}$  are the basis functions of  $X_{0;h}$  and  $X_h(T_i)$ , respectively, we have

$$\begin{aligned} \mathbf{u} &= \sum_k U_k \mathbf{w}_k, \\ \mathbf{u}^{(i)} &= \sum_j U_j^{(i)} \mathbf{w}_j^{(i)}. \end{aligned}$$

The variational problem (5.7) can then be written as a linear system

$$AU = F.$$

The local matrices  $A^{(i)}$  can be represented as

$$\begin{bmatrix} A_{II}^{(i)} & A_{IB}^{(i)} \\ A_{BI}^{(i)} & A_{BB}^{(i)} \end{bmatrix},$$

where we divide the local vectors  $U^{(i)}$  into two subvectors,  $U_I^{(i)}$  and  $U_B^{(i)}$ , of degrees of freedom corresponding to faces (edges, for  $n = 2$ ) inside  $T_i$  and on  $\partial T_i$ , respectively.

Since the variables interior to the substructures are associated with only one substructure, they can be eliminated in parallel across the substructures, using a direct method, and the reduced system

$$SU_B = G, \quad (5.8)$$

only involves the variables corresponding to the degrees of freedom on the interface  $\Gamma$ . Once the solution  $U_B$  of (5.8) is found, the local values  $U_I^{(i)}$  of the solution can be obtained by solving one local problem for each subdomain.

The local Schur complements are

$$S^{(i)} := A_{BB}^{(i)} - A_{BI}^{(i)} \left( A_{II}^{(i)} \right)^{-1} A_{IB}^{(i)},$$

and they are always defined since the matrices  $\{A_{II}^{(i)}\}$  are invertible.

With  $U_B$  a vector containing the coefficients relative to the degrees of freedom on  $\Gamma$ , let  $\tilde{R}_i$  be the restriction matrix, such that  $\tilde{R}_i U_B$  contains the coefficients relative to the degrees of freedom on  $\partial T_i$ . The global Schur complement and the vector  $G$  can then be obtained by subassembling local contributions:

$$\begin{aligned} S &= \sum_{T_i \in \mathcal{T}_H} \tilde{R}_i^T S^{(i)} \tilde{R}_i, \\ G &= F_B - \sum_{T_i \in \mathcal{T}_H} \tilde{R}_i^T A_{BI}^{(i)} \left( A_{II}^{(i)} \right)^{-1} F_I^{(i)}. \end{aligned}$$

For a substructure  $T_i$  and a vector  $U_B^{(i)}$ , it immediately follows that

$$U_B^{(i)T} S^{(i)} U_B^{(i)} = \min_{V_B^{(i)} = U_B^{(i)}} V^{(i)T} A^{(i)} V^{(i)}, \quad (5.9)$$

and that the minimum is obtained for the vector  $U^{(i)}$  that satisfies

$$A_{II}^{(i)} U_{II}^{(i)} + A_{IB}^{(i)} U_B^{(i)} = 0. \quad (5.10)$$

We recall that, if  $U^{(i)}$  are the degrees of freedom of a local vector  $\mathbf{u}$ , (5.10) is equivalent to (5.4), and, consequently, (5.10) defines the harmonic functions.

We recall that, if  $\mathbf{u} \in X_h(T_i)$ , its normal component  $\mathbf{u} \cdot \mathbf{n}$  on  $\partial T_i$  belongs to  $S_h(\partial T_i)$ , the space of piecewise constant functions on  $\partial T_i$ . Let

$$\{\psi_k^{(i)}, f_k \in \mathcal{F}_h, f_k \subset \partial T_i\},$$

be the basis functions of  $S_h(\partial T_i)$ , with  $\psi_k^{(i)}$  equal to one on the face  $f_k$  (edge, if  $n = 2$ ) and vanishing on the other part. Since the degrees of freedom of the space  $X_h(T_i)$  are the values of the normal component on the fine faces  $f \subset \bar{T}_i$ , then given a vector  $U_B^{(i)} = \Psi$  of degrees of freedom on  $\partial T_i$ , there is a unique function  $\psi \in S_h(\partial T_i)$ , such that

$$\psi = \sum_k \Psi_k \psi_k^{(i)}.$$

Consequently, a vector  $U_B^{(i)}$  of local degrees of freedom on  $\partial T_i$  also represents degrees of freedom of  $S_h(\partial T_i)$ . For  $\psi$  and  $\phi$  in  $S_h(\partial T_i)$ , the following local bilinear form is then well-defined

$$s_{T_i}(\psi, \phi) := \Psi^{(i)T} S^{(i)} \Phi^{(i)}, \quad \psi = \sum_k \Psi_k^{(i)} \psi_k^{(i)}, \quad \phi = \sum_k \Phi_k^{(i)} \phi_k^{(i)}.$$

In the same way, the set of global vectors  $U_B$  of degrees of freedom on  $\Gamma$  also represents the set of degrees of freedom of  $S_h(\Gamma)$ , and, for  $\psi$  and  $\phi$  in  $S_h(\Gamma)$ , we can define the global bilinear form

$$s(\psi, \phi) := \sum_{T_i \in \mathcal{T}_H} \Psi^{(i)T} S^{(i)} \Phi^{(i)}.$$

Let

$$\{\psi_k, f_k \in \mathcal{F}_h, f_k \subset \Gamma\},$$

be the basis functions of  $S_h(\Gamma)$

With these definitions, (5.9) and (5.10) give, for  $\psi \in S_h(\partial T_i)$ ,

$$s_{T_i}(\psi, \psi) = \min_{\substack{\mathbf{u} \in X_h(T_i) \\ \mathbf{u} \cdot \mathbf{n} = \psi}} a_{T_i}(\mathbf{u}, \mathbf{u}) = a_{T_i}(\mathcal{H}_{T_i} \psi, \mathcal{H}_{T_i} \psi), \quad (5.11)$$

and, for  $\psi \in S_h(\Gamma)$ ,

$$s(\psi, \psi) = \min_{\substack{\mathbf{u} \in X_{0,h} \\ \mathbf{u} \cdot \mathbf{n} = \psi}} a(\mathbf{u}, \mathbf{u}) = a(\mathcal{H}\psi, \mathcal{H}\psi) = \sum_{T_i \in \mathcal{T}_H} a_{T_i}(\mathcal{H}_{T_i} \psi^{(i)}, \mathcal{H}_{T_i} \psi^{(i)}), \quad (5.12)$$

where  $\psi^{(i)} = \psi|_{\partial T_i}$ . In (5.11) and (5.12), the normal component  $\mathbf{u} \cdot \mathbf{n}$  is taken on  $\partial T_i$  and  $\Gamma$ , respectively.

Finally, the variational formulation of (5.8) can be given as:  
 Find  $\psi \in S_h(\Gamma)$ , such that,

$$s(\psi, \phi) = \int_{\Gamma} g\psi \, ds, \quad \psi \in S_h(\Gamma), \quad (5.13)$$

where  $g := \sum_k G_k \psi_k$ .

## 5.4 Description of the algorithms

We will build a Schwarz preconditioner for the Schur complement system (5.8), corresponding to the variational problem (5.13). Because of (5.12), instead of working with functions in  $S_h(\Gamma)$  and the bilinear form  $s(\cdot, \cdot)$ , we can work with the space of harmonic extensions  $\widetilde{X}_{0,h}$  and the original bilinear form  $a(\cdot, \cdot)$ .

An important element in the definition of a Neumann–Neumann method is a set of scaling functions defined on the boundaries of the substructures, which involve the values of the coefficients of the partial differential equation. The use of these functions can ensure that the condition number of the corresponding preconditioned system be independent of the jumps of the coefficients across  $\Gamma$ ; see [11, 19, 34, 37, 16, 24, 51, 22, 38, 54]. Here, we propose a set of scaling functions, which involve only the values of one coefficient of (5.1). An important feature of our method is that it is independent of jumps of both coefficients  $a$  and  $B$  in (5.1). This is due to the particular divergence-free extension employed in the proof of Lemma 5.6.2; see Lemma 4.3.7. Because of the nature of the degrees of freedom in  $X_{0,h}$ , our scaling functions will be particularly simple, compared to those for problems in  $H^1(\Omega)$ .

Following [51, 52], our family of scaling functions will depend on a parameter

$$\delta \geq 1/2. \quad (5.14)$$

Let  $T$  be a substructure. We define a piecewise constant function  $\mu_T \in S_h(\partial T)$  by

$$\mu_{T|_f} \equiv \frac{\sum_D \gamma_D^\delta}{\gamma_T^\delta}, \quad f \in \mathcal{F}_h, \quad f \subset \partial T, \quad (5.15)$$

where  $\gamma_D$  and  $\gamma_T$  are the largest eigenvalues of the coefficient matrices  $B_D$  and  $B_T$ , respectively, as in (5.3). Here, the sum is taken over the substructures that share the face  $f$  (edge, if  $n = 2$ ). We remark that if the coefficient matrix  $B$  is constant,  $\mu_{T|_f}$  is the total number of subdomains to which  $f$  belongs. In addition, due to the nature of the degrees of freedom in  $X_{0;h}$ , this sum in (5.15) always has just two terms, and the function  $\mu_T$  belongs to the subspace  $S_H(\partial T)$ , of piecewise constant functions on the coarse faces (edges)  $F \subset \partial T$ . We will also need the corresponding function in  $S_h(\Gamma)$ , still denoted by  $\mu_T$ , obtained from  $\mu_T$  by extending it by zero to all of  $\Gamma$ . Given two substructures  $T$  and  $D$  that have a common face (edge, if  $n = 2$ )  $\overline{F} = \overline{T} \cap \overline{D}$ , we will also use the notation

$$\mu_{T;D} := \mu_{T|_F} = \mu_{D|_F}.$$

We remark that if Neumann conditions are considered on some part of the boundary  $\partial\Omega_N \subset \partial\Omega$ , the functions  $\mu_T$  are also defined on  $\partial\Omega_N$ . In this case, the sum in (5.15) has only one term, if  $f \subset \partial\Omega_N$ , and  $\mu_{T|_f} = 1$ .

For  $\delta = 1$ , the same counting functions are considered in [16], where a Neumann–Neumann method for the mixed approximation of the Laplace equation is studied.

We now define the pseudoinverses  $\{\mu_T^\dagger\}$  of the functions  $\{\mu_T\}$  on  $\Gamma$ , by

$$\mu_{T|_f}^\dagger \equiv \mu_{T|_f}^{-1}, \quad f \subset \partial T; \quad \mu_{T|_f}^\dagger \equiv 0, \quad f \subset \Gamma \setminus \partial T. \quad (5.16)$$

The functions  $\{\mu_T^\dagger\}$  are also constant on each coarse face  $F \subset \mathcal{F}_H$ .

It is immediate that  $\{\mu_T^\dagger\}$  is a partition of unity on  $\Gamma$ :

$$0 \leq \mu_T^\dagger \leq 1, \quad \sum_{T \in \mathcal{T}_H} \mu_T^\dagger \equiv 1, \quad \text{a.e. on } \Gamma.$$

In order to define a Schwarz algorithm, we need a family of subspaces and a bilinear form for each of them. Given a substructure  $T$ , we define  $\widetilde{X}_T \subset \widetilde{X}_{0;h}$ , as the space of harmonic extensions, that vanish on  $\Gamma \setminus \partial T$ . We remark that the support of a function  $\mathbf{u} \in \widetilde{X}_T$  is contained in the closure of the union of  $T$  and the substructures with a common face (edge, if  $n = 2$ ) with  $T$ . Since the degrees of freedom of the Raviart–Thomas spaces are defined on the faces (edges, if  $n = 2$ ) of the triangulation, the harmonic extension  $\mathbf{u}$  vanishes on the substructures that

share only a vertex with  $T$  and, if  $n = 3$ , also on the substructures that share only an edge with  $T$ .

We define the following decomposition of the space of harmonic extensions:

$$\widetilde{X}_{0;h} = \widetilde{X}_{0;H} + \sum_{T \in \mathcal{T}_H} \widetilde{X}_T. \quad (5.17)$$

Our next step is to define suitable bilinear forms on the subspaces. On the coarse space, we employ the original bilinear form  $a(\cdot, \cdot)$ .

On the space  $\widetilde{X}_T$ , we define an approximate bilinear form. The corresponding local problem only involves the solution of a Neumann problem on the substructure  $T$ . It is defined by

$$\tilde{a}_T(\mathbf{u}, \mathbf{v}) := a_T(\mathcal{H}_T(\mu_T \mathbf{u} \cdot \mathbf{n}), \mathcal{H}_T(\mu_T \mathbf{v} \cdot \mathbf{n})), \quad \mathbf{u}, \mathbf{v} \in \widetilde{X}_T; \quad (5.18)$$

cf. [51]. We note that the local bilinear form is built with the original one, defined in the substructure  $T$ , and with the harmonic extensions of the traces on  $\partial T$ , scaled by  $\mu_T$ .

We will consider a hybrid Schwarz preconditioner, where one solves first the global problem and then the local ones, in parallel. The error propagation operator is given by

$$E := (I - \sum_{T \in \mathcal{T}_H} Q_T)(I - P_0),$$

where the orthogonal projection  $P_0$  and the operators  $\{Q_T\}$  are defined by

$$\begin{aligned} P_0 : \widetilde{X}_{0;h} &\rightarrow \widetilde{X}_{0;H}; & a(P_0 u, v) &= a(u, v), & v &\in \widetilde{X}_{0;H} \\ Q_T : \widetilde{X}_{0;h} &\rightarrow \widetilde{X}_T; & \tilde{a}_T(Q_T u, v) &= a(u, v), & v &\in \widetilde{X}_T. \end{aligned}$$

The corresponding Schwarz operator is

$$I - E = P_0 + \sum_{T \in \mathcal{T}_H} Q_T (I - P_0).$$

In the following, we will employ the symmetrized operator, obtained by an additional coarse solve,

$$\begin{aligned} Q_{hyb} &:= I - (I - P_0) \left( I - \sum_{T \in \mathcal{T}_H} Q_T \right) (I - P_0) \\ &= P_0 + (I - P_0) \left( \sum_{T \in \mathcal{T}_H} Q_T \right) (I - P_0) = P_0 + \sum_{T \in \mathcal{T}_H} \tilde{Q}_T, \end{aligned} \quad (5.19)$$

where

$$\tilde{Q}_T := (I - P_0) Q_T (I - P_0), \quad T \in \mathcal{T}_H.$$

Since  $P_0$  is a projection, this can be done at no extra cost.

We choose this hybrid algorithm since the local bilinear forms (5.18), though coercive on the spaces  $\tilde{X}_T$ , are not uniformly coercive with respect to  $H$ . In order to have a coercivity constant that is independent of  $H$ , the local bilinear forms have to be defined on smaller spaces. In Section 5.6, we will show that the local operators  $Q_T$  need to be defined on the subspace  $\text{Ran}(I - P_0)$ , and their image has to be projected on  $\text{Ran}(I - P_0)$ , for their norm to be independent of  $H$ ; see Lemma 2.3.2. We refer to Section 5.7, for some remarks on the implementation of Neumann–Neumann methods.

Similar hybrid algorithms have been employed successfully in some Neumann–Neumann methods for scalar or vector equations in  $H^1(\Omega)$ ; see [37, 38, 16, 54, 61]. For these methods, the local operators  $Q_T$  are not defined on the whole space but only on  $\text{Ran}(I - P_0)$  and the local bilinear forms are coercive only on local spaces contained in  $\text{Ran}(I - P_0)$ . For our methods, the situation is somewhat different, since the local problems are always solvable, but a good stability constant is obtained only on local spaces contained in  $\text{Ran}(I - P_0)$ .

## 5.5 Technical tools

In this section, we will modify some results proven in Section 4.3.3 for the two-dimensional case, and prove a technical lemma.

We first consider  $\rho_H$ , the interpolation operator onto the coarse space. The stability estimate in Lemma 4.3.1, for  $n = 3$ , can easily be proved for  $n = 2$ , by modifying the proof of Lemma 4.2.1 for  $H(\mathbf{curl}; \Omega)$ .

Let  $T$  be a substructure. A closer look at the proof of Lemma 4.3.7 shows that it is valid for both  $n = 2$ , as well as  $n = 3$ . Consequently, for  $n = 2, 3$ , a divergence free extension can be found

$$\tilde{\mathcal{H}}_T : S_{0;h}(\partial T) \rightarrow X_h(T),$$



such that (4.45) holds. We remark that a similar result also holds for  $H(\mathbf{curl}; \Omega)$  and  $n = 2$ . In particular, given a function  $\mu \in S_{0,h}(\partial T)$ , a curl-free extension  $\widetilde{\mathcal{H}}_T \mu$  can be found into the Nédélec space defined on  $T$ , such that (4.45) holds. In the proof of Lemma 4.3.7, it is enough to choose  $\mathbf{u} := \mathbf{curl} \phi$  and  $\widetilde{\mathcal{H}}_T \mu := \Pi_h^{\mathcal{N}^{\mathcal{D}^1}} \mathbf{u}$ .

For  $n = 2, 3$ , define  $V_h(\partial T) \subset H^{\frac{1}{2}}(\partial T)$  as

$$V_h(\partial T) := Q_h(\partial T) + B_h(\partial T);$$

see Section 4.3.3. Here  $Q_h(\partial T)$  is the space of all continuous piecewise bilinear (linear, for  $n = 2$ ) functions and  $B_h(\partial T)$  a space of bubble functions vanishing on the faces (edges)  $f \in \mathcal{F}_h$ ,  $f \subset \partial T$ :

$$\begin{aligned} Q_h(\partial T) &:= \{ \phi \in C^0(\partial T), \phi|_f \in \mathbb{Q}_1(f), f \subset \partial T, f \in \mathcal{F}_h \}, \\ B_h(\partial T) &:= \{ \phi \in C^0(\partial T), \phi|_f = \alpha_f \varphi_1 \cdots \varphi_{2(n-1)}, f \subset \partial T, f \in \mathcal{F}_h, \alpha_f \in \mathbb{R} \}, \end{aligned}$$

where  $\varphi_i$ ,  $1 \leq i \leq 2^{(n-1)}$ , are the nodal basis functions that span  $\mathbb{Q}_1(f)$  on the face (edge)  $f$ .

Lemma 4.3.5 is then valid for both  $n = 2$  and  $n = 3$ . The proof given in Section 4.3.3 for  $n = 3$ , can also be carried over to  $n = 2$ , by noticing that Lemmas 4.3.2, 4.3.3, and 4.3.4 are also valid for  $n = 2$ .

It remains to prove Lemma 4.3.6, for  $n = 2$ . The proof follows that of Section 4.3.3, but a different Sobolev-type inequality is employed; see (5.25) and (5.26).

**Lemma 5.5.1** *Let  $n = 2$  and let  $T$  be in  $\mathcal{T}_H$ . Let  $\{\mu_E, E \subset \partial T\}$  be functions in  $S_{0,h}(\partial T)$ , which vanish on  $\partial T \setminus E$  and let  $\mu := \sum_{E \subset \partial T} \mu_E$ . Then there exists a constant  $C$ , independent of  $h$  and  $\mu_H$ , such that,  $\forall \mu_H \in S_H(\partial T)$ ,*

$$\|\mu_E\|_{-\frac{1}{2}; \partial T}^2 \leq C(1 + \log H/h) \left( (1 + \log H/h) \|\mu + \mu_H\|_{-\frac{1}{2}; \partial T}^2 + \|\mu\|_{-\frac{1}{2}; \partial T}^2 \right).$$

*Proof.* Using Lemmas 4.3.5 and 4.3.3, we have

$$\|\mu_E\|_{-\frac{1}{2}; \partial T} \leq C \left( \sup_{\substack{\phi_Q \in Q_h(\partial T) \\ \phi_Q \neq \text{const.}}} \frac{\langle \mu_E, \phi_Q \rangle}{|\phi_Q|_{\frac{1}{2}; \partial T}} + \sup_{\substack{\phi_B \in B_h(\partial T) \\ \phi_B \neq 0}} \frac{\langle \mu_E, \phi_B \rangle}{|\phi_B|_{\frac{1}{2}; \partial T}} \right). \quad (5.20)$$

Let  $\vartheta_E$  be the function given in the proof of Lemma 4.2.1 and let  $I_h$  be the nodal interpolation operator onto  $Q_h(\partial T)$ . If, for any  $\phi_Q \in Q_h(\partial T)$ , we define the weighted average  $c_{\phi_Q}$  by

$$c_{\phi_Q} := \frac{\int_E I_h(\vartheta_E \phi_Q) ds}{\int_E \vartheta_E ds},$$

we can write

$$\sup_{\substack{\phi_Q \in Q_h(\partial T) \\ \phi_Q \neq \text{const.}}} \frac{\langle \mu_E, \phi_Q \rangle}{|\phi_Q|_{\frac{1}{2}; \partial T}} = \sup_{\substack{\phi_Q \in Q_h(\partial T) \\ \phi_Q \neq \text{const.}}} \frac{\langle \mu_E, \phi_Q - c_{\phi_Q} \rangle}{|\phi_Q - c_{\phi_Q}|_{\frac{1}{2}; \partial T}} = \sup_{\substack{\phi_Q \in Q_h(\partial T), \\ \phi_Q \neq 0, c_{\phi_Q} = 0}} \frac{\langle \mu_E, \phi_Q \rangle}{|\phi_Q|_{\frac{1}{2}; \partial T}}. \quad (5.21)$$

In the last term of (5.21), the  $H^{\frac{1}{2}}$ -seminorm can be replaced by the full norm, because of (4.33). We next decompose  $\phi_B$  into the sum of terms  $\phi_{B;E}$  supported on individual edges  $E \subset \partial T$

$$\phi_B = \sum_{\substack{E \in \mathcal{F}_H \\ E \subset \partial T}} \phi_{B;E}. \quad (5.22)$$

Similarly, we decompose  $\phi_Q$  into the sum of contributions supported on individual edges  $E \subset \partial T$ ,

$$\phi_{Q;E} := \vartheta_E \phi_Q, \quad E \subset \partial T$$

and a remainder  $\phi_{Q;w}$ :

$$\phi_{Q;w} := \phi_Q - \sum_{E \subset \partial T} \phi_{Q;E}. \quad (5.23)$$

We remark that  $\phi_{Q;w}$  is the sum of four contributions, one for each vertex of  $\partial T$ , and has support contained in the union of the two fine edges in  $\mathcal{F}_h$  that end at that vertex.

Local inverse estimates combined with interpolation arguments easily give

$$|\phi_{B;E}|_{\frac{1}{2}; \partial T}^2 \leq C |\phi_B|_{\frac{1}{2}; \partial T}^2. \quad (5.24)$$

Similar arguments give

$$|\phi_{Q;w}|_{\frac{1}{2}; \partial T}^2 \leq C \frac{1}{h} \|\phi_{Q;w}\|_{0; \partial T}^2 \leq C \|\phi_{Q;w}\|_{L^\infty(\partial T)}^2. \quad (5.25)$$

Using [23, Lemma 3.3], we have,

$$\|\phi_{Q;w}\|_{L^\infty(\partial T)}^2 \leq C(1 + \log H/h) \|\phi_Q\|_{\frac{1}{2}; \partial T}^2; \quad (5.26)$$

see also [12, Lemma 2.3], [21, Lemma 1], and [54, Lemma 7, p. 170], for a proof of similar Sobolev–type inequalities. Combining (5.25) and (5.26), we find

$$\|\phi_{Q;w}\|_{\frac{1}{2};\partial T}^2 \leq C(1 + \log H/h) \|\phi_Q\|_{\frac{1}{2};\partial T}^2. \quad (5.27)$$

Using the inequality  $\|u^h\|_{1;T} \leq C\|u^h\|_{1/2;\partial T}^2$ , which is valid for discrete harmonic functions, and the same argument as in [54, p. 172, Th. 3], we have,

$$\|\phi_{Q;E}\|_{\frac{1}{2};\partial T}^2 \leq C(1 + \log H/h)^2 \|\phi_Q\|_{\frac{1}{2};\partial T}^2; \quad (5.28)$$

see also [23, Th. 5.1] and [22, Lemma 4.5], for proofs of similar inequalities.

By using the splitting (5.23), we find

$$\begin{aligned} \langle \mu_E, \phi_Q \rangle &= \sum_{\hat{E} \subset \partial T} \langle \mu_E, \phi_{Q;\hat{E}} \rangle + \langle \mu_E, \phi_{Q;w} \rangle \\ &= \langle \mu, \phi_{Q;E} \rangle + \langle \mu_E, \phi_{Q;w} \rangle. \end{aligned} \quad (5.29)$$

Since  $I_h(\vartheta_E \phi_Q) = \phi_{Q;E} = I_h(\vartheta_E \phi_{Q;E})$  and since, according to (5.21), we can always assume that  $c_{\phi_Q} = 0$ , we obtain

$$\langle \mu_H, \phi_{Q;E} \rangle = 0, \quad \forall \mu_H \in S_H(\partial T),$$

and  $c_{\phi_{Q;E}} = 0$ . The first term on the right side of (5.29) can be bounded by means of (5.28)

$$|\langle \mu, \phi_{Q;E} \rangle| = |\langle \mu + \mu_H, \phi_{Q;E} \rangle| \leq C(1 + \log H/h) \|\phi_Q\|_{\frac{1}{2};\partial T} \|\mu + \mu_H\|_{-\frac{1}{2};\partial T}. \quad (5.30)$$

The second term on the right side of (5.29) can be bounded using the following argument: For each  $\phi_{Q;w}$  there is a unique  $\tilde{\phi}_{B;E} \in B_h(\partial T)$  such that

$$\int_e \phi_{Q;w} ds = \int_e \tilde{\phi}_{B;E} ds, \quad e \in \mathcal{F}_h, \quad e \subset F,$$

with  $\tilde{\phi}_{B;E} = 0$  on  $\partial T \setminus E$ . Moreover, this mapping is continuous

$$\|\tilde{\phi}_{B;E}\|_{\frac{1}{2};\partial T}^2 \leq C \frac{1}{h} \|\tilde{\phi}_{B;E}\|_{0;\partial T}^2 \leq C \frac{1}{h} \|\phi_{Q;w}\|_{0;\partial T}^2 \leq C \|\phi_{Q;w}\|_{\frac{1}{2};\partial T}^2.$$

By means of this bound and (5.27), we finally obtain

$$\begin{aligned} |\langle \mu_E, \phi_{Q;w} \rangle| &= |\langle \mu_E, \tilde{\phi}_{B;E} \rangle| = |\langle \mu, \tilde{\phi}_{B;E} \rangle| \leq C \|\mu\|_{-\frac{1}{2};\partial T} \|\phi_{Q;w}\|_{\frac{1}{2};\partial T} \\ &\leq C(1 + \log H/h)^{1/2} \|\mu\|_{-\frac{1}{2};\partial T} \|\phi_Q\|_{\frac{1}{2};\partial T}. \end{aligned} \quad (5.31)$$

Using (5.24), we find for the second term on the right hand side of (5.20)

$$\begin{aligned} \frac{|\langle \mu_E, \phi_B \rangle|}{|\phi_B|_{\frac{1}{2}; \partial T}} &= \frac{|\langle \mu, \phi_{B;E} \rangle|}{|\phi_B|_{\frac{1}{2}; \partial T}} \leq \frac{\|\mu\|_{-\frac{1}{2}; \partial T} \|\phi_{B;E}\|_{\frac{1}{2}; \partial T}}{|\phi_B|_{\frac{1}{2}; \partial T}} \\ &\leq C \frac{\|\mu\|_{-\frac{1}{2}; \partial T} |\phi_{B;E}|_{\frac{1}{2}; \partial T}}{|\phi_B|_{\frac{1}{2}; \partial T}} \leq C \|\mu\|_{-\frac{1}{2}; \partial T}. \end{aligned} \quad (5.32)$$

The proof is completed by combining (5.20), (5.21), (4.33), (5.23), (5.30), (5.31), and (5.32).  $\square$

We end this section with the following lemma.

**Lemma 5.5.2** *Let  $n = 2, 3$  and let  $T_1$  and  $T_2$  be two substructures with a common face  $F \in \mathcal{F}_H$  (edge, if  $n = 2$ ). Let  $\mu_F$  be a function in  $L^2(\partial T_1 \cup \partial T_2)$ , that vanishes outside  $F$ . Then there is a positive constant  $C$ , that only depends on the aspect ratios of  $T_1$  and  $T_2$ , such that*

$$\|\mu_F\|_{-\frac{1}{2}; \partial T_1} \leq C \|\mu_F\|_{-\frac{1}{2}; \partial T_2}.$$

*Proof.* We will only give the proof for the three-dimensional case. The case of  $n = 2$  can be proved in the same way.

Let  $\hat{T}$  be the unit cube, and let  $\mathcal{F}_1$  and  $\mathcal{F}_2$  be two functions that map  $T_1$  and  $T_2$ , respectively, onto  $\hat{T}$ , respectively, such that  $\mathcal{F}_1(x) = \mathcal{F}_2(x)$ ,  $\forall x \in F$ .

We have

$$\begin{aligned} \|\mu_F\|_{-\frac{1}{2}; \partial T_1} &= \sup_{\psi \in H^{\frac{1}{2}}(\partial T_1)} \frac{\langle \mu_F, \psi \rangle}{\|\psi\|_{\frac{1}{2}; \partial T_1}} \\ &\leq C_1 \sup_{\hat{\psi} \in H^{\frac{1}{2}}(\partial \hat{T})} \frac{H_{T_1}^2 \langle \hat{\mu}, \hat{\psi} \rangle}{H_{T_1}^{\frac{1}{2}} \|\hat{\psi}\|_{\frac{1}{2}; \partial \hat{T}}} \leq C_1 C_2 \left( \frac{H_{T_1}}{H_{T_2}} \right)^{\frac{3}{2}} \sup_{\psi \in H^{\frac{1}{2}}(\partial T_2)} \frac{\langle \mu_F, \psi \rangle}{\|\psi\|_{\frac{1}{2}; \partial T_2}}, \end{aligned}$$

where the constants  $C_1$  and  $C_2$  only depend on the aspect ratios of the substructures and  $\hat{\mu}(\hat{x}) := \mu_F(\mathcal{F}_1(\hat{x})) = \mu_F(\mathcal{F}_2(\hat{x}))$ . The product  $C_1 C_2 (H_{T_1}/H_{T_2})^{3/2}$  can then be bounded by a constant that only depends on the aspect ratios of the two substructures.  $\square$

## 5.6 Main result

In this section, we will prove a logarithmic bound for the condition number of the hybrid operator  $T_{hyb}$ , introduced in Section 5.4. We refer to [61], for similar proofs for a hybrid method for the Laplace equation.

**Lemma 5.6.1** *We have*

$$a(T_{hyb}\mathbf{u}, \mathbf{u}) \geq a(\mathbf{u}, \mathbf{u}), \quad \mathbf{u} \in \widetilde{X}_{0;h}.$$

*Proof.* We will first prove a lower bound for the smallest eigenvalue of the operator

$$\sum_{T \in \mathcal{T}_H} Q_T.$$

Given a function  $\mathbf{u} \in \widetilde{X}_{0;h}$ , for  $T \in \mathcal{T}_H$ , let

$$\mathbf{u}_T := \mathcal{H}(\mu_T^\dagger(\mathbf{u} \cdot \mathbf{n}|_\Gamma)) \in \widetilde{X}_T, \quad (5.33)$$

where the partition of unity  $\{\mu_T^\dagger\}$  is defined in (5.16). We remark that  $\mathbf{u}_T$  is obtained from  $\mathbf{u}$  by taking its normal component on  $\Gamma$  and multiplying it by the cut-off function  $\mu_T^\dagger$ , obtaining a function that is non-zero only on  $\partial T$ . We finally extend it harmonically into  $T$  and its neighboring substructures.

Since  $\{\mu_T^\dagger\}$  is a partition of unity on  $\Gamma$  and the vectors  $\mathbf{u}$  and  $\mathbf{u}_T$  are all harmonic extensions, we have

$$\mathbf{u} = \sum_{T \in \mathcal{T}_H} \mathbf{u}_T.$$

In view of Lemma 2.3.1, we have to bound the sum of the energies of the  $\mathbf{u}_T$ . Using the definition of  $\mathbf{u}_T$  and the fact that the functions  $\{\mu_T^\dagger\}$  are the pseudoinverses of the  $\{\mu_T\}$ , we have

$$\begin{aligned} \sum_{T \in \mathcal{T}_H} \tilde{a}_T(\mathbf{u}_T, \mathbf{u}_T) &= \sum_{T \in \mathcal{T}_H} a_T(\mathcal{H}_T(\mu_T \mathbf{u}_T \cdot \mathbf{n}), \mathcal{H}_T(\mu_T \mathbf{u}_T \cdot \mathbf{n})) \\ &= \sum_{T \in \mathcal{T}_H} a_T(\mathbf{u}, \mathbf{u}) = a(\mathbf{u}, \mathbf{u}). \end{aligned}$$

Lemma 2.3.1, ensures that the smallest eigenvalue of  $\sum_{T \in \mathcal{T}_H} Q_T$  is one. The same quantity is also a lower bound for the smallest eigenvalue of  $T_{hyb}$  since  $P_0$  is an orthogonal projection. In fact,

$$\begin{aligned} a(T_{hyb} \mathbf{u}, \mathbf{u}) &= a \left( P_0 \mathbf{u} + \sum_{T \in \mathcal{T}_H} \tilde{Q}_T \mathbf{u}, \mathbf{u} \right) \\ &= a(P_0 \mathbf{u}, P_0 \mathbf{u}) + a \left( \left( \sum_{T \in \mathcal{T}_H} Q_T \right) (I - P_0) \mathbf{u}, (I - P_0) \mathbf{u} \right) \geq a(\mathbf{u}, \mathbf{u}). \end{aligned}$$

□

In order to bound the largest eigenvalue, we will first prove an upper bound for the norm of the local operators  $\{\tilde{Q}_T\}$ ; see Lemma 2.3.2.

**Lemma 5.6.2** *Let  $T$  be a substructure. Then there is a constant  $C$ , independent of  $h$ ,  $H$ , the coefficients  $a$  and  $B$ , and the parameter  $\delta$ , such that*

$$\|\tilde{Q}_T\|_a \leq C \eta \left( 1 + \log \frac{H}{h} \right)^2,$$

where

$$\|\tilde{Q}_T\|_a^2 := \sup_{\mathbf{u} \in \tilde{X}_{0,h}} \frac{a(\tilde{Q}_T \mathbf{u}, \tilde{Q}_T \mathbf{u})}{a(\mathbf{u}, \mathbf{u})},$$

and

$$\eta := \max_{T \in \mathcal{T}_H} \{\eta_T\} := \max_{T \in \mathcal{T}_H} \max \left\{ \frac{\gamma_T}{\beta_T}, \frac{\gamma_T H_T^2}{a_T} \right\}. \quad (5.34)$$

*Proof.* Let  $\Pi_H : X_{0,h} \rightarrow \tilde{X}_{0,H}$  be the interpolation operator defined in Section 5.2. Since  $P_0$  is an orthogonal projection and it has the same range as  $\Pi_H$ , we have

$$(I - P_0)(I - \Pi_H) = I - P_0,$$

and we can then write

$$\tilde{Q}_T = (I - P_0) Q_T (I - P_0) = (I - P_0)(I - \Pi_H) Q_T (I - P_0). \quad (5.35)$$

It is therefore enough to estimate the norm of

$$(I - \Pi_H) Q_T,$$

when applied to  $\text{Ran}(I - P_0)$ .

Let  $\mathbf{u} \in \text{Ran}(I - P_0)$ , and  $\mathbf{w} := (I - \Pi_H) Q_T \mathbf{u}$ . The support of functions in  $\widetilde{X}_T$  extends to the neighboring substructures of  $T$ , while the approximate bilinear form  $\widetilde{a}_T(\cdot, \cdot)$  only involves the values of  $\mathbf{w}$  in  $T$ . We will first bound the energy of  $\mathbf{w}$  in  $T$ , and then that from the neighboring substructures, in terms of  $\widetilde{a}_T(\mathbf{w}, \mathbf{w})$ . We remark that we only need to consider the substructures that have a common face (edge, if  $n = 2$ ) with  $T$ . We also remark that  $\mathbf{w}$  is discrete harmonic. Let  $D$  be one of these substructures and  $\overline{F} = \partial T \cap \partial D$ . Using then the fact that  $\mathbf{w} \cdot \mathbf{n}$  has mean value zero on  $F$  and vanishes elsewhere on  $\partial D$ , and Lemma 4.3.7, we have

$$\begin{aligned} a_D(\mathbf{w}, \mathbf{w}) &\leq a_D\left(\widetilde{\mathcal{H}}_D(\mathbf{w} \cdot \mathbf{n}), \widetilde{\mathcal{H}}_D(\mathbf{w} \cdot \mathbf{n})\right) \\ &\leq \gamma_D \left\| \widetilde{\mathcal{H}}_D(\mathbf{w} \cdot \mathbf{n}) \right\|_{0;D}^2 \leq C \gamma_D \|\mathbf{w} \cdot \mathbf{n}\|_{-\frac{1}{2};\partial D}^2, \end{aligned} \quad (5.36)$$

with a constant  $C$  that does not depend on the diameter of  $D$ . Using Lemma 5.5.2 gives

$$\gamma_D \|\mathbf{w} \cdot \mathbf{n}\|_{-\frac{1}{2};\partial D}^2 \leq C \gamma_D \|\vartheta_F \mathbf{w} \cdot \mathbf{n}\|_{-\frac{1}{2};\partial T}^2 = C \frac{\gamma_D}{\mu_{T;D}^2} \|\vartheta_F(\mu_T \mathbf{w} \cdot \mathbf{n})\|_{-\frac{1}{2};\partial T}^2, \quad (5.37)$$

where  $\vartheta_F$  is identically one on  $F$  and vanishes on the rest of  $\partial T$ . Lemma 4.3.6 (Lemma 5.5.1, if  $n = 2$ ) and the fact that  $\mu_T \mathbf{w} \cdot \mathbf{n}$  has mean value zero on each face (edge, if  $n = 2$ ) of  $T$  ensures that the last term in (5.37) can be bounded by

$$\begin{aligned} &C \frac{\gamma_D}{\mu_{T;D}^2} \left(1 + \log \frac{H}{h}\right) \cdot \\ &\left( \|\mu_T \mathbf{w} \cdot \mathbf{n}\|_{-\frac{1}{2};\partial T}^2 + \left(1 + \log \frac{H}{h}\right) \|\mu_T \mathbf{w} \cdot \mathbf{n} + \psi_H\|_{-\frac{1}{2};\partial T}^2 \right), \end{aligned} \quad (5.38)$$

where  $\psi_H$  is an arbitrary function of  $S_H(\partial T)$ .

Combining (5.36), (5.37), and (5.38), we obtain

$$\begin{aligned} a_D(\mathbf{w}, \mathbf{w}) &\leq \frac{\gamma_D}{\mu_{T;D}^2} \left(1 + \log \frac{H}{h}\right) \cdot \\ &\left( \|\mu_T \mathbf{w} \cdot \mathbf{n}\|_{-\frac{1}{2};\partial T}^2 + \left(1 + \log \frac{H}{h}\right) \|\mu_T \mathbf{w} \cdot \mathbf{n} + \psi_H\|_{-\frac{1}{2};\partial T}^2 \right). \end{aligned} \quad (5.39)$$

The second term in (5.39) can be bounded by taking  $\psi_H = -\mu_T (\Pi_H Q_T \mathbf{u}) \cdot \mathbf{n}$ , and using the trace estimate (2.4), and the definition (5.18),

$$\begin{aligned}
& \|\mu_T \mathbf{w} \cdot \mathbf{n} + \psi_H\|_{-\frac{1}{2}; \partial T}^2 = \|\mu_T (Q_T \mathbf{u}) \cdot \mathbf{n}\|_{-\frac{1}{2}; \partial T}^2 \\
& \leq C \left( H_T^2 \|\operatorname{div} (\mathcal{H}_T (\mu_T (Q_T \mathbf{u}) \cdot \mathbf{n}))\|_{0; T}^2 + \|\mathcal{H}_T (\mu_T (Q_T \mathbf{u}) \cdot \mathbf{n})\|_{0; T}^2 \right) \\
& \leq C \frac{\eta}{\gamma_T} a_T (\mathcal{H}_T (\mu_T (Q_T \mathbf{u}) \cdot \mathbf{n}), \mathcal{H}_T (\mu_T (Q_T \mathbf{u}) \cdot \mathbf{n})) \\
& = C \frac{\eta}{\gamma_T} \tilde{a}_T (Q_T \mathbf{u}, Q_T \mathbf{u}).
\end{aligned} \tag{5.40}$$

For the first term in (5.39), we use the definition of  $\mathbf{w}$  and obtain

$$\|\mu_T \mathbf{w} \cdot \mathbf{n}\|_{-\frac{1}{2}; \partial T}^2 \leq 2 \|\mu_T (Q_T \mathbf{u}) \cdot \mathbf{n}\|_{-\frac{1}{2}; \partial T}^2 + 2 \|\mu_T (\Pi_H Q_T \mathbf{u}) \cdot \mathbf{n}\|_{-\frac{1}{2}; \partial T}^2. \tag{5.41}$$

A bound for the second term in (5.41) can be found in the following way:

It can easily be checked that the normal component of the vector

$$\mathbf{w}_H := \rho_H (\mathcal{H}_T (\mu_T (Q_T \mathbf{u}) \cdot \mathbf{n})),$$

on  $\partial T$  is equal to  $\mu_T (\Pi_H Q_T \mathbf{u}) \cdot \mathbf{n}$ . We remark that  $\mathbf{w}_H$  is obtained by first extending the normal trace  $(\mu_T (Q_T \mathbf{u}) \cdot \mathbf{n})$  harmonically into  $T$  and then interpolating into the coarse space  $X_{0; H}$ . Using the trace estimate (2.4) and the stability estimates for  $\rho_H$  in Lemma 4.3.1, we find

$$\begin{aligned}
& \|\mu_T (\Pi_H Q_T \mathbf{u}) \cdot \mathbf{n}\|_{-\frac{1}{2}; \partial T}^2 = \|\mathbf{w}_H \cdot \mathbf{n}\|_{-\frac{1}{2}; \partial T}^2 \leq C \left( H_T^2 \|\operatorname{div} \mathbf{w}_H\|_{0; T}^2 + \|\mathbf{w}_H\|_{0; T}^2 \right) \\
& \leq C \left( 1 + \log \frac{H}{h} \right) \left( H_T^2 \|\operatorname{div} (\mathcal{H}_T (\mu_T (Q_T \mathbf{u}) \cdot \mathbf{n}))\|_{0; T}^2 + \|\mathcal{H}_T (\mu_T (Q_T \mathbf{u}) \cdot \mathbf{n})\|_{0; T}^2 \right) \\
& \leq C \frac{\eta}{\gamma_T} \left( 1 + \log \frac{H}{h} \right) a_T (\mathcal{H}_T (\mu_T (Q_T \mathbf{u}) \cdot \mathbf{n}), \mathcal{H}_T (\mu_T (Q_T \mathbf{u}) \cdot \mathbf{n})) \\
& = C \frac{\eta}{\gamma_T} \left( 1 + \log \frac{H}{h} \right) \tilde{a}_T (Q_T \mathbf{u}, Q_T \mathbf{u}).
\end{aligned} \tag{5.42}$$

Finally, combining (5.39), (5.40), and (5.42), we obtain

$$a_D(\mathbf{w}, \mathbf{w}) \leq C \eta \left( 1 + \log \frac{H}{h} \right)^2 \frac{\gamma_D}{\mu_{T; D}^2 \gamma_T} \tilde{a}_T (Q_T \mathbf{u}, Q_T \mathbf{u}). \tag{5.43}$$



An estimate for the energy  $a_T(\mathbf{w}, \mathbf{w})$  can be found in a similar way:

If a substructure  $D$  shares a face (edge, if  $n = 2$ ) with  $T$ , let  $\overline{F}_D := \partial T \cap \partial D$  be the common face. Since  $\mathbf{w} \cdot \mathbf{n}$  has mean value zero on each face of  $\partial T$ , Lemma 4.3.7 can still be applied. We have

$$\begin{aligned}
a_T(\mathbf{w}, \mathbf{w}) &\leq a_T\left(\widetilde{\mathcal{H}}_T(\mathbf{w} \cdot \mathbf{n}), \widetilde{\mathcal{H}}_T(\mathbf{w} \cdot \mathbf{n})\right) \leq \gamma_T \left\| \widetilde{\mathcal{H}}_T(\mathbf{w} \cdot \mathbf{n}) \right\|_{0;T}^2 \\
&\leq C \gamma_T \|\mathbf{w} \cdot \mathbf{n}\|_{-\frac{1}{2};\partial T}^2 = \gamma_T \left\| \sum_D \vartheta_{F_D}(\mathbf{w} \cdot \mathbf{n}) \right\|_{-\frac{1}{2};\partial T}^2 \\
&\leq C \sum_D \frac{\gamma_T}{\mu_{T;D}^2} \|\vartheta_{F_D}(\mu_T \mathbf{w} \cdot \mathbf{n})\|_{-\frac{1}{2};\partial T}^2,
\end{aligned} \tag{5.44}$$

where the sum is taken over the substructures  $D$  that share a face (edge, if  $n = 2$ ) with  $T$ , and  $\vartheta_{F_D}$  is equal to one on  $F_D$  and vanishes on the rest of  $\partial T$ . Lemma 4.3.6 (Lemma 5.5.1, if  $n = 2$ ) thus gives the following bound for the last term in (5.44):

$$\begin{aligned}
C \sum_D \frac{\gamma_T}{\mu_{T;D}^2} \left(1 + \log \frac{H}{h}\right) \cdot \\
\left( \|\mu_T \mathbf{w} \cdot \mathbf{n}\|_{-\frac{1}{2};\partial T}^2 + \left(1 + \log \frac{H}{h}\right) \|\mu_T \mathbf{w} \cdot \mathbf{n} + \psi_H\|_{-\frac{1}{2};\partial T}^2 \right),
\end{aligned} \tag{5.45}$$

where  $\psi_H$  is an arbitrary function of  $S_H(\partial T)$ .

An upper bound for (5.45) can be obtained in the same way as for (5.39). (5.44) and (5.45) give

$$a_T(\mathbf{w}, \mathbf{w}) \leq C \eta \left(1 + \log \frac{H}{h}\right)^2 \left( \sum_D \frac{1}{\mu_{T;D}^2} \right) \tilde{a}_T(Q_T \mathbf{u}, Q_T \mathbf{u}). \tag{5.46}$$

Employing (5.43) and (5.46), and summing over the substructures that share a face (edge) with  $T$ , we obtain

$$a(\mathbf{w}, \mathbf{w}) \leq C \eta \left(1 + \log \frac{H}{h}\right)^2 \left( \sum_D \frac{\gamma_T + \gamma_D}{\mu_{T;D}^2 \gamma_T} \right) \tilde{a}_T(Q_T \mathbf{u}, Q_T \mathbf{u}).$$

It can easily be checked that the terms

$$\frac{\gamma_T + \gamma_D}{\mu_{T;D}^2 \gamma_T} = \frac{(\gamma_T + \gamma_D) \gamma_T^{2\delta}}{(\gamma_T^\delta + \gamma_D^\delta)^2 \gamma_T},$$

are homogeneous functions of  $\gamma_T$  and  $\gamma_D$ , and can be bounded by 2, independently of  $\gamma_T, \gamma_D > 0$ , and  $\delta \geq 1/2$ . We then obtain

$$a(\mathbf{w}, \mathbf{w}) \leq C \eta \left(1 + \log \frac{H}{h}\right)^2 \tilde{a}_T(Q_T \mathbf{u}, Q_T \mathbf{u}).$$

Using the definition of  $Q_T$  and the fact that we have chosen  $\mathbf{u} \in \text{Ran}(I - P_0)$ , we can write

$$\begin{aligned} a(\mathbf{w}, \mathbf{w}) &\leq C \eta \left(1 + \log \frac{H}{h}\right)^2 a(\mathbf{u}, Q_T \mathbf{u}) \\ &= C \eta \left(1 + \log \frac{H}{h}\right)^2 a(\mathbf{u}, (I - P_0)Q_T(I - P_0)\mathbf{u}) \\ &= C \eta \left(1 + \log \frac{H}{h}\right)^2 a(\mathbf{u}, \mathbf{w}). \end{aligned}$$

By applying Schwarz inequality, we finally obtain

$$a((I - \Pi_H)Q_T \mathbf{u}, (I - \Pi_H)Q_T \mathbf{u}) = a(\mathbf{w}, \mathbf{w}) \leq C \eta^2 \left(1 + \log \frac{H}{h}\right)^4 a(\mathbf{u}, \mathbf{u}),$$

and the proof is completed by noting that  $(I - P_0)$  is an orthogonal projection.  $\square$

**Lemma 5.6.3** *There is a constant  $C$ , independent of  $h, H, \mathbf{u}$ , the coefficients  $a$  and  $B$ , and the parameter  $\delta$ , such that*

$$a(T_{hyb} \mathbf{u}, \mathbf{u}) \leq C \eta \left(1 + \log \frac{H}{h}\right)^2 a(\mathbf{u}, \mathbf{u}), \quad \mathbf{u} \in \tilde{X}_{0;h}.$$

*Proof.* The proof employs the previous Lemma and a standard coloring argument; see, e.g., [54, p. 165] or [6, Th. 4.1]. We present it here for completeness.

Let  $T$  be a substructure and define  $\Omega_T$  as the union of  $T$  and the substructures that have a common face (edge, if  $n = 2$ ) with  $T$ . Let  $\chi_T$  be the characteristic function of  $\Omega_T$ . We have, for  $\mathbf{u} \in \tilde{X}_{0;h}$ ,

$$\begin{aligned} a\left(\sum_T \tilde{Q}_T \mathbf{u}, \sum_T \tilde{Q}_T \mathbf{u}\right) &= \sum_{T,D} a\left(\chi_T \tilde{Q}_T \mathbf{u}, \chi_D \tilde{Q}_D \mathbf{u}\right) \\ &\leq \sum_{T,D} a\left(\chi_D \tilde{Q}_T \mathbf{u}, \chi_D \tilde{Q}_T \mathbf{u}\right)^{1/2} a\left(\chi_T \tilde{Q}_D \mathbf{u}, \chi_T \tilde{Q}_D \mathbf{u}\right)^{1/2} \\ &\leq \sum_{T,D} a\left(\chi_D \tilde{Q}_T \mathbf{u}, \chi_D \tilde{Q}_T \mathbf{u}\right) \leq C \sum_T a\left(\tilde{Q}_T \mathbf{u}, \tilde{Q}_T \mathbf{u}\right). \end{aligned} \tag{5.47}$$

In the last step, we have used the fact that, in the sum over  $T$  and  $D$ , every integral over a single substructure is counted at most 6 times (4 times, if  $n = 2$ ), the number of faces (edges) of a substructure. Using Lemma 5.6.2, we can then write

$$\begin{aligned} \sum_T a(\tilde{Q}_T \mathbf{u}, \tilde{Q}_T \mathbf{u}) &\leq \sum_T a(\tilde{Q}_T \mathbf{u}, \mathbf{u}) \|\tilde{Q}_T\|_a \\ &\leq C \eta \left(1 + \log \frac{H}{h}\right)^2 a\left(\sum_T \tilde{Q}_T \mathbf{u}, \mathbf{u}\right). \end{aligned} \quad (5.48)$$

Combining (5.47) and (5.48) and using Schwarz inequality, we obtain

$$a\left(\sum_T \tilde{Q}_T \mathbf{u}, \sum_T \tilde{Q}_T \mathbf{u}\right) \leq C \eta^2 \left(1 + \log \frac{H}{h}\right)^4 a(\mathbf{u}, \mathbf{u}).$$

Another application of Schwarz inequality gives

$$a\left(\sum_T \tilde{Q}_T \mathbf{u}, \mathbf{u}\right) \leq C \eta \left(1 + \log \frac{H}{h}\right)^2 a(\mathbf{u}, \mathbf{u}),$$

and the bound for  $T_{hyb}$  is obtained by noting that  $P_0$  is an orthogonal projection.

□

Lemmas 5.6.1 and 5.6.3 combine to give the following theorem.

**Theorem 5.6.1** *There is a constant  $C$ , independent of  $h$ ,  $H$ , the coefficients  $a$  and  $B$ , and the parameter  $\delta$ , such that*

$$\kappa(T_{hyb}) \leq C \eta \left(1 + \log \frac{H}{h}\right)^2,$$

where  $\eta$  is the constant in Lemma 5.6.2.

We remark that the same constant  $\eta$  also appears in the estimates for the edge and face-space methods in Chapter 4; see (4.12) and (4.50).

The estimate given in Theorem 5.6.1 remains bounded when the coefficient matrix  $B$  tends to zero, but becomes unbounded when  $a$  becomes small. The following lemma ensures that in the limit case  $a = 0$ , the condition number of the hybrid operator is bounded independently of  $H/h$  and the jumps of the coefficient  $B$ .

**Lemma 5.6.4** *In the limit case  $a = 0$ , there is a constant  $C$ , independent of  $h$ ,  $H$ , the coefficient matrix  $B$ , and the parameter  $\delta$ , such that*

$$\kappa(T_{hyb}) \leq C \xi,$$

where

$$\xi := \max_{T \in \mathcal{T}_H} \left\{ \frac{\gamma_T}{\beta_T} \right\}.$$

*Proof.* It is immediate to check that Lemma 5.6.1 still holds. It is then enough to prove a bound for  $\|\tilde{Q}_T\|_a$ , as in Lemma 5.6.2, since the coloring argument in the proof of Lemma 5.6.3 can also be employed in the limit case  $a = 0$ .

Let  $T$  be a substructure and let  $\tilde{Q}_T = (I - P_0)Q_T(I - P_0)$  be defined in Section 5.4. Since  $a = 0$ , the bilinear forms  $a(\cdot, \cdot)$  and  $a_T(\cdot, \cdot)$  are just weighted  $L^2$  scalar products.

Let  $\mathbf{u} \in \tilde{X}_{0,h}$ , and  $\mathbf{w} := Q_T \mathbf{u} \in \tilde{X}_T$ . The proof is similar to the one of Lemma 5.6.2. The support of functions in  $\tilde{X}_T$  extends to the neighboring substructures of  $T$ , while the approximate bilinear form  $\tilde{a}_T(\cdot, \cdot)$  only involves the values of  $\mathbf{w}$  in  $T$ . We will first bound the energy of  $\mathbf{w}$  in  $T$ , and then that from the neighboring substructures, in terms of  $\tilde{a}_T(\mathbf{w}, \mathbf{w})$ . We remark that we only need to consider the substructures that have a common face (edge, if  $n = 2$ ) with  $T$ . We also remark that  $\mathbf{w}$  is discrete harmonic. Let  $D$  be one of these substructures and  $\bar{F} = \partial T \cap \partial D$ . We have

$$\begin{aligned} a_D(\mathbf{w}, \mathbf{w}) &\leq a_D(\hat{\mathcal{H}}_D(\mathbf{w} \cdot \mathbf{n}), \hat{\mathcal{H}}_D(\mathbf{w} \cdot \mathbf{n})) \\ &\leq \gamma_D \left\| \hat{\mathcal{H}}_D(\mathbf{w} \cdot \mathbf{n}) \right\|_{0;D}^2 \leq C \gamma_D \sum_{f \subset \bar{F}} h_f^n \lambda_f(\mathbf{w})^2, \end{aligned} \tag{5.49}$$

where  $\hat{\mathcal{H}}_D(\mathbf{w} \cdot \mathbf{n})$  is the extension by zero of  $\mathbf{w} \cdot \mathbf{n}$  into  $D$  and, for the last inequality, we have used (2.28).

The last term in (5.49) can be bounded using the fact that the function  $\mu_T$  is constant on  $F$  and the degree of freedom  $\lambda_f(\mathbf{w})$  is the normal component of  $\mathbf{w}$  on

$f \subset F$ . We can then write

$$\begin{aligned}
\sum_{f \subset F} h_f^n \lambda_f(\mathbf{w})^2 &= \frac{1}{\mu_{D;T}^2} \sum_{f \subset F} \mu_{D;T}^2 h_f^n \lambda_f(\mathbf{w})^2 \\
&= \frac{1}{\mu_{D;T}^2} \sum_{f \subset F} h_f^n \lambda_f(\mathcal{H}_T(\mu_T \mathbf{w} \cdot \mathbf{n}))^2 \\
&\leq \frac{1}{\mu_{D;T}^2} \sum_{f \subset \bar{T}} h_f^n \lambda_f(\mathcal{H}_T(\mu_T \mathbf{w} \cdot \mathbf{n}))^2 \\
&\leq C \frac{1}{\mu_{D;T}^2} \|\mathcal{H}_T(\mu_T \mathbf{w} \cdot \mathbf{n})\|_{0;T}^2 \\
&\leq C \xi \frac{1}{\mu_{D;T}^2 \gamma_T} a_T(\mathcal{H}_T(\mu_T \mathbf{w} \cdot \mathbf{n}), \mathcal{H}_T(\mu_T \mathbf{w} \cdot \mathbf{n})) \\
&= C \xi \frac{1}{\mu_{D;T}^2 \gamma_T} \tilde{a}_T(\mathbf{w}, \mathbf{w}),
\end{aligned} \tag{5.50}$$

where we have also used (2.28). Combining (5.49) and (5.50), and using the definition of  $\mathbf{w}$ , we obtain

$$a_D(\mathbf{w}, \mathbf{w}) \leq C \xi \frac{\gamma_D}{\mu_{D;T}^2 \gamma_T} \tilde{a}_T(Q_T \mathbf{u}, Q_T \mathbf{u}); \tag{5.51}$$

see (5.43).

An estimate for the energy  $a_T(\mathbf{w}, \mathbf{w})$  can be found in a similar way:

If a substructure  $D$  shares a face (edge, if  $n = 2$ ) with  $T$ , let  $\bar{F}_D := \partial T \cap \partial D$  be the common face. We have

$$\begin{aligned}
a_T(\mathbf{w}, \mathbf{w}) &\leq a_T(\hat{\mathcal{H}}_T(\mathbf{w} \cdot \mathbf{n}), \hat{\mathcal{H}}_T(\mathbf{w} \cdot \mathbf{n})) \\
&\leq \gamma_T \|\hat{\mathcal{H}}_T(\mathbf{w} \cdot \mathbf{n})\|_{0;T}^2 \leq C \gamma_T \sum_{f \subset \partial T} h_f^n \lambda_f(\mathbf{w})^2,
\end{aligned} \tag{5.52}$$

where  $\hat{\mathcal{H}}_T(\mathbf{w} \cdot \mathbf{n})$  is the extension by zero of  $\mathbf{w} \cdot \mathbf{n}$  into  $T$  and, for the last inequality, we have used (2.28).

The right hand side of (5.52) can be bounded using similar arguments as in (5.50):

$$\begin{aligned}
\gamma_T \sum_{f \subset \partial T} h_f^n \lambda_f(\mathbf{w})^2 &\leq C \gamma_T \sum_{F_D \subset \partial T} \frac{1}{\mu_{D;T}^2} \sum_{f \subset F_D} h_f^n \lambda_f(\mathcal{H}_T(\mu_T \mathbf{w} \cdot \mathbf{n}))^2 \\
&\leq C \sum_{F_D \subset \partial T} \frac{\gamma_T}{\mu_{D;T}^2} \sum_{f \subset \bar{T}} h_f^n \lambda_f(\mathcal{H}_T(\mu_T \mathbf{w} \cdot \mathbf{n}))^2 \\
&\leq C \xi a_T (\mathcal{H}_T(\mu_T \mathbf{w} \cdot \mathbf{n}), \mathcal{H}_T(\mu_T \mathbf{w} \cdot \mathbf{n})) \sum_{F_D \subset \partial T} \frac{1}{\mu_{D;T}^2} \\
&= C \xi \tilde{a}_T(Q_T \mathbf{u}, Q_T \mathbf{u}) \sum_{F_D \subset \partial T} \frac{1}{\mu_{D;T}^2},
\end{aligned} \tag{5.53}$$

where we have used (2.28) and the definition of  $\mathbf{w}$ .

Employing (5.51), (5.52), and (5.53), and summing over the substructures that share a face (edge, if  $n = 2$ ) with  $T$ , we obtain

$$a(\mathbf{w}, \mathbf{w}) \leq C \xi \left( \sum_D \frac{\gamma_T + \gamma_D}{\mu_T^2 \gamma_T} \right) \tilde{a}(Q_T \mathbf{u}, Q_T \mathbf{u}),$$

and a bound for  $\|\tilde{Q}_T\|_a$  can then be found as in the proof of Lemma 5.6.2.  $\square$

We remark that Lemma 5.6.4 gives an optimal bound for the limit case  $a = 0$ . Thus, as the ratio between the coefficients  $B$  and  $a$  becomes large, we expect an upper bound for the condition number which is independent of  $H/h$ ; see the numerical results in the next section.

## 5.7 Numerical results

In this section, we present some numerical results on the performance of the hybrid Neumann–Neumann method described in the previous sections, when varying the diameters of the coarse and fine meshes, and the coefficients  $a$  and  $B$ . We will only consider two–dimensional problems.

The hybrid operator is given in (5.19). The matrix representation of the projection  $P_0$  is

$$B_H S := (\tilde{R}_H^T S_H^{-1} \tilde{R}_H) S,$$

where  $\tilde{R}_H^T$  is the natural extension matrix from the coarse space into the fine space, defined on the interface  $\Gamma$ , and  $S_H$  is the matrix representation of the bilinear form

$s(\cdot, \cdot)$  on the coarse space, defined by

$$S_H := \tilde{R}_H S \tilde{R}_H^T.$$

We remark that, if  $n_H$  is the dimension of the coarse space,  $n_H$  applications of the Schur complement are required, in order to calculate  $S_H$ . Since the basis functions of the coarse space are supported on single coarse edges (faces, if  $n = 3$ ), only the solution of at most two Dirichlet problems on two substructures are required for the application of  $S$  to a coarse basis function.

For a generic substructure  $T_i$ , the matrix representation of the local operator  $Q_{T_i}$  is

$$B_i S := \left( \tilde{R}_i^T D_i^{-1} S_i^{-1} D_i^{-1} \tilde{R}_i \right) S;$$

see (5.18). Here the natural extension  $\tilde{R}_i^T$  maps the local degrees of freedom on  $\partial T_i$  into the corresponding global ones on  $\Gamma$ , the diagonal matrix  $D_i$  represents the multiplication by the scaling function  $\mu_{T_i}$ , and  $S_i$  is the Schur complement of the local bilinear form  $a_{T_i}(\cdot, \cdot)$ , with respect to the variables on  $\partial T_i$ . The matrix  $S_i$  does not need to be calculated explicitly, but the action of its inverse on a local vector can be calculated by solving a Neumann problem on the substructure  $T_i$ ; see [54, Sect. 4.2.1]. We also note that, as is often the case for Neumann–Neumann methods, the local averaging operators  $\{D_i^{-1}\}$  satisfy

$$\sum_i \tilde{R}_i D_i^{-1} \tilde{R}_i = Id;$$

see, e.g., [22, 54].

We have considered the domain  $\Omega = (0, 1)^2$  and uniform rectangular triangulations  $\mathcal{T}_h$  and  $\mathcal{T}_H$ . The fine triangulation  $\mathcal{T}_h$  consists of  $n^2$  square elements, with  $h = 1/n$ . The matrix  $B$  is given by

$$B = \text{diag}\{b, b\}.$$

In Table 5.1, we show the estimated condition number and the number of iterations in order to obtain a reduction of the norm of the preconditioned residual by a factor  $10^{-6}$ , as a function of the dimensions of the fine and coarse meshes. For a fixed ratio  $H/h$ , the condition number and the number of iterations are quite

Table 5.1: Estimated condition number and number of CG iterations necessary for a reduction of  $10^{-6}$  of the norm of the preconditioned residual (in parentheses), versus  $H/h$  and  $n$ . Case of  $a = 1$ ,  $b = 1$ .

$H/h$	32	16	8	4	2
n=32	-	3.075 (4)	2.881 (10)	2.182 (8)	1.505 (5)
n=64	4.004 (4)	3.791 (11)	3.023 (10)	2.113 (7)	1.508 (5)
n=128	4.860 (12)	3.985 (11)	2.935 (8)	2.033 (6)	x
n=192	-	3.978 (10)	2.854 (7)	1.974 (5)	x
n=256	5.112 (12)	4.01 (10)	2.854 (7)	1.974 (5)	x

insensitive to the dimension of the fine mesh. Our results compare very well with those for finite element approximations in  $H^1$  of the Laplace equation; see, e.g. [54], and with those for the iterative substructuring method based on individual edges, described in Chapter 4; see Table 4.1.

In Figure 5.1, we plot the results of Table 5.1, together with the best second order logarithmic polynomial least-square fit. The relative fitting error is about 2.8 per cent. Our numerical results are therefore in good agreement with the theoretical bound obtained in the previous section and suggest that our bound is sharp.

In Table 5.2, we show some results when the ratio of the coefficients  $b$  and  $a$  is changed. For a fixed value of  $n = 128$  and  $a = 1$ , the estimated condition number and the number of iterations are shown as a function of  $H/h$  and  $b$ . In accordance with Theorem 5.6.1, the condition number is independent of the ratio  $b/a$ , when  $b/a \leq 1$ . Table 5.2 also shows that, in practice, this holds for  $b/a \geq 1$ , and that, when  $b/a$  is very large, the condition number tends to be independent of  $H/h$ . Our numerical results then confirm our analysis of the limit case  $a = 0$ , in Lemma 5.6.4. The numerical results in Table 5.2 compare very well with those in Table 4.2.

We finally consider some cases where the coefficients have jumps. In Table 5.3, we show some results when the coefficient  $b$  has jumps across the substructures. We



Table 5.2: Estimated condition number and number of CG iterations necessary for a reduction of  $10^{-6}$  of the norm of the preconditioned residual (in parentheses), versus  $H/h$  and  $b$ . Case of  $n = 128$  and  $a = 1$ .

$H/h$	4	8	16	32
b=1e-5	2.033 (6)	2.935 (8)	3.988 (11)	4.871 (12)
b=1e-4	2.033 (6)	2.936 (8)	3.988 (11)	4.871 (12)
b=1e-3	2.033 (6)	2.936 (8)	3.988 (11)	4.871 (12)
b=1e-2	2.033 (6)	2.936 (8)	3.988 (11)	4.871 (12)
b=1e-1	2.033 (6)	2.935 (8)	3.988 (11)	4.87 (12)
b=1	2.033 (6)	2.935 (8)	3.985 (11)	4.86 (12)
b=1e+1	2.032 (6)	2.931 (8)	3.959 (11)	4.765 (12)
b=1e+2	2.026 (6)	2.881 (8)	3.705 (10)	4.15 (10)
b=1e+3	1.932 (5)	2.507 (7)	2.806 (8)	2.862 (7)
b=1e+4	1.613 (4)	1.717 (5)	1.751 (5)	1.771 (5)
b=1e+5	1.124 (3)	1.134 (3)	1.15 (3)	1.154 (3)

consider the checkerboard distribution shown in Figure 4.2, where  $b$  is equal to  $b_1$  in the shaded area and to  $b_2$  elsewhere. For a fixed value of  $n = 128$ ,  $b_1 = 100$ , and  $a = 1$ , the estimated condition number and the number of iterations are shown as a function of  $H/h$  and  $b_2$ . For  $b_2 = 100$ , the coefficient  $b$  has a uniform distribution, and this corresponds to a minimum for the condition number and the number of iterations. When  $b_2$  decreases or increases, the condition number and the number of iterations also increase, but they can still be bounded independently of  $b_2$ . The results in Table 5.3 compare very well with those in Table 4.3.

In Table 5.4, we show some results when the coefficient  $a$  has jumps. We consider the checkerboard distribution shown in Figure 4.2, where  $a$  is equal to  $a_1$  in the shaded area and to  $a_2$  elsewhere. For a fixed value of  $n = 128$ ,  $a_1 = 0.01$ , and  $b = 1$ , the estimated condition number and the number of iterations are shown as a function of  $H/h$  and  $a_2$ . We remark that for  $a_2 = 0.01$ , the coefficient  $a$  has a uniform distribution. A slight increase in the number of iterations and the condition number is observed, when  $a_2$  is decreased or increased and when  $H/h$  is large.

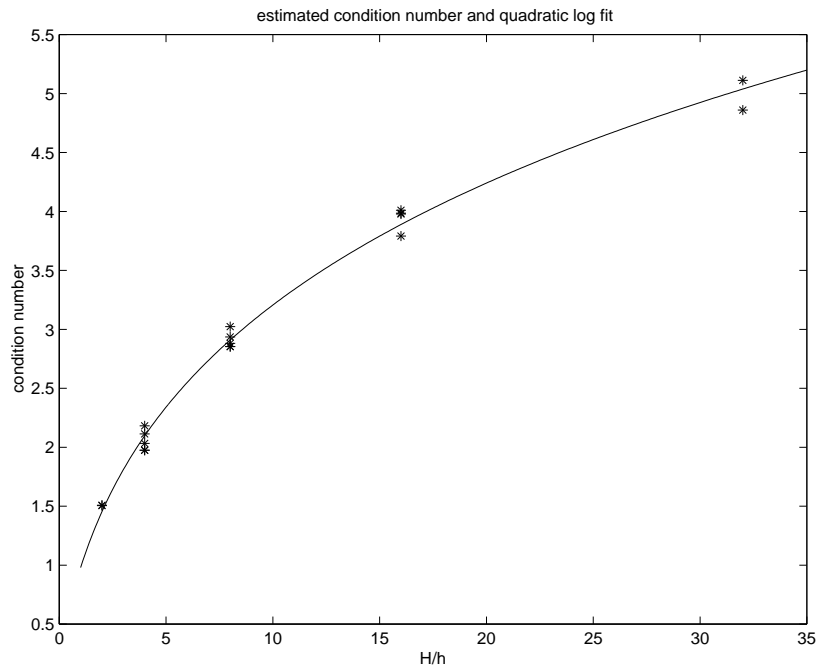


Figure 5.1: Estimated condition number from Table 5.1 (asterisk) and least-square second order logarithmic polynomial (solid line), versus  $H/h$ ; relative fitting error about 2.8 per cent.

Finally, we recall that when Maxwell's equations are discretized with an implicit time-scheme, the time step is related to the ratio  $b/a$ . The iterative substructuring method presented in this chapter therefore appears very attractive for the solution of linear systems arising from the finite element approximation of time-dependent Maxwell's equations.

Table 5.3: Checkerboard distribution for  $b$ :  $(b_1, b_2)$ . Estimated condition number and number of CG iterations for a reduction of  $10^{-6}$  of the norm of the preconditioned residual (in parentheses), versus  $H/h$  and  $b_2$ . Case of  $n = 128$ ,  $a = 1$ , and  $b_1 = 100$ .

$H/h$	4	8	16
$b_2 = 1e - 4$	5.344 (14)	7.514 (16)	9.989 (19)
$b_2 = 1e - 3$	5.321 (14)	7.481 (16)	9.945 (19)
$b_2 = 1e - 2$	5.248 (13)	7.379 (16)	9.81 (19)
$b_2 = 1e - 1$	5.031 (12)	7.073 (15)	9.402 (18)
$b_2 = 1$	4.442 (11)	6.239 (14)	8.289 (17)
$b_2 = 1e + 1$	3.249 (8)	4.532 (11)	5.987 (14)
$b_2 = 1e + 2$	2.026 (6)	2.881 (8)	3.705 (10)
$b_2 = 1e + 3$	3.15 (8)	4.138 (11)	4.932 (13)
$b_2 = 1e + 4$	3.556 (9)	4.043 (11)	4.384 (13)
$b_2 = 1e + 5$	2.638 (8)	3.24 (11)	3.912 (13)
$b_2 = 1e + 6$	2.417 (8)	3.176 (11)	3.919 (13)

Table 5.4: Checkerboard distribution for  $a$ :  $(a_1, a_2)$ . Estimated condition number and number of CG iterations for a reduction of  $10^{-6}$  of the norm of the preconditioned residual (in parentheses), versus  $H/h$  and  $a_2$ . Case of  $n = 128$ ,  $b = 1$ , and  $a_1 = 0.01$ .

$H/h$	4	8	16
$a_2 = 1e - 7$	2.1 (6)	3.399 (9)	5.909 (13)
$a_2 = 1e - 6$	2.1 (6)	3.196 (9)	5.537 (13)
$a_2 = 1e - 5$	2.059 (6)	2.882 (8)	4.165 (11)
$a_2 = 1e - 4$	2.051 (6)	2.857 (8)	3.403 (10)
$a_2 = 1e - 3$	1.944 (5)	2.853 (8)	3.611 (10)
$a_2 = 1e - 2$	2.026 (6)	2.881 (8)	3.705 (10)
$a_2 = 1e - 1$	2.032 (6)	2.933 (8)	3.948 (11)
$a_2 = 1$	2.033 (6)	2.938 (8)	3.975 (11)
$a_2 = 1e + 1$	2.033 (6)	2.939 (8)	3.977 (11)
$a_2 = 1e + 2$	2.033 (6)	2.939 (8)	3.978 (11)
$a_2 = 1e + 3$	2.033 (6)	2.939 (8)	3.978 (11)

# Bibliography

- [1] Robert A. Adams. *Sobolev Spaces*. Academic Press New York, 1975.
- [2] Ana Alonso and Alberto Valli. Some remarks on the characterization of the space of tangential traces of  $H(\text{rot}; \Omega)$  and the construction of an extension operator. *Manuscripta Math.*, 89:159–178, 1996.
- [3] Ana Alonso and Alberto Valli. An optimal domain decomposition preconditioner for low-frequency time-harmonic Maxwell equations. *Math. Comp.*, 68(226):607, 1999.
- [4] Chérif Amrouche, Christine Bernardi, Monique Dauge, and Vivette Girault. Vector potentials in three-dimensional nonsmooth domains. Technical Report R 96001, Laboratoire d'Analyse Numérique, Université Pierre et Marie Curie, Paris, 1996.
- [5] Douglas N. Arnold, Richard S. Falk, and Ragnar Winther. Multigrid preconditioning in  $H(\text{div})$  on non-convex polygons. *Comput. and Appl. Math.*, 1997. Submitted.
- [6] Douglas N. Arnold, Richard S. Falk, and Ragnar Winther. Preconditioning in  $H(\text{div})$  and applications. *Math. Comp.*, 66:957–984, 1997.
- [7] Douglas N. Arnold, Richard S. Falk, and Ragnar Winther. Multigrid in  $H(\text{div})$  and  $H(\text{curl})$ . Technical Report 13 1997/98, Mittag-Leffler Institute, 1998.
- [8] Franck Assous, Pierre Degond, Ernst Heintze, Pierre-Arnaud Raviart, and J. Segre. On a finite element method for solving 3D Maxwell equations. *J. Comput. Phys.*, 109:222–237, 1993.

- [9] Faker Ben Belgacem and Christine Bernardi. Spectral element discretization of the Maxwell equations. Technical Report R 97027, Laboratoire d'Analyse Numérique, Université Pierre et Marie Curie, Paris, 1997.
- [10] Alain Bossavit. A rationale for edge elements in 3d field computations. *IEEE Trans. Mag.*, 24:74–79, 1988.
- [11] Jean-François Bourgat, Roland Glowinski, Patrick Le Tallec, and Marina Vidrascu. Variational formulation and algorithm for trace operator in domain decomposition calculations. In Tony Chan, Roland Glowinski, Jacques Périaux, and Olof Widlund, editors, *Domain Decomposition Methods*, pages 3–16, Philadelphia, PA, 1989. SIAM.
- [12] James H. Bramble and Jinchao Xu. Some estimates for a weighted  $L^2$  projection. *Math. Comp.*, 56:463–476, 1991.
- [13] Susanne Brenner. A multigrid algorithm for the lowest order Raviart-Thomas mixed triangular finite element method. *SIAM J. Numer. Anal.*, 29:647–678, 1992.
- [14] Franco Brezzi and Michel Fortin. *Mixed and hybrid finite element methods*. Springer-Verlag, New York, 1991.
- [15] Patrick Ciarlet, Jr. and Jun Zou. Fully discrete finite element approaches for time-dependent Maxwell equations. Technical Report TR MATH-96-31 (105), Department of Mathematics, The Chinese University of Hong Kong, 1996.
- [16] Lawrence C. Cowsar, Jan Mandel, and Mary F. Wheeler. Balancing domain decomposition for mixed finite elements. *Math. Comp.*, 64(211):989–1015, July 1995.
- [17] Monique Dauge. *Elliptic boundary value problems on corner domains*. Lecture Notes in Mathematics 1341. Springer-Verlag, New York, 1988.
- [18] Robert Dautray and Jaques-Louis Lions. *Mathematical analysis and numerical methods for science and technology*. Springer-Verlag, New York, 1988.

- [19] Yann-Hervé De Roeck and Patrick Le Tallec. Analysis and test of a local domain decomposition preconditioner. In Roland Glowinski, Yuri Kuznetsov, Gérard Meurant, Jacques Périaux, and Olof Widlund, editors, *Fourth International Symposium on Domain Decomposition Methods for Partial Differential Equations*, pages 112–128. SIAM, Philadelphia, PA, 1991.
- [20] Jim Douglas, Jr. and Jean E. Roberts. Global estimates for mixed methods for 2nd order elliptic equations. *Math. Comp.*, 44:39–52, 1985.
- [21] Maksymilian Dryja. A method of domain decomposition for 3-D finite element problems. In Roland Glowinski, Gene H. Golub, Gérard A. Meurant, and Jacques Périaux, editors, *First International Symposium on Domain Decomposition Methods for Partial Differential Equations*, pages 43–61, Philadelphia, PA, 1988. SIAM.
- [22] Maksymilian Dryja, Barry F. Smith, and Olof B. Widlund. Schwarz analysis of iterative substructuring algorithms for elliptic problems in three dimensions. *SIAM J. Numer. Anal.*, 31(6):1662–1694, December 1994.
- [23] Maksymilian Dryja and Olof B. Widlund. Domain decomposition algorithms with small overlap. *SIAM J. Sci. Comput.*, 15(3):604–620, May 1994.
- [24] Maksymilian Dryja and Olof B. Widlund. Schwarz methods of Neumann-Neumann type for three-dimensional elliptic finite element problems. *Comm. Pure Appl. Math.*, 48(2):121–155, February 1995.
- [25] Richard E. Ewing and Junping Wang. Analysis of the Schwarz algorithm for mixed finite element methods. *RAIRO Mathematical Modelling and Numerical Analysis*, 26(6):739–756, 1992.
- [26] Vivette Girault and Pierre-Arnaud Raviart. *Finite Element Methods for Navier-Stokes Equations*. Springer-Verlag, New York, 1986.
- [27] Roland Glowinski and Mary F. Wheeler. Domain decomposition and mixed finite element methods for elliptic problems. In Roland Glowinski, Gene H. Golub, Gérard A. Meurant, and Jacques Périaux, editors, *First International*

*Symposium on Domain Decomposition Methods for Partial Differential Equations*, Philadelphia, PA, 1988. SIAM.

- [28] P. Grisvard. *Elliptic problems in nonsmooth domains*. Pitman Publishing, Boston, 1985.
- [29] Ralf Hiptmair. *Multilevel Preconditioning for Mixed Problems in Three Dimensions*. PhD thesis, Mathematisches Institut, Universität Augsburg, 1996.
- [30] Ralf Hiptmair. Multigrid method for  $H(\text{div})$  in three dimensions. Technical Report 368, Institut für Mathematik, Universität Augsburg, 1997. To appear in ETNA.
- [31] Ralf Hiptmair. Multigrid method for Maxwell's equations. Technical Report 374, Institut für Mathematik, Universität Augsburg, 1997. Submitted to SIAM J. Numer. Anal.
- [32] Ralf Hiptmair and Ronald H. W. Hoppe. Multilevel methods for mixed finite elements in three dimensions. Technical Report 359, Mathematisches Institut, Universität Augsburg, Germany, October 1996.
- [33] Ralf Hiptmair and Andrea Toselli. Overlapping and multilevel Schwarz methods for vector valued elliptic problems in three dimensions. In *Parallel Solution of PDEs, IMA Volumes in Mathematics and its Applications*, Berlin, 1998. Springer-Verlag. To appear.
- [34] Patrick Le Tallec, Yann-Hervé De Roeck, and Marina Vidrascu. Domain-decomposition methods for large linearly elliptic three dimensional problems. *J. of Computational and Applied Mathematics*, 34, 1991.
- [35] Rolf Leis. *Initial Boundary Value Problems in Mathematical Physics*. B.G. Teubner, Stuttgart, 1986.
- [36] Jan Mandel. Balancing domain decomposition. *Comm. Numer. Meth. Engrg.*, 9:233–241, 1993.

- [37] Jan Mandel and Marian Brezina. Balancing domain decomposition: Theory and computations in two and three dimensions. Technical Report UCD/CCM 2, Center for Computational Mathematics, University of Colorado at Denver, 1993.
- [38] Jan Mandel and Marian Brezina. Balancing domain decomposition for problems with large jumps in coefficients. *Math. Comp.*, 65:1387–1401, 1996.
- [39] Tarek P. Mathew. Schwarz alternating and iterative refinement methods for mixed formulations of elliptic problems, part I: Algorithms and Numerical results. *Numer. Math.*, 65(4):445–468, 1993.
- [40] Tarek P. Mathew. Schwarz alternating and iterative refinement methods for mixed formulations of elliptic problems, part II: Theory. *Numer. Math.*, 65(4):469–492, 1993.
- [41] Peter Monk. Analysis of a finite element method for Maxwell’s equations. *SIAM J. Numer. Anal.*, 19(3):714–729, 1992.
- [42] Peter Monk. An analysis of Nédélec’s method for the spatial discretization of Maxwell’s equations. *J. Comp. Appl. Math.*, 47:101–102, 1993.
- [43] Claus Müller. *Foundations of the mathematical theory of electromagnetic waves*. Springer-Verlag, Berlin, 1969.
- [44] Jean-Claude Nédélec. Mixed finite elements in  $R^3$ . *Numer. Math.*, 35:315–341, 1980.
- [45] Jean-Claude Nédélec. A new family of mixed finite elements in  $R^3$ . *Numer. Math.*, 50:57–81, 1986.
- [46] Jindřich Nečas. *Les méthodes directes en théorie des équations elliptiques*. Academia, Prague, 1967.
- [47] Dianne P. O’Leary and Olof B. Widlund. Capacitance matrix methods for the Helmholtz equation on general three dimensional regions. *Math. Comp.*, 33:849–879, 1979.



- [48] Pierre-Arnaud Raviart and J. M. Thomas. A mixed finite element method for 2-nd order elliptic problems. In A. Dold and B. Eckmann, editors, *Mathematical Aspects of Finite Element Methods*. Springer, 1975. Lecture Notes of Mathematics, Volume 606.
- [49] Alfio Quarteroni and Alberto Valli. *Numerical approximation of partial differential equations*. Springer-Verlag, Berlin, 1994.
- [50] Alfio Quarteroni and Alberto Valli. *Domain decomposition methods for partial differential equations*. Oxford University Press, Oxford, 1998.
- [51] Marcus V. Sarkis. Two-level Schwarz methods for nonconforming finite elements and discontinuous coefficients. In N. Duane Melson, Thomas A. Mantueffel, and Steve F. McCormick, editors, *Proceedings of the Sixth Copper Mountain Conference on Multigrid Methods, Volume 2*, number 3224, pages 543–566, Hampton VA, 1993. NASA.
- [52] Marcus V. Sarkis. *Schwarz Preconditioners for Elliptic Problems with Discontinuous Coefficients Using Conforming and Non-Conforming Elements*. PhD thesis, Courant Institute, New York University, September 1994.
- [53] Marcus V. Sarkis. Nonstandard coarse spaces and Schwarz methods for elliptic problems with discontinuous coefficients using non-conforming elements. *Numer. Math.*, 77(3):383–406, 1997.
- [54] Barry F. Smith, Petter E. Bjørstad, and William D. Gropp. *Domain Decomposition: Parallel Multilevel Methods for Elliptic Partial Differential Equations*. Cambridge University Press, 1996.
- [55] Andrea Toselli. Some numerical results using an additive Schwarz method for Maxwell’s equations. Technical Report 726, Courant Institute of Mathematical Sciences, New York University, November 1996.
- [56] Andrea Toselli. Overlapping Schwarz methods for Maxwell’s equations in three dimensions. Technical Report 736, Courant Institute of Mathematical Sciences, New York University, June 1997. Submitted to Numer. Math.

- [57] Andrea Toselli, Olof B. Widlund, and Barbara I. Wohlmuth. An iterative substructuring method for Maxwell's equations in two dimensions. Technical Report 768, Department of Computer Science, Courant Institute, 1998. Submitted to Math. Comput.
- [58] Rüdiger Verfürth. *A review of a posteriori error estimation and adaptive mesh-refinement techniques*. Teubner-Verlag, Stuttgart, 1996.
- [59] Olof B. Widlund. Iterative substructuring methods: Algorithms and theory for elliptic problems in the plane. In Roland Glowinski, Gene H. Golub, Gérard A. Meurant, and Jacques Périaux, editors, *First International Symposium on Domain Decomposition Methods for Partial Differential Equations*, Philadelphia, PA, 1988. SIAM.
- [60] Olof B. Widlund. Exotic coarse spaces for Schwarz methods for lower order and spectral finite elements. In David E. Keyes and Jinchao Xu, editors, *Seventh International Conference of Domain Decomposition Methods in Scientific and Engineering Computing*, volume 180 of *Contemporary Mathematics*, pages 131–136. AMS, 1994. Held at Penn State University, October 27-30, 1993.
- [61] Olof B. Widlund. Domain decomposition methods for elliptic partial differential equations. In *Error control and adaptivity in scientific computing*, 1998. Lecture notes based on talks given at a NATO summer school in Antalya, Turkey, August 1998. To appear.
- [62] Barbara I. Wohlmuth, Andrea Toselli, and Olof B. Widlund. An iterative substructuring method for Raviart–Thomas vector fields in three dimensions. Technical Report 775, Department of Computer Science, Courant Institute, 1998. Submitted to SIAM J. Numer. Anal.